NASA CR-72245
JANUARY 26, 1967

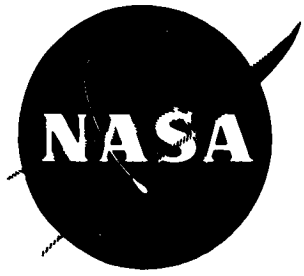

TOPICAL REPORT

DEFINITION OF SPACECRAFT AND RADIATOR INTERRELATIONS FOR NUCLEAR RANKINE SYSTEMS

by

R. D. Cockfield

prepared for

NATIONAL AERONAUTICS AND SPACE ADMINISTRATION

CONTRACT NASw-1449

ADVANCED NUCLEAR SYSTEMS OPERATION

GENERAL ELECTRIC

MISSILE AND SPACE DIVISION
Valley Forge Space Technology Center
P.O. Box 8555 • Philadelphia 1, Penna.

GENERAL ELECTRIC COMPANY

MISSILE AND SPACE DIVISION

KING OF PRUSSIA PARK (MAIL: P. O. BOX 8661, PHILADELPHIA, PA. 19101) ... TELEPHONE 969-2000

Subject: Contract NASw-1449

Gentlemen:

The Missile and Space Division of the General Electric Company encloses herewith for your retention Final Report of Task 'A' Topical Report, entitled Definition of Spacecraft and Radiator Interrelations for Nuclear Rankine Systems, prepared under subject contract.

This Report is furnished to you in accordance with instructions from NASA/Lewis Research Center.

Very truly yours,

Thurmae Anderson

Thurmae Anderson
Contract Analyst

a/
Enclosure

NASA CR-72 245
GE ANSO 6300-166
January 26, 1967

TOPICAL REPORT

DEFINITION OF SPACECRAFT AND RADIATOR INTERRELATIONS FOR NUCLEAR RANKINE SYSTEMS

by

R. D. Cockfield

prepared for

NATIONAL AERONAUTICS AND SPACE ADMINISTRATION

CONTRACT NASw-1449

Technical Management
NASA Lewis Research Center
Cleveland, Ohio
James P. Couch

ADVANCED NUCLEAR SYSTEMS OPERATION

GENERAL ELECTRIC

MISSILE AND SPACE DIVISION
Valley Forge Space Technology Center
P.O. Box 8555 • Philadelphia 1, Penna.

NOTICE

This report was prepared as an account of Government-sponsored work. Neither the United States nor the National Aeronautics and Space Administration (NASA), nor any person acting on behalf of NASA:

A) Makes any warranty or representation, expressed or implied with respect to the accuracy, completeness, or usefulness of the information contained in this report or that the use of any information, apparatus, method, or process disclosed in this report may not infringe privately-owned rights; or

B) Assumes any liabilities with respect to the use of, or for damages resulting from the use of any information, apparatus, method or process disclosed in this report.

As used above, "person acting on behalf of NASA" includes any employee or contractor of NASA, or employee of such contractor, to this extent that such employee or contractor of NASA, or employee of such contractor prepares, disseminates, or provides access to, any information pursuant to his employment or contract with NASA, or his employment with such contractor.

Request for copies of this report should be addressed to:

NASA
Office of Scientific and Technical Information
Box 33
College Park, Md. 20740

TABLE OF CONTENTS

LIST OF ILLUSTRATIONS

LIST OF ILLUSTRATIONS (Cont)

LIST OF ILLUSTRATIONS (Cont)

LIST OF ILLUSTRATIONS (Cont)

LIST OF TABLES

1. SUMMARY

This report summarizes the results of the first of three tasks being performed by the General Electric Company, Missile and Space Division for the National Aeronautics and Space Administration under contract NASw-1449 - A Study of Radiator Structural and Mechanical Requirements. The three tasks covered in this study are:

a. Definition of Spacecraft and Radiator Interrelations

b. Comparison of Load Bearing and Non-Load Bearing Radiators

c. Comparison of Direct Condensing and Indirect Radiators

The purpose of the first task is to investigate geometry, loading, and system interactions between large radiators for space nuclear systems and their launch vehicles, including extension of the radiator over the final propulsion stage. Results include the definition of limitations to radiator area, and the generation of parametric data on loads and radiation shielding weight with respect to radiator size and configuration. The shielding weights determined are appropriate to unmanned missions only. Considerably different conclusions may be reached if shielding appropriate to manned missions were considered.

An evaluation of the launch loads is made for three launch vehicles: the Saturn IB, and the Saturn V in both its two- and three-stage versions. These vehicles are compared in Figure 1-1.

The launch loads acting at the payload interface are determined as a function of radiator size and payload weight. Maximum limits for these loads are set by the structural capabilities of the launch vehicle, thereby yielding the radiating area limitations for each of the cases considered. Maximum areas for nominal payload weight are about 3080 square feet for the Saturn IB, 3240 square feet for the three-stage Saturn V, and 12,400 square feet for the two-stage Saturn V.

The feasibility of utilizing the upper stages for additional radiator area is investigated, using two approaches: a sheath type radiator that fits over the stage to minimize interference between the payload and launch vehicle, and an integral radiator requiring redesign and possible requalification of the propulsion stage. Maximum feasible area additions are determined to be 2200 square feet by using the S-IVB stage, and 5040 square feet by using the S-II stage.

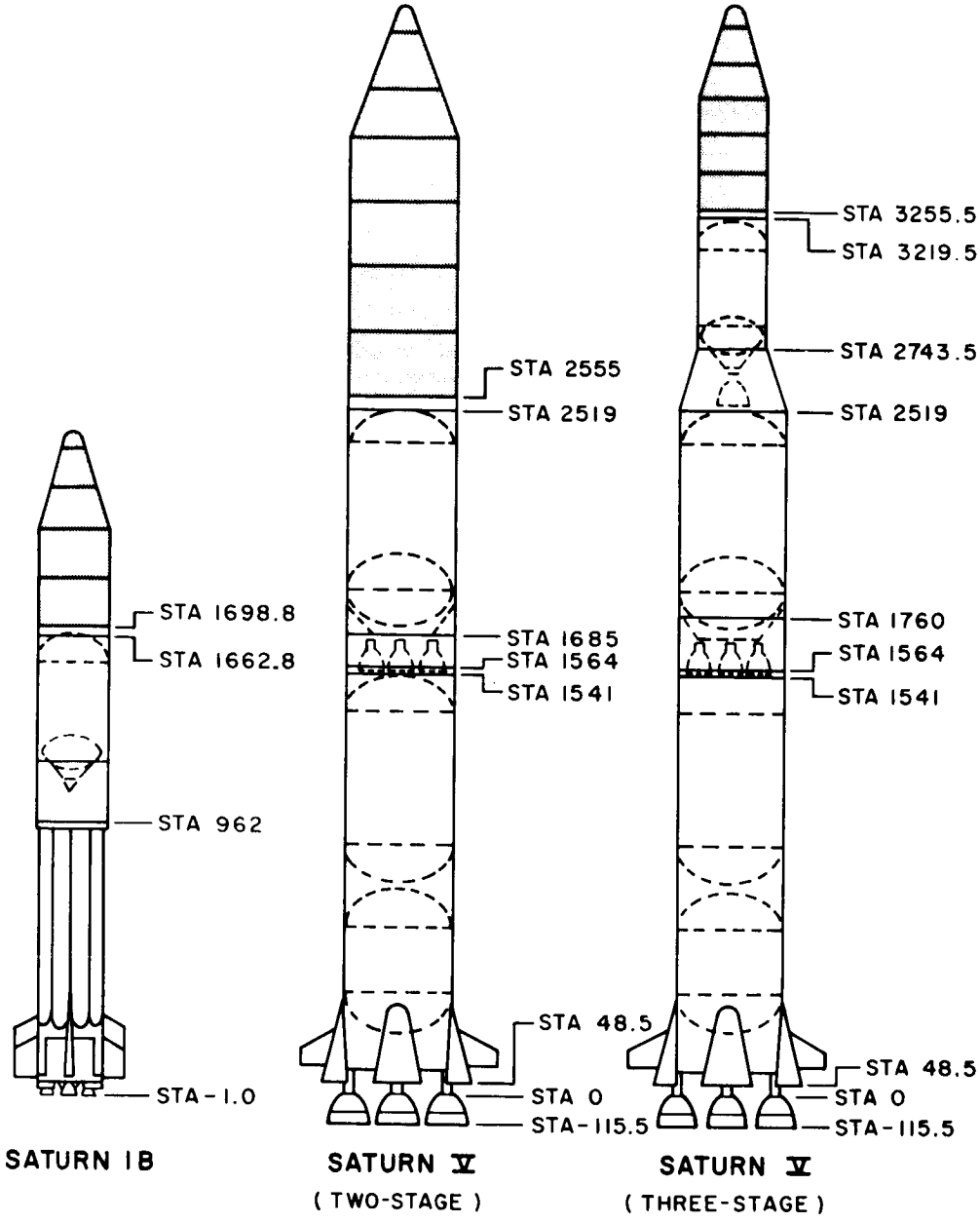

VEHICLE NAME	STAGE DESIGNATION	STAGE CONTRACTOR	PROPULSION
SATURN IB	S-IB S-IVB	CHRYSLER DOUGLAS	8 X ROCKETDYNE H-1 1 X ROCKETDYNE J-2
SATURN V (TWO-STAGE)	S-IC S-II	BOEING NAA	5 X ROCKETDYNE F-1 5 X ROCKETDYNE J-2
SATURN V (THREE-STAGE)	S-IC S-II S-IVB	BOEING NAA DOUGLAS	5 X ROCKETDYNE F-1 5 X ROCKETDYNE J-2 1 X ROCKETDYNE J-2

Figure 1-1. Comparison of Saturn Launch Vehicles

A parametric study of nuclear radiation shielding is included for both conical and flat panel radiator configurations in order to show the interaction with radiator geometry. Both configurations require the same weight of primary shielding. For conical radiators, secondary shielding weights are shown to be significant for large radiator cone angles, but at cone angles of 10 degrees and less, the radiator does not project beyond the shadow of the primary shield and no secondary shielding is required. The secondary shielding associated with flat panel radiators is found to be significantly less for comparable angles, yielding weights that are relatively insensitive to radiator geometry.

An evaluation of the effect of launch loads on the optimization of radiator design is also included in this report. This shows the structural capability of a beryllium cone-cylinder radiator, optimized to meet normal thermal and meteoroid protection requirements, to be a good match with the launch loads on the Saturn vehicles.

Detailed conclusions resulting from this task are presented in Section 6. of this report.

2. SPACECRAFT CONFIGURATION

Thermal considerations favor the use of a flat panel configuration for the radiator of a nuclear electric spacecraft. Typical examples are the JPL "Space Cruiser" (Reference 2-1) and the thermionic powerplants studied by Pratt and Whitney (Reference 2-2). This concept requires a separate support structure for the radiator, and an aerodynamic fairing to cover the entire vehicle. By utilizing a cone-cylinder arrangement, the radiator forms a shell structure enclosing the booster payload envelope. This arrangement permits the radiator to serve as the primary vehicle structure and aerodynamic fairing, taking advantage of the inherently rugged construction that results from meeting the thermal and meteoroid protection requirements.

Because the cone-cylinder radiator can reject heat from only one surface, its specific weight is generally heavier than a flat panel configuration. However, a complete evaluation of the two concepts must compare their total effect on spacecraft weight, accounting for the structure, aerodynamic fairing, and differences in nuclear radiation shielding requirements. Such a comparison will be the subject of a later topical report of this study. The objective at present is to examine the interrelations of both these concepts in terms of radiating area capabilities, launch loads and spacecraft integration.

2.1 NUCLEAR SHIELDING INTERACTIONS

Numerous studies of nuclear electric spacecraft for unmanned missions have identified the desirability of locating the reactor at the top of the vehicle and the scientific payload at the base with the nuclear radiation shielding adjacent to the reactor. The radiator enters this relationship by its configuration, overall length, and cone angle.

A flat panel radiator will require local lobes of secondary shielding where it projects outside the shadow of the primary shield. On the other hand, a conical radiator will require a secondary shield that is a conical frustrum surrounding the primary shield. The overall length of the radiator is related to the separation distance between reactor and scientific payload, while the cone angle determines the extent by which the radiator projects beyond the shadow of the primary shield.

To examine these interactions, a parametric analysis of shield weight was made for both the conical and flat panel radiator configurations. Assumptions used in the analysis are listed

in Table 2-1. Two reactor sizes were considered, corresponding to the two classes of spacecraft sizes. The smaller size corresponds to a power system suitable for launch on the Saturn IB or three-stage Saturn V vehicle. The larger size corresponds to the class of spacecraft that would be launched by a two-stage Saturn V.

TABLE 2-1. ASSUMPTIONS USED IN NUCLEAR RADIATION SHIELD ANALYSIS

Reactor diameter:	2.0 feet and 2.5 feet
Reactor 1/d:	1.0
Reactor power:	7.6 Mw_t and 30.4 Mw_t
Gamma shielding:	Tungsten
Neutron shielding:	Lithium Hydride
Payload dose:	10^{11} nvt neutrons 10^{6} rad gamma

Data from Reference 2-3 were used to estimate the relationship between radiation flux and reactor thermal power. Although the radiation damage tolerance of the payload equipment will depend upon the materials used and local shielding provided, permissible unmanned payload dosages used for the analysis are typical of current practices.

The method of analysis follows that used in Reference 2-4, except that geometrical relations were established for flat panel radiators as shown by Figure 2-1. Shield density includes a factor to account for stainless steel encapsulation of lithium hydride neutron shielding. This encapsulation is adequate to provide structural support and meteoroid protection. The latter is needed since a puncture of the shield would result in loss of hydrogen from the lithium hydride, resulting in radiation damage to the payload.

Results of the analysis are shown in Figures 2-2, 2-3, 2-4, and 2-5. It may be seen that the secondary shield weight for a conical radiator is a substantial penalty when large cone angles are used. However, when the half-cone angle is 10 degrees or less, the radiator projection beyond the shadow of the primary shield is small or absent so that secondary shielding weight becomes negligible. The bottom curve in each figure is the weight of the primary shield alone.

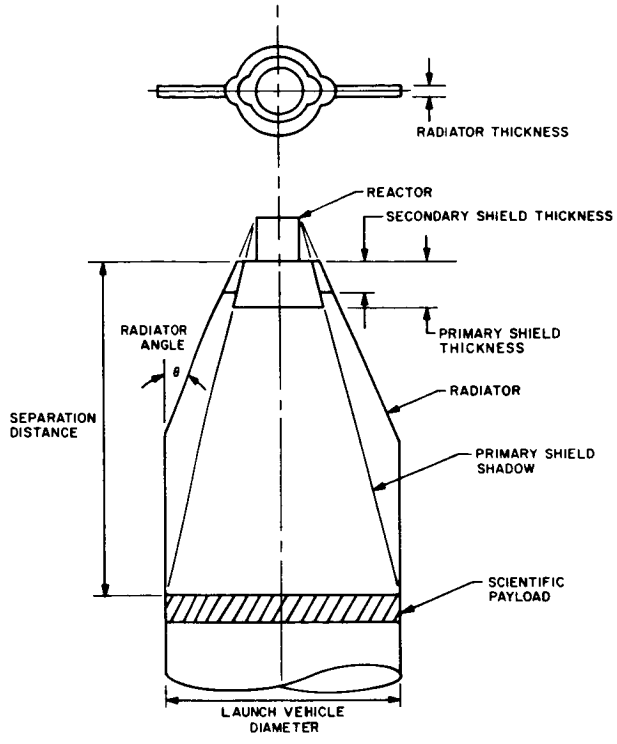

Figure 2-1. Shield Geometry for Flat Panel Radiator

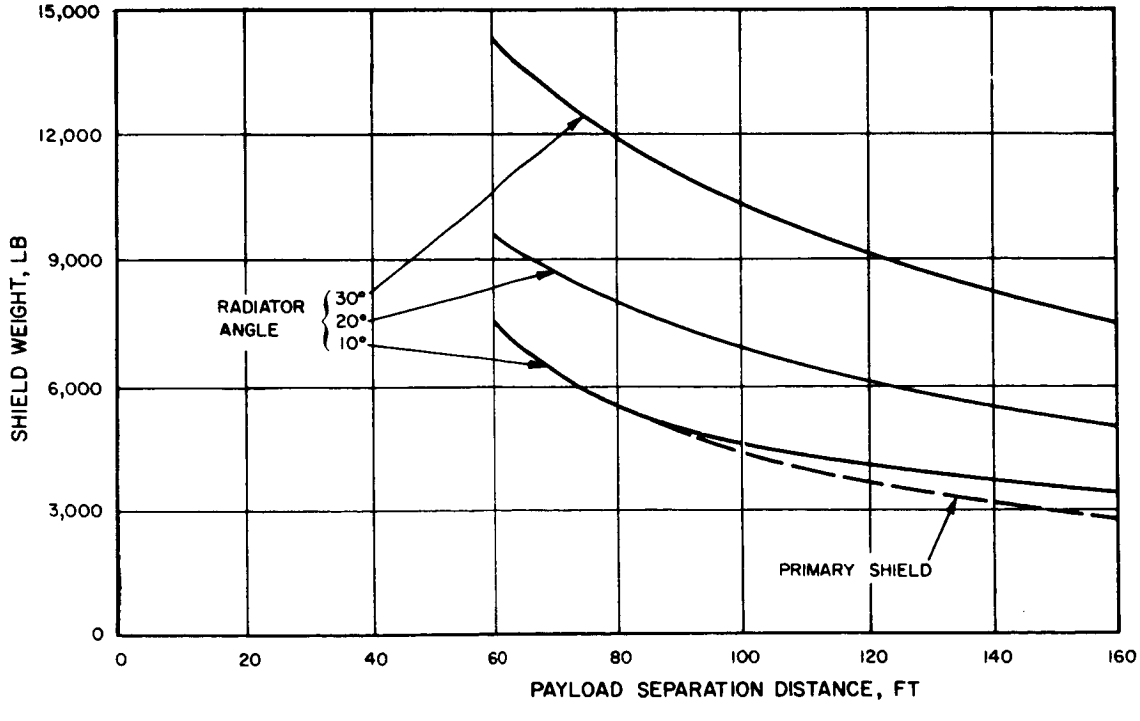

Figure 2-2. Shield Weight for Conical Radiator on 33-Foot-Diameter Launch Vehicle

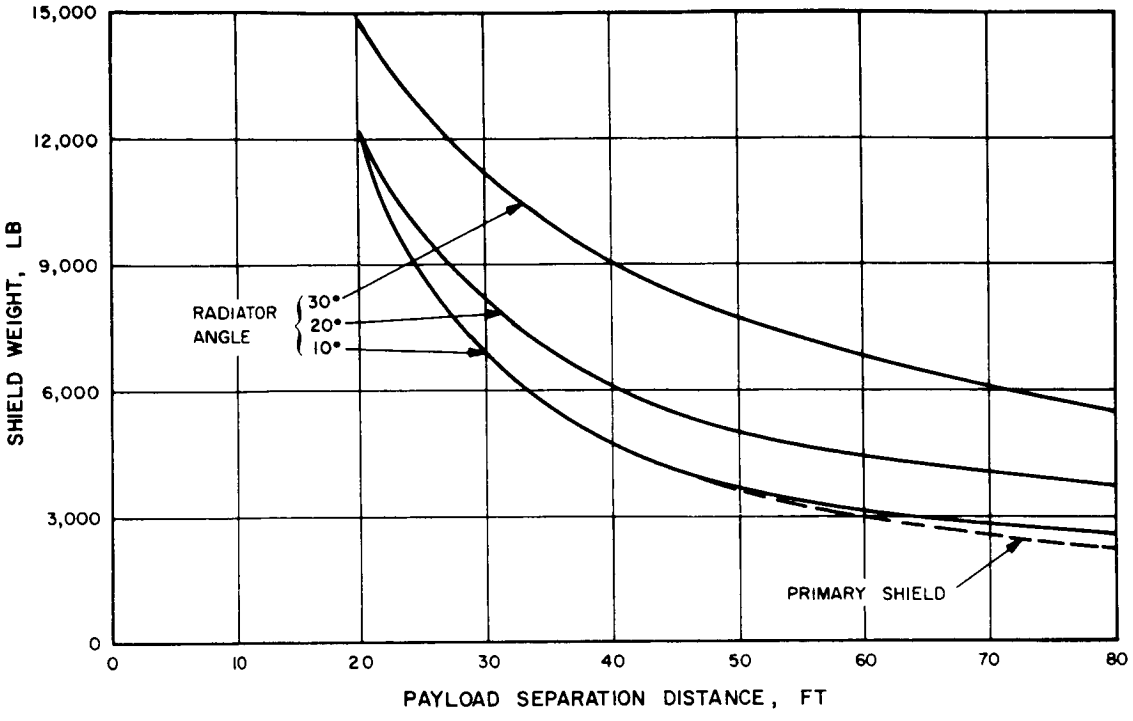

Figure 2-3. Shield Weight for Conical Radiator on 21.7-Foot-Diameter Launch Vehicle

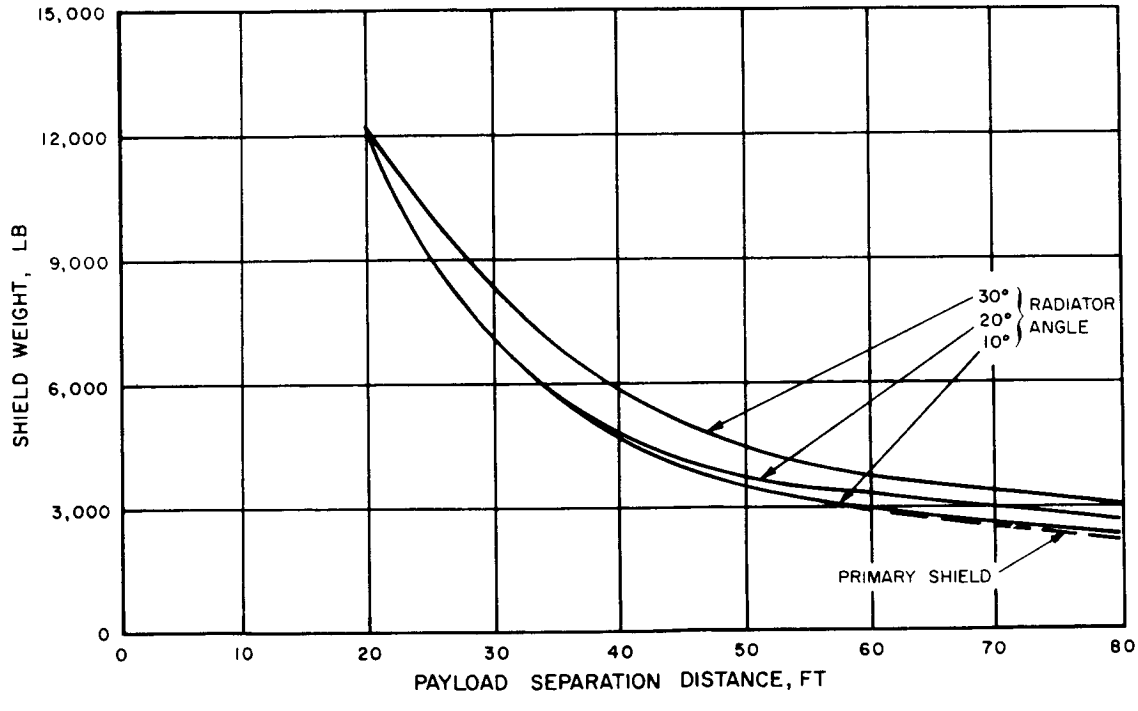

Figure 2-4. Shield Weight for Flat Panel Radiator on 21.7-Foot-Diameter Launch Vehicle

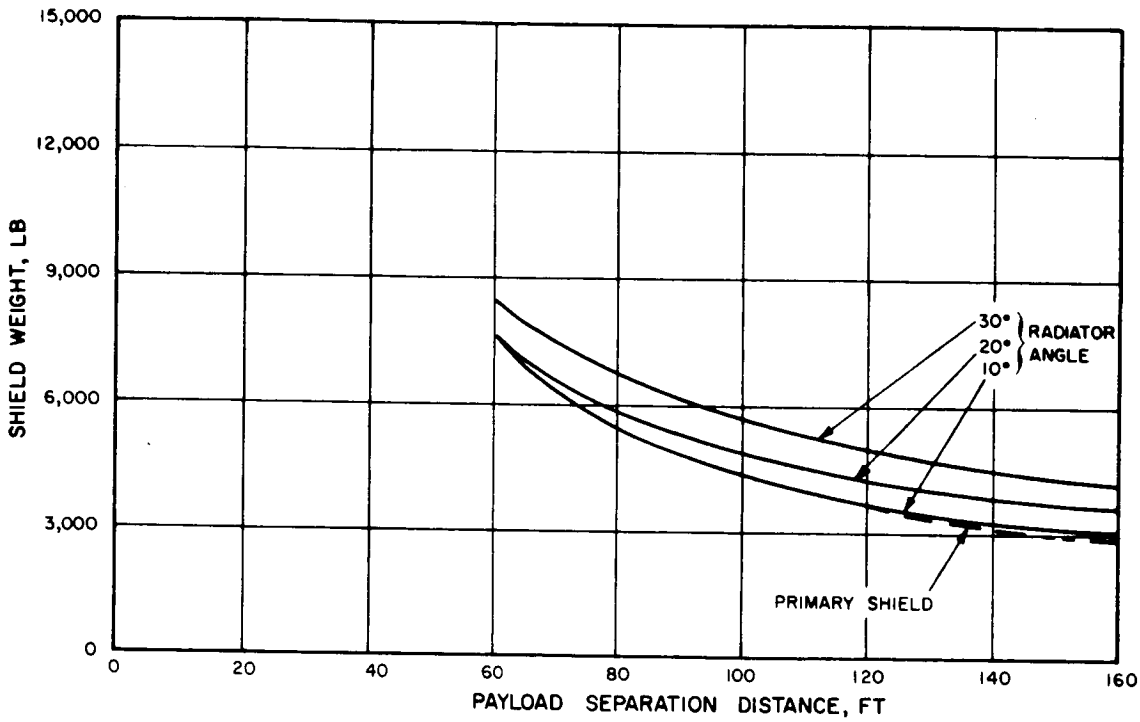

Figure 2-5. Shield Weight for Flat Panel Radiator on 33-Foot-Diameter Launch Vehicle

The higher power level assumed for the larger class of spacecraft is compensated by the larger separation distance so that primary shield weights on the two classes of spacecraft are comparable. Shield weights for the flat panel radiator differ from those of the cylindrical radiator only in the secondary shield. The local lobes used with the flat panel radiator result in a considerable reduction of the secondary shield weight, so that less penalty results from the use of a large radiator angle. For the flat panel radiator, this angle also applies to the aerodynamic fairing that covers it. Therefore, it is appropriate to refer to it as a cone angle, regardless of the radiator configuration.

2.2 RADIATOR AREA RELATIONS

When viewed in plan form, both the conical and flat panel radiator appear as shown in Figure 2-6. With appropriate assumptions for the dimensions of the reactor and shield to account for the area not available at the nose of the spacecraft, it is possible to determine the total radiator area as a function of the two significant parameters, half-cone angle (θ) and overall length. Since the base of the radiator will be assumed to match the diameter of the launch

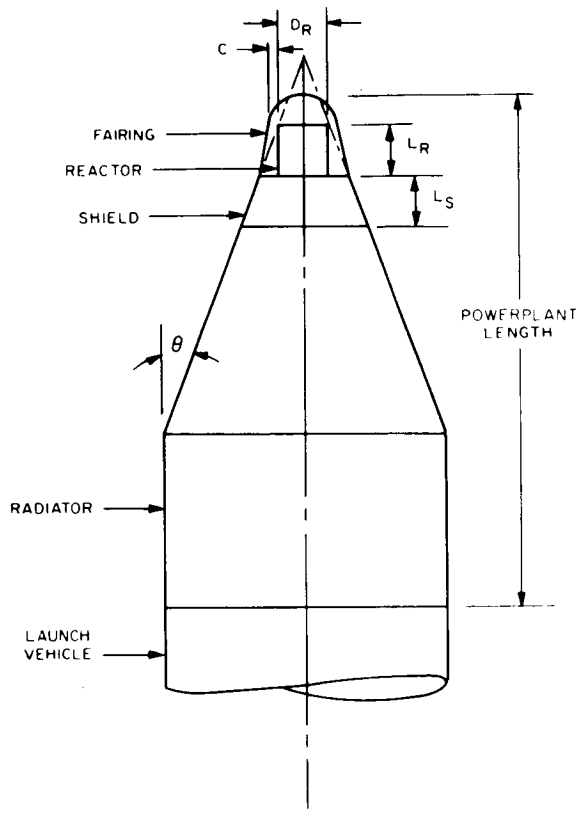

Figure 2-6. Powerplant Geometry for Area Calculations

vehicle at the interface, the length of conical section (trapezoidal for the flat panel) is uniquely determined by these two parameters. It is convenient to express the radiator size in terms of overall powerplant length, defined as the distance from the tip of the nose on the aerodynamic fairing to the base of the radiator. This permits plotting of all data on a single base and is consistent with the measurement of distances for loads analysis.

Using the dimensions listed in Table 2-2, radiator areas were determined for half-cone angles of 10 degrees, 20 degrees, 30 degrees and for launch vehicle diameters of 21.7 feet and 33 feet. Results are shown in Figures 2-7 and 2-8. The flat panel radiator areas differ from conical radiator areas only by the factor $2/\pi$, taking into account that the flat panel radiator is able to radiate from both front and back surfaces. It is important to note that the flat panel areas are idealized; that is, no reduction is taken into account to allow for the clearance required between the radiator and the aerodynamic fairing that encloses it, nor for space allotted for the power conversion equipment and the scientific payload. No corresponding area is lost on the conical radiator since it can serve as its own aerodynamic fairing and the power conversion equipment and scientific payload can be mounted inside it.

TABLE 2-2. DIMENSIONS USED FOR RADIATOR AREA ANALYSIS

Reactor diameter:	2.0 feet	(D_R)
Reactor length:	2.0 feet	(L_R)
Shield thickness:	3.0 feet	(L_S)
Fairing clearance:	4.0 inches	(C)
Launch vehicle diameter	21.7 and 33 feet	

The reactor and shield dimensions assumed for the purpose of determining radiator area are appropriate to the smaller class size of spacecraft, suitable for launch on the Saturn IB and three-stage Saturn V vehicles. However, these dimensions do not change significantly over a wide range of power levels, so that their use in determining the radiator areas for spacecraft to be launched on the two-stage Saturn V vehicle introduces negligible error.

The cut-off limits shown on Figures 2-7 and 2-8 are for combinations of cone angle and length that result in a match between the base of the cone and the launch vehicle diameter. Below this line, a nonradiating adapter structure would be required to match the radiator to the launch vehicle.

As used in this study, the spacecraft configuration for a cone-cylinder radiator follows the pattern of an unmanned interplanetary probe mission vehicle as developed in the Navigator Studies (Reference 2-5) and is shown in simplified form in Figure 2-9. The radiator acts as the primary structure, supporting the reactor, shield and power conversion equipment. During launch, an aerodynamic fairing covers only the reactor. The scientific payload and electric propulsion system are mounted inside the radiator and are supported directly on the booster interface. Similar configurations have been used for studies of Lunar Cargo and Manned Mars missions using nuclear power (References 2-6 and 2-7). By using this configuration for the development of launch loads, data can be obtained which apply to both the conical radiator and the flat panel radiator, provided the external fairing shapes and mass distributions are similar. The aerodynamic fairing over the flat panel radiator will see only the aerodynamic loads, while the inertia loads will be carried by a separate, expendable structure. The conical radiator, acting as both aerodynamic fairing and primary structure will see the combined effect of aerodynamic and inertia loads.

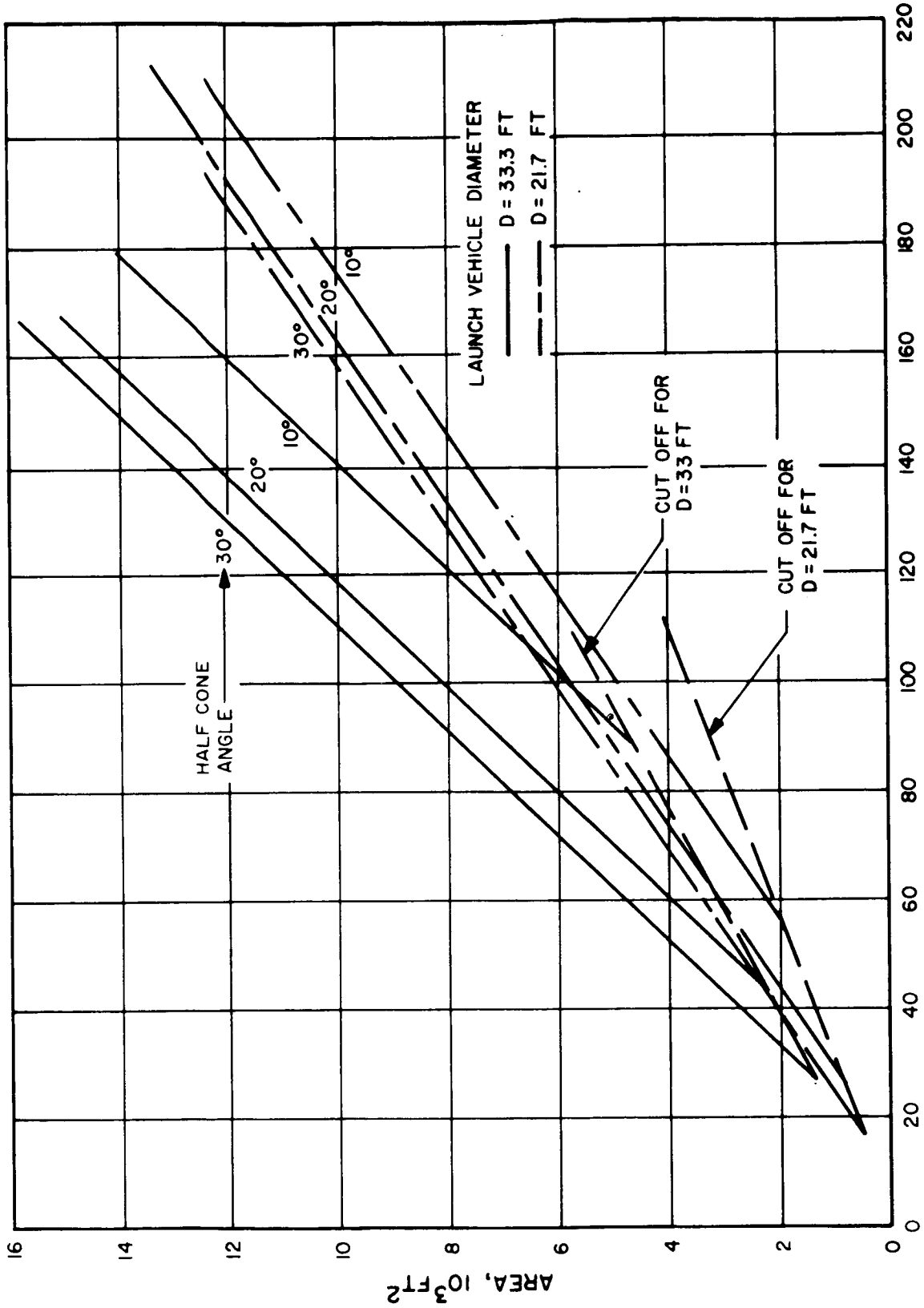

Figure 2-7. Radiator Area for Cone-Cylinder Configuration

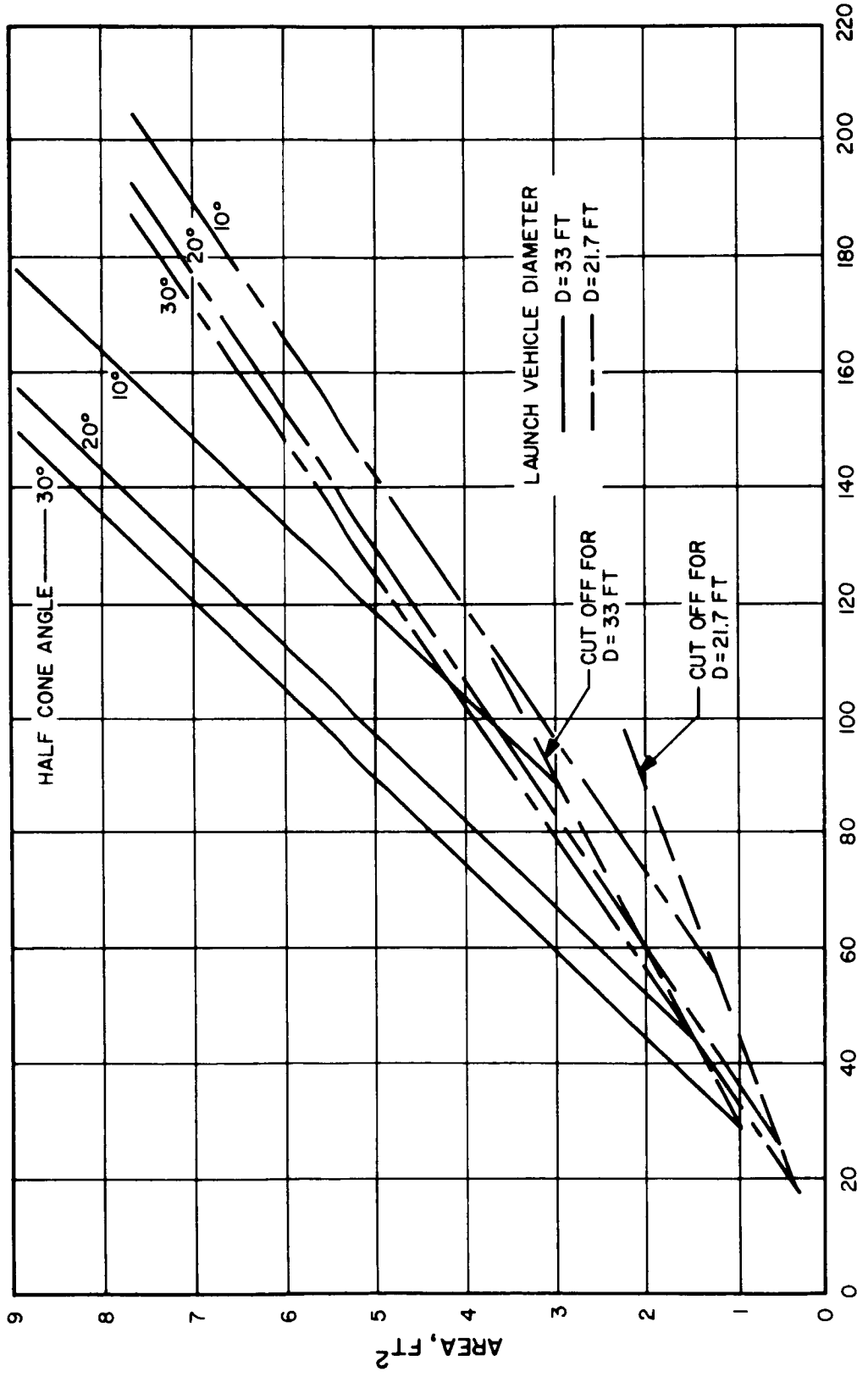

Figure 2-8. Radiator Area for Flat Panel Configuration

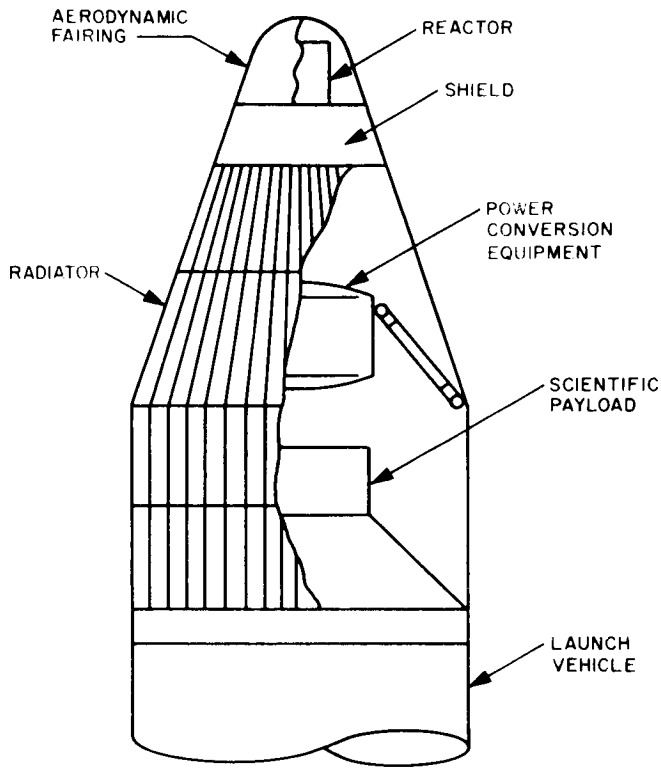

Figure 2-9. Spacecraft Launch Configuration

2.3 REFERENCES

2-1. Beale, R.J., Speiser, E.W., Womack, J.R. "The Electric Space Cruiser for High-Energy Missions," Technical Report No. 32-404, Jet Propulsion Laboratory, June 1963.

2-2. Buatti, A.V., Schmitt, J.W. "Design Study of High Power In-Pile Nuclear Thermionic Space Powerplant," NASA CR-54172, July 30, 1964.

2-3. Cochran, D.L. and Friedman, S.T. "Preliminary Shield Design for Nuclear Electric Space Powerplants," AIEE Paper 62-1236.

2-4. Freedman, S.I. "Study of Nuclear Brayton Cycle Power System," NASA/CR-54397, August 1965.

2-5. Larson, J.W. "Research on Spacecraft and Powerplant Integration - Spacecraft Analysis Topical Report," NAS CR-54159, July 24, 1964.

2-6. Larson, J.W. "Electrically Propelled Cargo Vehicle for Sustained Lunar Supply Operations - Topical Report Nuclear Powerplant Analysis (U)," Contract NAS 8-11207, May 1966.

2-7. Coates, G.L. and Brown, H. "Study of Low Acceleration Space Transport Systems - Phase I Study Report," Contract NAS 8-11423, June 30, 1965.

3. LAUNCH LOADS ANALYSIS

The load conditions which determine the structural requirements of a spacecraft occur during launch. These loads may come from many sources: aerodynamic pressure and turbulence, acceleration due to thrust and attitude control maneuvers, engine noise, thrust transients, shocks due to fairing and stage separations, etc. Each of these sources may create loads locally that determine the design of local structure. However, the major forces acting on a launch vehicle and its payload occur during powered flight and act as shown in Figure 3-1.

The relative wind acts at an angle-of-attack α, which is composed of an attitude error or steering angle and a wind induced angle-of-attack, α_W.

$$\alpha_W = \tan^{-1} \frac{W}{V} \approx \frac{W}{V}$$

where

W = wind speed

V = vehicle velocity

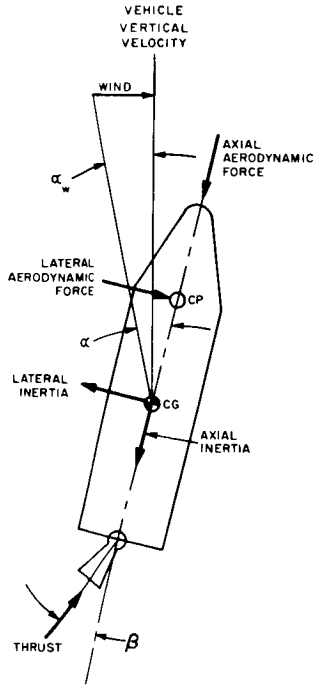

Figure 3-1. Launch Loads in Powered Flight

The resulting aerodynamic loads can be resolved into axial and normal components corresponding to drag and lift, as shown. These forces are balanced by the inertia forces and the thrust force acting at a gimbal angle, β.

The determination of the unknown quantities, accelerations, angle-of-attack and gimbal angle, is a complex dynamic problem. For solution it requires modeling of the launch vehicle dynamic characteristics, as it flies a chosen trajectory through an atmosphere of varying density, with proper representation of varying wind velocity, including gusts. Once these parameters have been determined for a specific launch vehicle and launch condition, however, the forces can be analyzed as for a free body in equilibrium. Hence the launch loads acting on the payload section of the vehicle depend on such parameters as the trajectory, wind speed, and attitude control system performance. These parameters will be discussed before presenting the loads analysis.

3.1 DISCUSSION OF LAUNCH PARAMETERS

3.1.1 TRAJECTORY CHARACTERISTICS

For purposes of launch load analysis, trajectory data were used which were most readily available. The trajectories are for Apollo payloads, the Saturn IB launch to 100-nautical mile circular orbit and the Saturn V launch to lunar orbit. The initial boost to 100 nautical miles for the Saturn V launch provides data which are applicable to a two-stage vehicle.

Typical missions employing large nuclear power systems would normally require an initial earth orbit higher than 100 nautical miles. For example, typical Navigator payloads and their orbits are compared with Apollo payloads in Table 3-1. The use of Apollo trajectory data for load analysis is judged to be adequately realistic for preliminary evaluation purposes because of compensating factors. For instance, it is likely that direct ascent to a higher orbit would not be used. Instead, transfer would be made from a 100-nautical mile orbit using an additional chemical stage (transtage). In this case, the initial trajectory to 100 nautical miles, during which critical launch loads occur, would be identical to the Apollo trajectories.

TABLE 3-1. COMPARISON OF APOLLO PAYLOADS AND TYPICAL NAVIGATOR PAYLOADS

MISSION	LAUNCH VEHICLE	PAYLOAD WEIGHT (LB)	PAYLOAD LENGTH (FT)	ORBIT
Apollo	Saturn IB	32,000	81.6	100 n. mi.
	Saturn V	101,000	81.6	beyond escape
Navigator	Saturn IB	28,000	54.3	300 n. mi.
	Saturn V (3-stage)	95,000	54.3	beyond escape
	Saturn V (2-stage)	240,000	128 *	300 n. mi.

* Comparable to length of Apollo payload plus S-IVB stage = 143 feet.

The trajectory parameters required for payload analysis of the S-IB and S-V are plotted in Figures 3-2 and 3-3 (References 3-1 and 3-2). In addition, the maximum "$q\alpha$" conditions are as follows:

Saturn IB

Dynamic pressure	582 lb/ft^2
Mach number	1.05
Angle-of-attack	8.4^o
Axial acceleration	2.0g
Lateral acceleration	0.2g

Saturn V

Dynamic pressure	741 lb/ft^2
Mach number	1.35
Angle-of-attack	9.3^o
Axial acceleration	2.0g
Lateral acceleration	0.2g

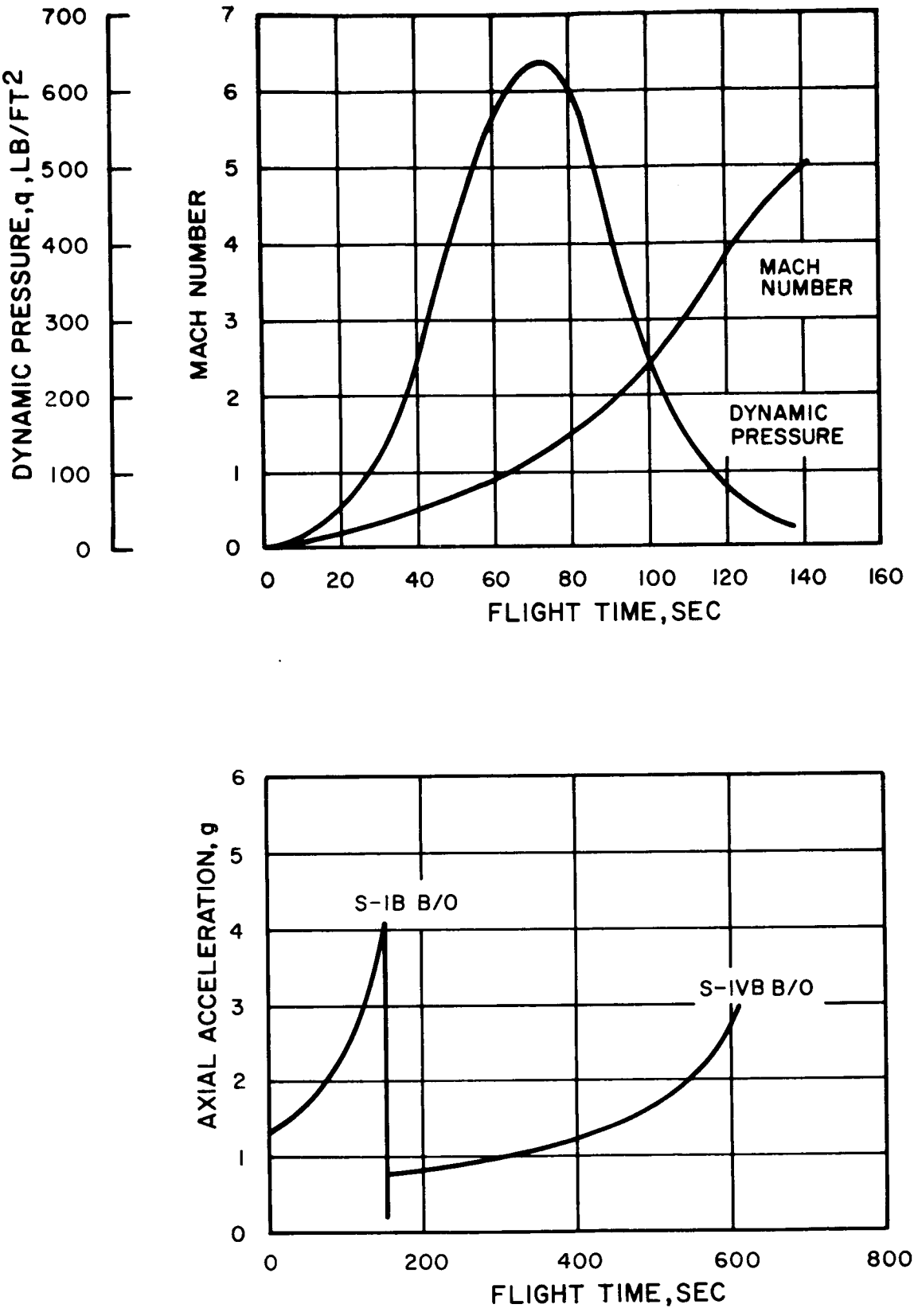

Figure 3-2. Trajectory Data for Saturn IB Launch Vehicle

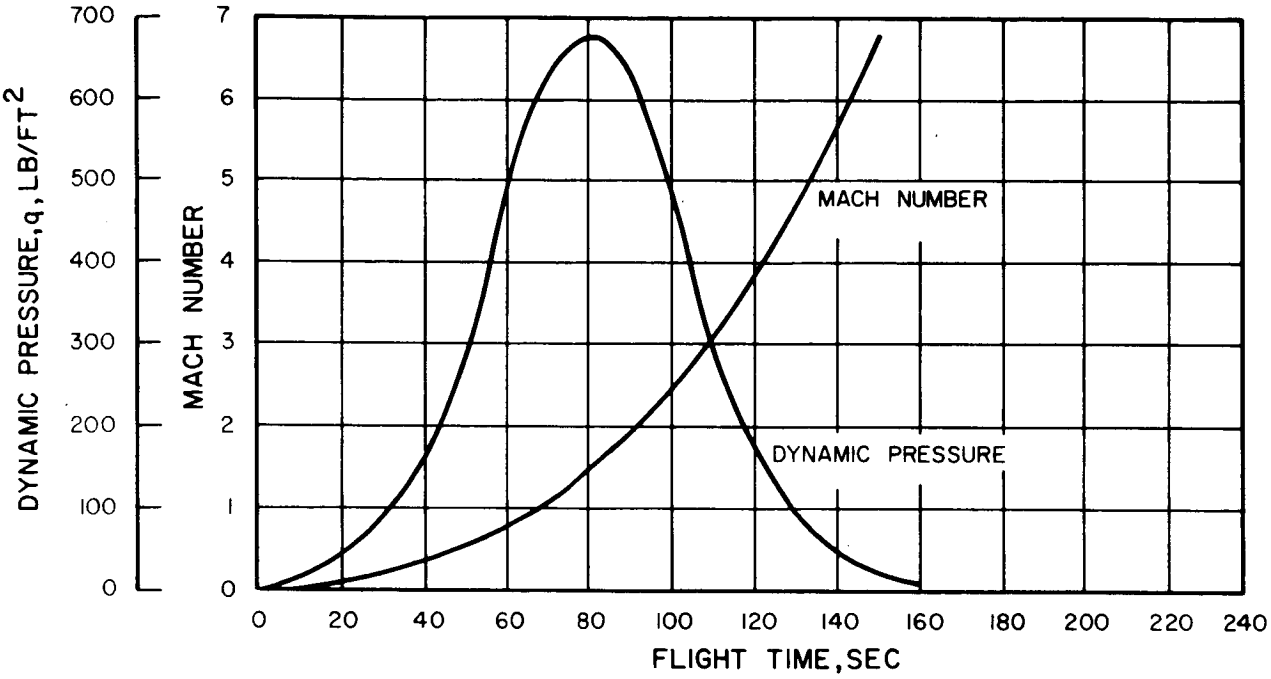

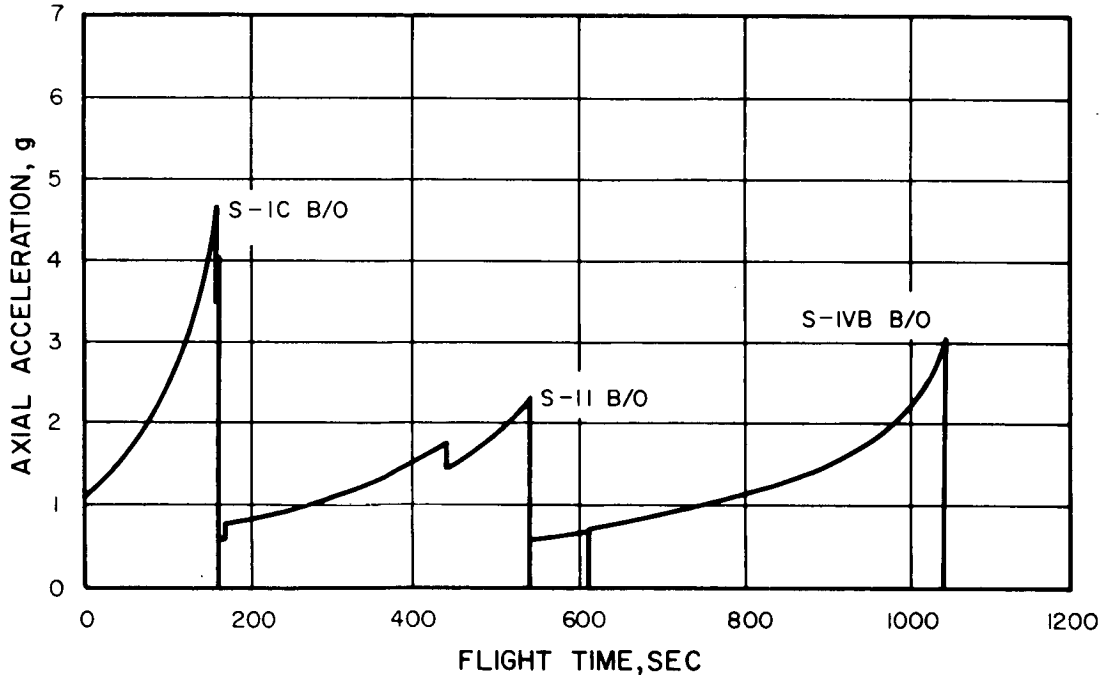

Figure 3-3. Trajectory Data for Saturn V Launch Vehicle

3.1.2 DESIGN WINDS

The "design wind" used in determining launch load conditions is based on measurements at Cape Kennedy over a span of several years. The winds are typically specified by giving wind speed and wind shear as a function of altitude for different probability levels. The winds used for the Apollo payload are 95-percent probable wind speed values with associated 99-percent probable wind shear values. These probabilities are selected to give a high launch probability and an even higher probability of not having to abort a mission after a decision to launch has been made. The lower probability for wind speed is acceptable because wind speed measurements can be made up until a few hours before launch, whereas wind shear measurements are not as easily obtained.

Using the wind speed and shear profile shown in Figure 3-4 and the vehicle trajectory to relate altitude and time, a wind history can be constructed, as shown in Figure 3-5. In this figure, a rectangular gust has been superimposed at the time of peak wind speed. Because the largest shears and gust values are unlikely to occur at the same time, reduced gust and shear values are used to obtain the profile used for design purposes.

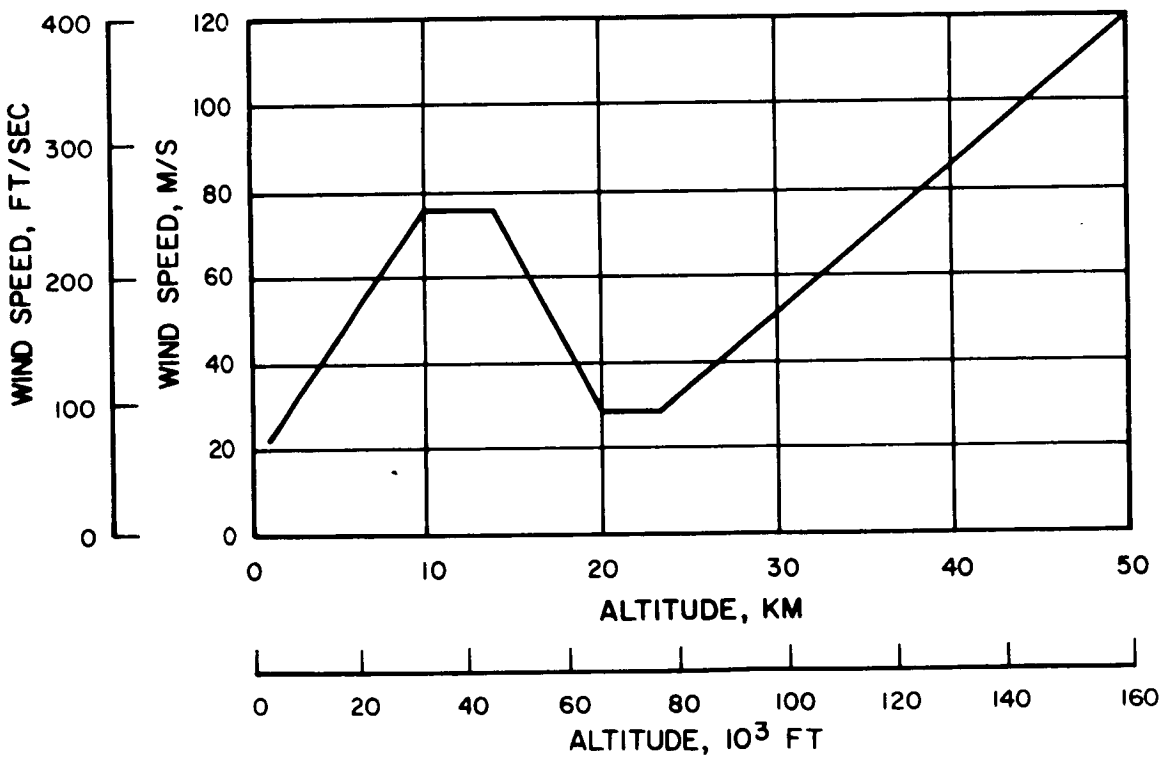

Figure 3-4. Design Wind Speed

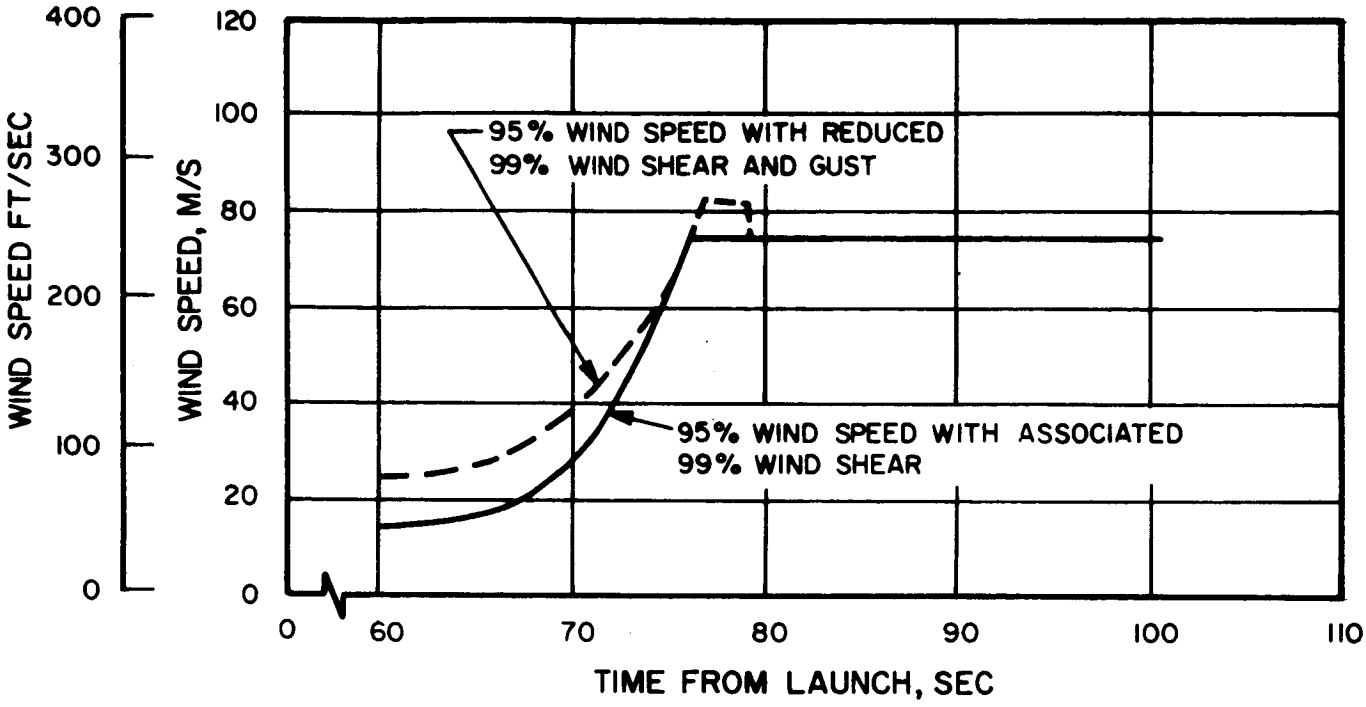

Figure 3-5. Synthetic Wind Profile

Because wind speeds are seasonal, it is possible to obtain alleviation of the wind condition by restricting the launch to certain dates. This is illustrated by Figure 3-6, which shows the probability that the design wind will not be exceeded during any month. Restriction of the launch date to the three most favorable months, July, August, and September, permits a reduction in the 95-percent probable wind speed from 246 feet per second (75 meters per second) to 95 feet per second (28 meters per second). Or, as an alternate philosopy, the reduction in design wind speed can be obtained at the expense of a reduced probability of launch opportunity.

3.1.3 ATTITUDE CONTROL SYSTEM EFFECTS

The launch vehicle attitude control system has an important role in determining structural loads. The primary objective of the control system is to maintain a prescribed flight path with minimum drift. However, the design of the control system must also consider the reduction of structural loads. Because the thrust contribution to vehicle bending moment is of the same order of magnitude as the aerodynamic contributions, a trade-off must be made in

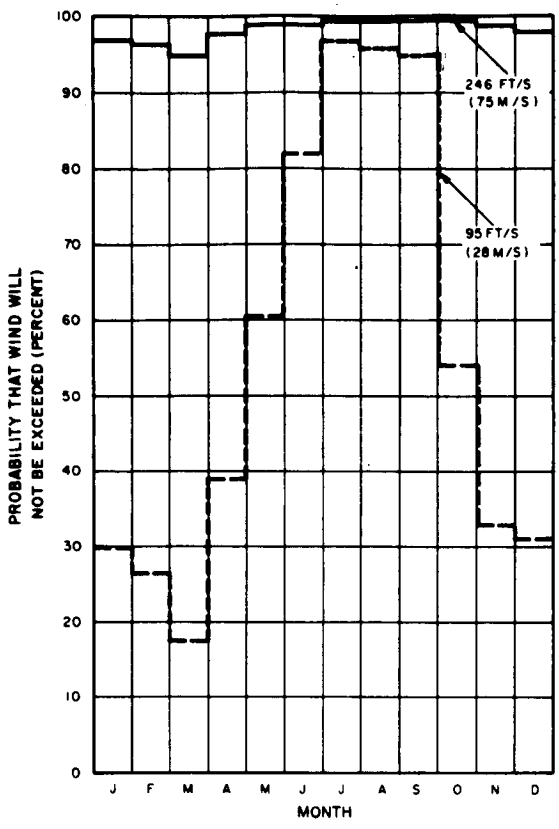

Figure 3-6. Launch Restrictions of Reduced Design Wind

selecting the control law. This is illustrated by Figure 3-7, which shows the bending moment at two stations on the Saturn V for increasing accelerometer gain. The accelerometer gain has been normalized by expressing it as a ratio of the gain for minimum drift. Increasing the accelerometer gain decreases the angle-of-attack while increasing the gimbal angle. Hence, a reduction in bending moment at station 30 is obtained at the expense of increased bending moment at station 10. The selection of the optimum gain must consider the structural design and the penalties involved at both vehicle stations.

Much of the current effort in improving control systems is directed toward development of "adaptive" systems. Typical of these is the "Switched Integral Controller" (Reference 3-3), shown by block diagram in Figure 3-8. In this system, the control law adapts to the magnitude of the wind. When the wind exceeds a predetermined value, the system switches from minimum drift to "load minimum" control, which reduces the bending moment at the expense of drift, by turning the vehicle to fly into the wind.

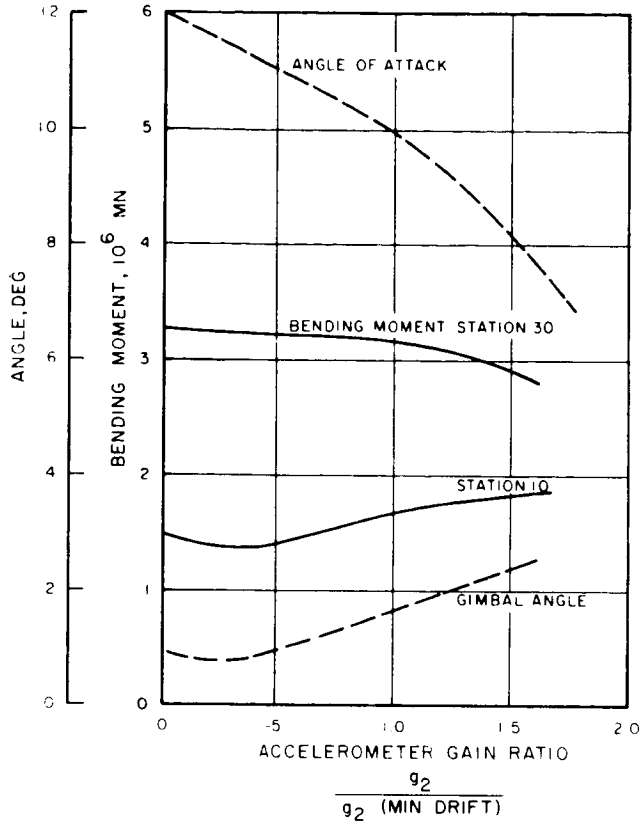

Figure 3-7. Effect of Accelerometer Gain on Vehicle Bending Moment

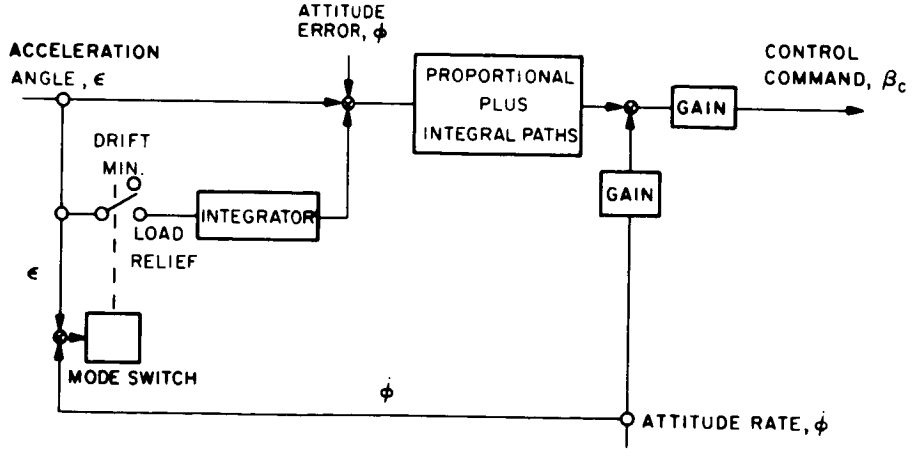

Figure 3-8. Block Diagram for Switch-Integral Controller

In addition to considering the rigid body dynamics of the launch vehicle, the design of the control system must also account for elastic effects. The dynamic bending modes of the launch vehicle are of concern, not only because they can cause control system instability, but they also contribute significantly to vehicle bending moments if they are not properly stabilized. If the elastic effects can be identified, the gimbal angle can be programmed to damp the oscillations. To do this requires a knowledge of the bending mode shapes and frequencies of the launch vehicle and payload.

It is apparent that the control system must be tailored to meet the requirements of a particular payload and mission. A proper determination of launch loads for payloads beyond Apollo should account for the optimization and possible improvements of the control system. Additional information on the load relief aspects of launch vehicle control systems can be obtained from References 3-4 through 3-8.

3.2 MAXIMUM "$q\alpha$" CONDITION

The condition resulting in the highest bending moment on the launch vehicle during powered flight occurs when the product of dynamic pressure and angle-of-attack is a maximum. This condition produces the critical launch loads on unpressurized sections at the forward end of the launch vehicle. The maximum "$q\alpha$" generally occurs later than the time at which dynamic pressure is a maximum.

An analysis of the maximum "$q\alpha$" condition will be shown, using data applicable to an Apollo payload, for various payload shapes and sizes. From this analysis will be determined the maximum payload area suitable for use as a radiator that can be obtained on the Saturn launch vehicles. The analysis will also provide the maximum launch loads on the payload structure. Aerodynamic and inertia loads will be calculated separately so that the data can also be applied to flat panel radiator configurations where the loads are carried by separate structures. For structures that carry inertia loads only, the maximum acceleration condition, to be discussed later, will be critical.

3.2.1 AERODYNAMIC LOADS

Aerodynamic loads were computed for both the axial and lateral directions. Since empirical data departs from theory in the transonic range, wind tunnel data were used in preference to theoretical solutions.

The axial aerodynamic loads were computed using the drag coefficients shown in Figure 3-9. These data are derived from test data reported in Reference 3-9. The circled points for a cone-angle of 15 degrees are taken from Reference 3-10. The effects of nose bluntness are neglected, since Reference 3-11 shows the effect to be small in the transonic range for bluntness ratios up to 0.2. (Bluntness ratio is defined as the ratio of the diameter of the spherical nose segment at the station of tangency to the cone base diameter.)

Values of fore drag coefficient from Reference 3-11 are less than those shown in Figure 3-9; however, the Reference 3-11 data were obtained with sting-mounted cones rather than with cone-cylinders. Since shock formation at the base of the cone influences the entire shock pattern in the transonic range, data from these two configurations cannot be compared.

Axial aerodynamic loads for each launch vehicle are shown in Figures 3-10 and 3-11 as a function of half-cone angle and distance from the nose. By plotting the data this way, the figures can be used for any size radiator. Note that no increase in axial load is shown aft of the cone-cylinder intersection, indicating that friction drag on the cylindrical section has been neglected.

Lateral aerodynamic loads were determined using the method of Reference 3-12. This report describes an empirical method based on both theory and wind tunnel data. The data are presented in the form of a generalized loading function, involving the normal force coefficient slope, primarily for the convenience of aeroelasticians. However, by integration the forces can be found for each spherical, conical, or cylindrical section. The results are shown in Figures 3-12, 3-13, and 3-14 for the three launch vehicles. Note that for the conditions associated with the Saturn IB vehicle, a pronounced reversal of loads occurs several diameters aft of the cone-cylinder intersection, resulting from shock formation at the corner. This reversal is not apparent at the conditions applicable to the Saturn V launch vehicle.

3.2.2 INERTIA LOADS

The mass distribution used to determine inertia loads is based on the arrangement of components shown in Figure 2-9. Reactor and shield masses are lumped and are assumed to be supported at the top of the radiator. Power conversion equipment is assumed to be supported at the junction between the conical and cylindrical sections of the radiator. This is a logical

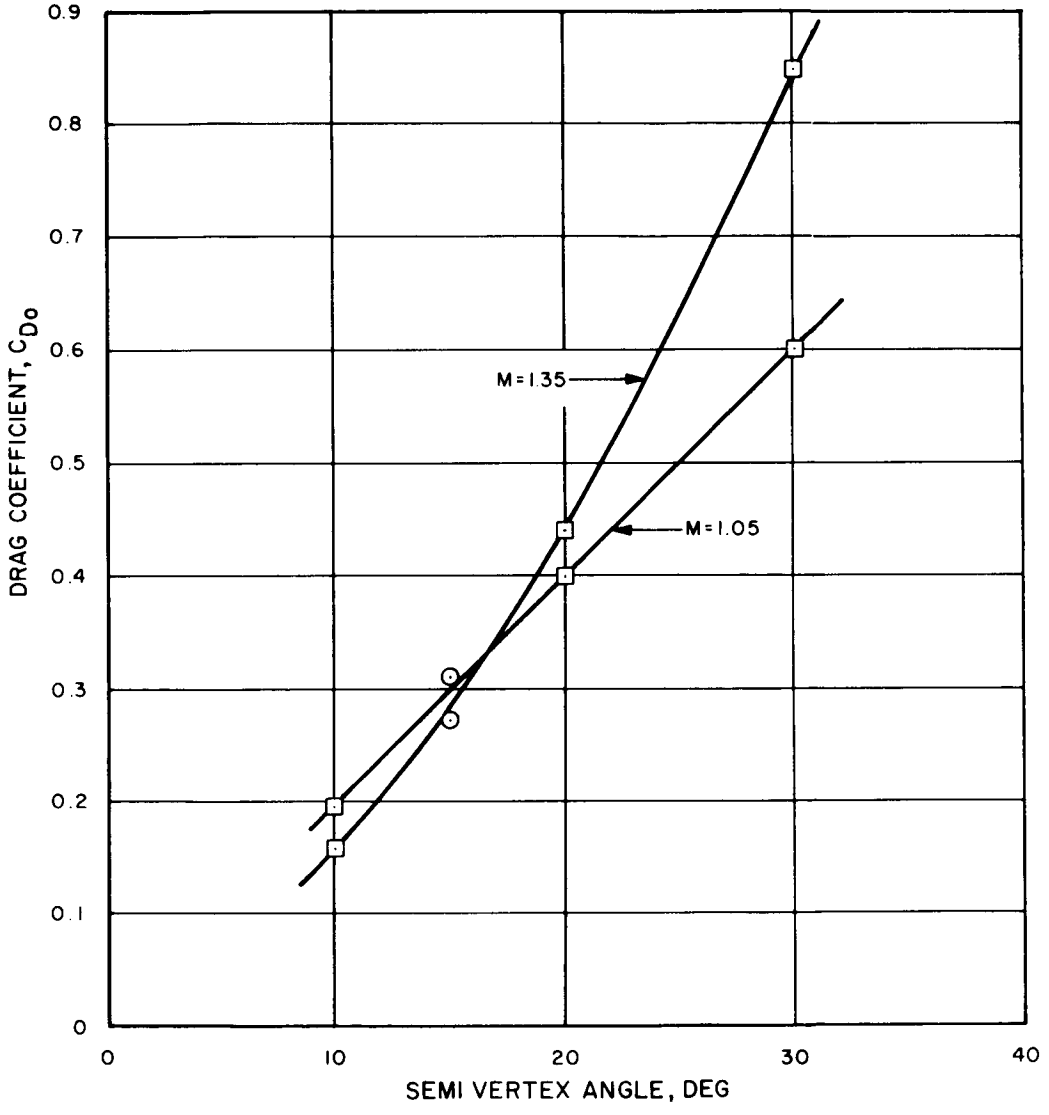

Figure 3-9. Drag Coefficient of Conical Head

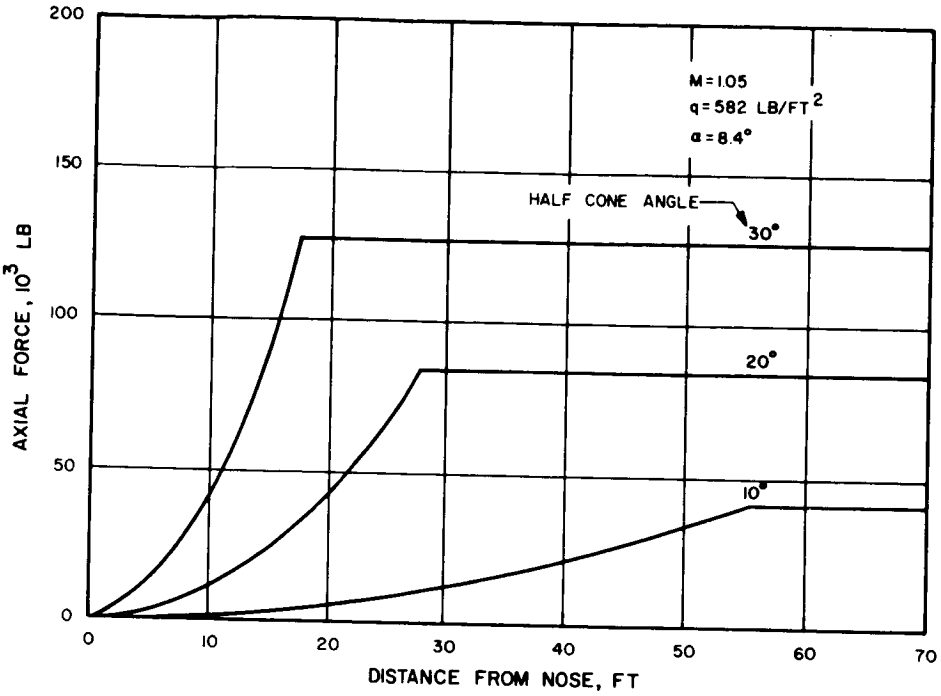

Figure 3-10. Axial Aerodynamic Load for Saturn IB Launch Vehicle

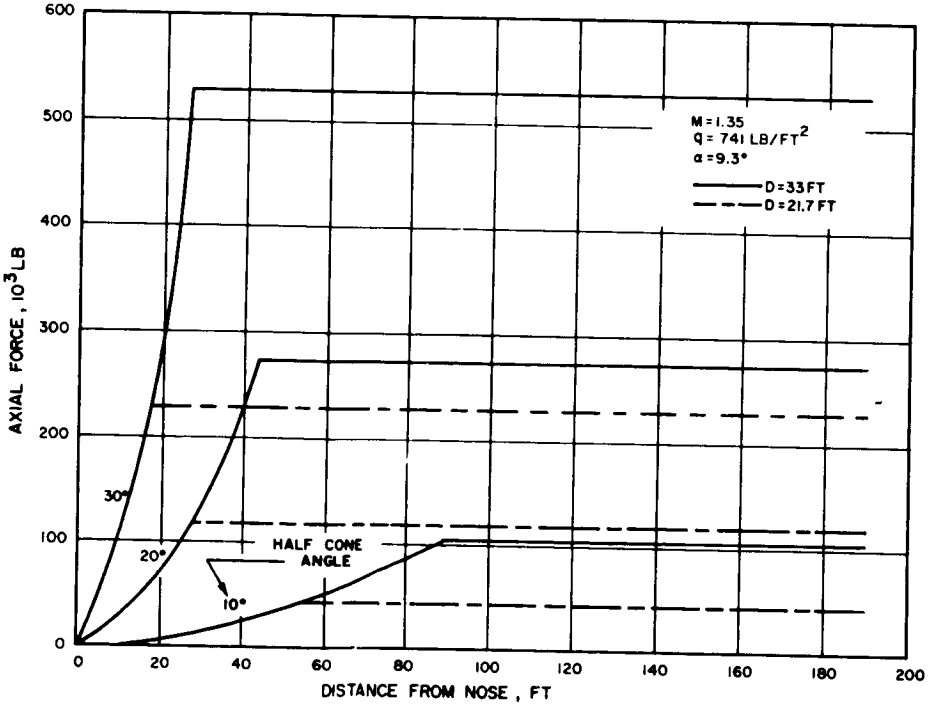

Figure 3-11. Axial Aerodynamic Load for Saturn V Launch Vehicle

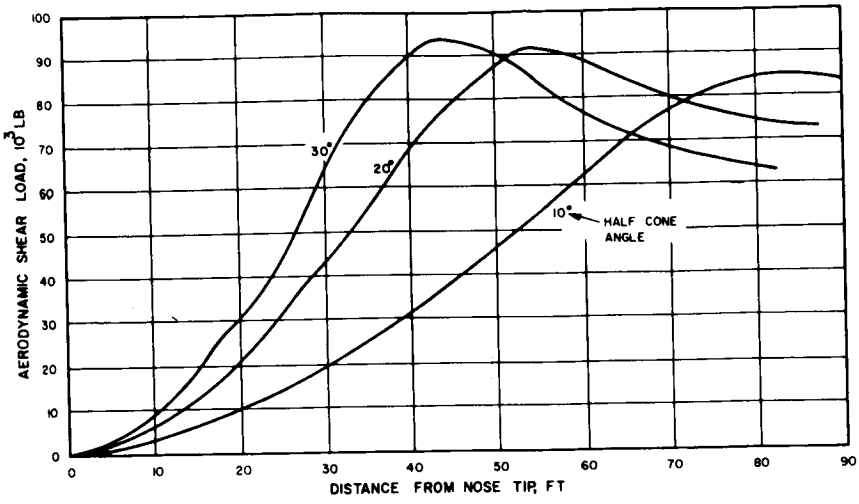

Figure 3-12. Aerodynamic Shear for Saturn IB Launch Vehicle

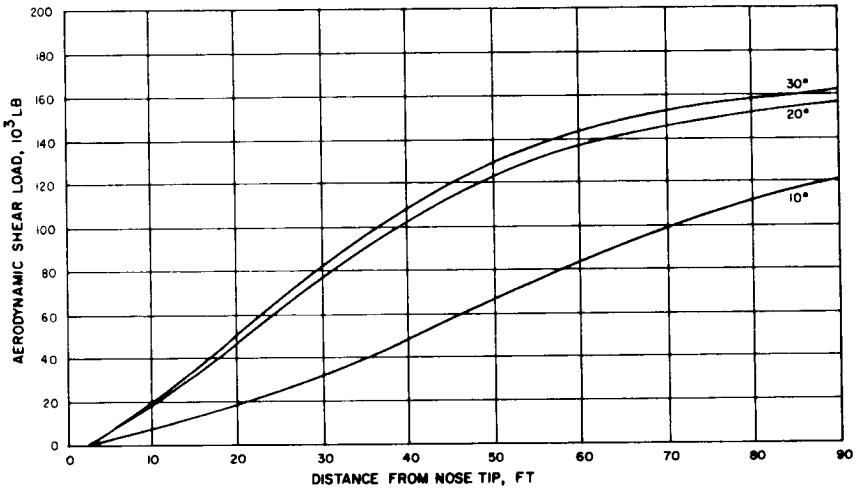

Figure 3-13. Aerodynamic Shear for Saturn V Launch Vehicle (Three-Stage)

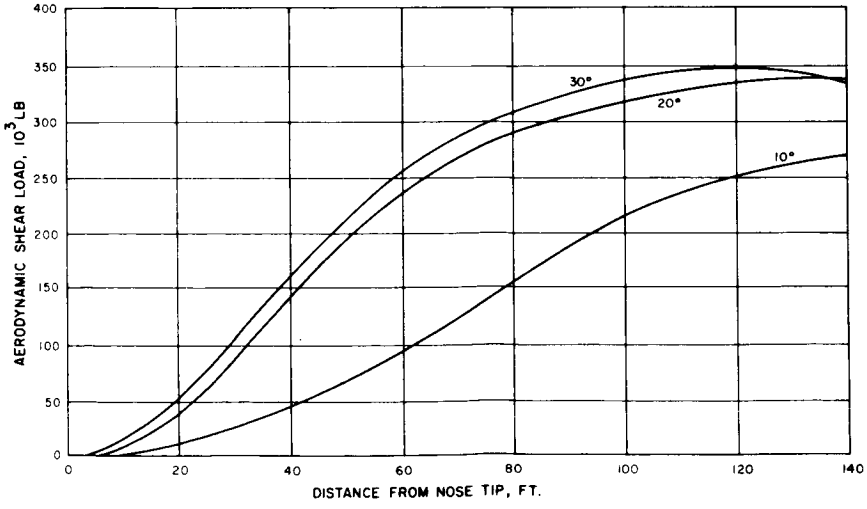

Figure 3-14. Aerodynamic Shear for Saturn V Launch Vehicle (Two-Stage)

support point since it is a junction between bays and will require a stiffening ring to withstand "kick" loads as well as to support circumferential header lines. Radiator mass is assumed to be uniformly distributed along its length. The remainder of the payload mass is assumed to be located near the base of the radiator and supported directly by the booster interface.

The masses used in the analysis are taken from the Navigator Studies, using the 1.2 Mw_e spacecraft on a 21.7-foot-diameter launch vehicle (the Saturn IB and the three-stage Saturn V) and the 4.8 Mw_e spacecraft on a 33-foot-diameter launch vehicle (the two-stage Saturn V), summarized in Table 3-2. These spacecraft are representative of Potassium-Rankine power systems, using beryllium radiators, for unmanned interplanetary probe missions. However, the mass distribution would not be significantly different for vehicles using other nuclear power systems and technologies. In any event, it will be seen that the inertia loads are much less significant than the aerodynamic loads at the maximum "$q\alpha$" condition.

TABLE 3-2. MASS SUMMARY FOR NUCLEAR SPACECRAFT

SYSTEM	MASS (10^3 LB)	
	SPACECRAFT "A"	SPACECRAFT "B"
Reactor and Shield	6.8	14
Power Conversion Equipment	9.8	41
Radiator	9.4	40
Payload (remainder)	65.5	147
Total	91.5	242

* Spacecraft "A" is 1.2 Mw_e for launch on three-stage Saturn V, and Saturn IB; Spacecraft "B" is 4.8 Mw_e for launch on two-stage Saturn V.

The axial and lateral inertia loads are derived by multiplying the mass distribution by the appropriate load factors. The results are shown in Figures 3-15 and 3-16. For spacecraft longer than the reference spacecraft, the radiator mass was assumed to continue as a linear distribution at the same rate.

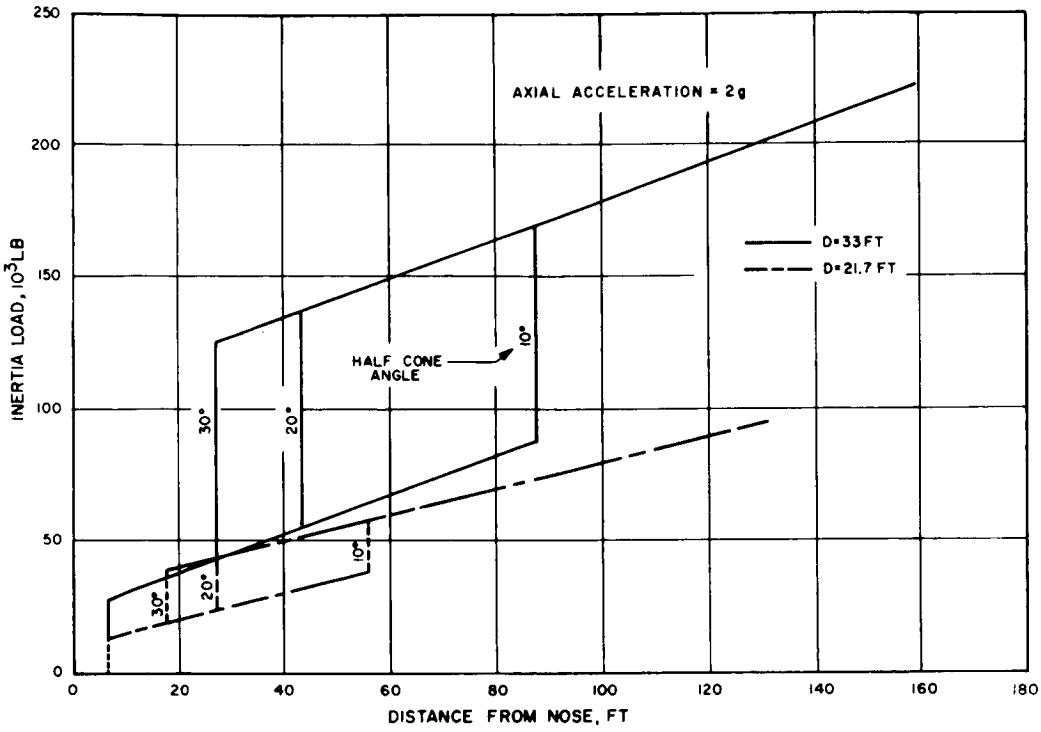

Figure 3-15. Axial Inertia Loads

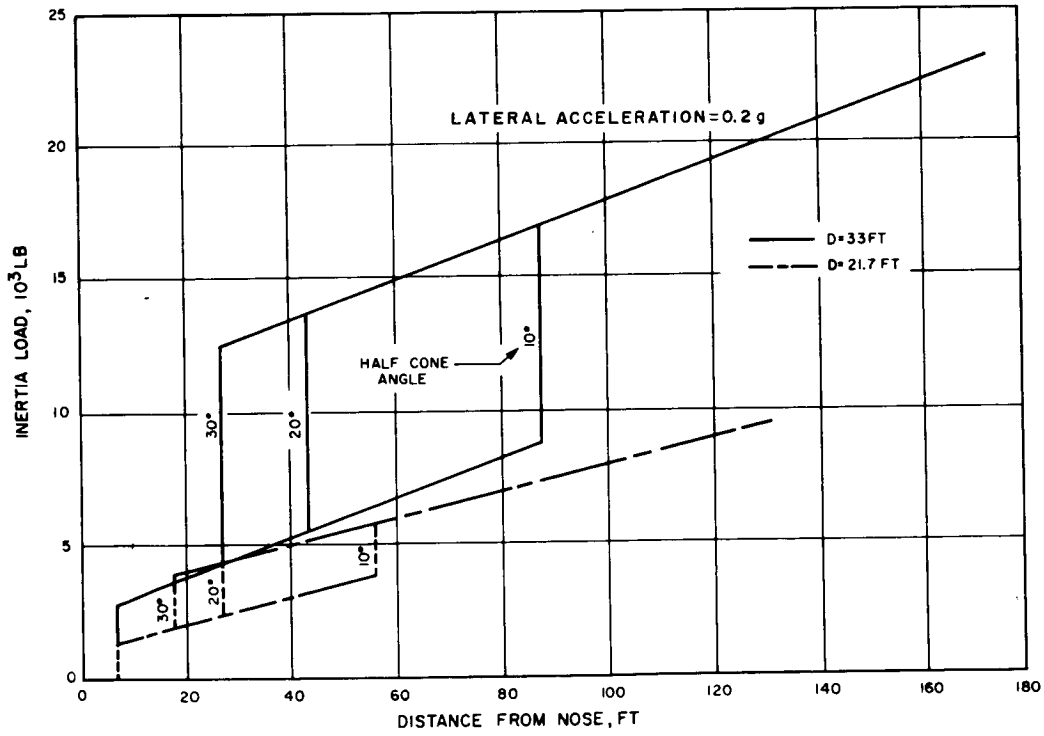

Figure 3-16. Lateral Inertia Shear Load

For simplicity, no account was taken for the variation in shield weight with radiator geometry in determining the inertia loads. For the conical radiator, this is a secondary effect since the aerodynamic loads are more significant. The shield weight used represents an average value. For the flat panel radiator, it has been shown that the shield weight is relatively insensitive to radiator geometry so that use of an approximate shield weight is acceptable.

3.2.3 DESIGN INFLUENCE OF COMBINED LOADS

To determine the loads for a conical radiator and the loads that the launch vehicle will see, it is necessary to combine the aerodynamic and inertia loads. Figures 3-17 through 3-22 show the combined axial and shear loads for the three launch vehicles. Integrating the shear loads gives the bending moments shown in Figures 3-23, 3-24, and 3-25.

The axial and bending components are then combined to give an equivalent axial load using the following relation:

$$P_{eq} = P_{axial} + 4M/D$$

where

P_{eq} = equivalent axial load
P_{axial} = axial load
M = bending moment
D = diameter

The results are shown in Figures 3-26, 3-27, and 3-28.

It should be noted that the loads derived in the preceeding analysis apply above the launch vehicle interface. The loads seen by the launch vehicle structure are obtained by adding to these loads the inertia contribution of the scientific payload mounted directly on the launch vehicle interface. (The term "scientific payload" is here intended to include all of the payload weight other than the powerplant). For example, consider a Saturn V launch vehicle having a total payload weight of 100,000 pounds, of which 25,000 pounds is the powerplant. The inertia contribution of the scientific payload would be 2 x (100,000-25,000) = 150,000 pounds. If the powerplant length is 77 feet and the radiator half-cone angle 10^o then from Figure 3-27, the equivalent axial load at the base of the radiator is 772 x 10^3 pounds. The load on the launch vehicle would then be 150,000 + 772,000 = 922,000 pounds

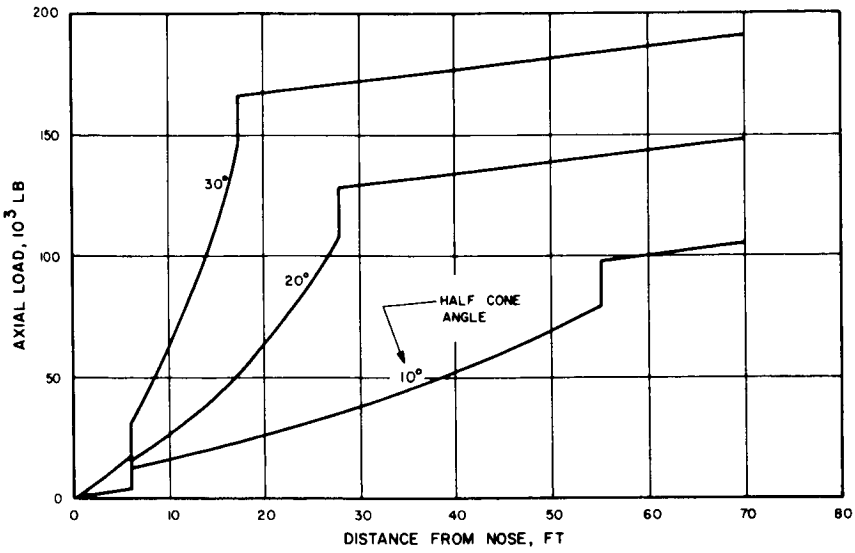

Figure 3-17. Combined Axial Load, Saturn IB Launch Vehicle

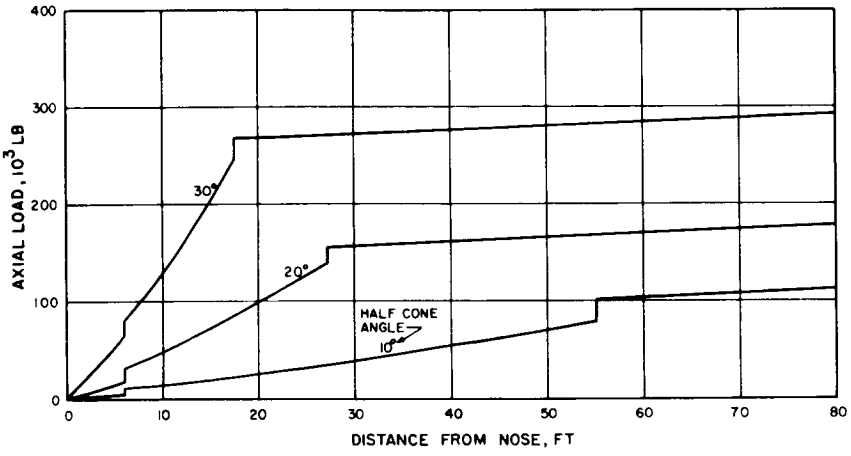

Figure 3-18. Combined Axial Load, Saturn V Launch Vehicle (Three-Stage)

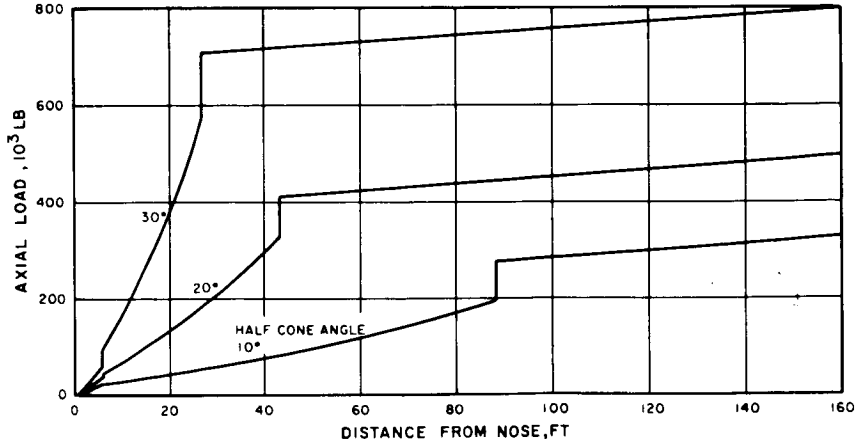

Figure 3-19. Combined Axial Load, Saturn V Launch Vehicle (Two-Stage)

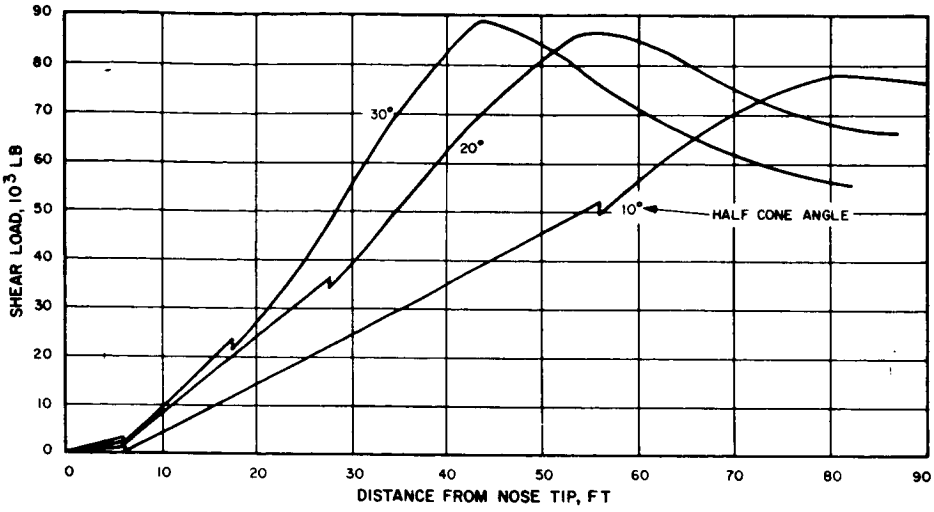

Figure 3-20. Combined Shear - Saturn IB Launch Vehicle

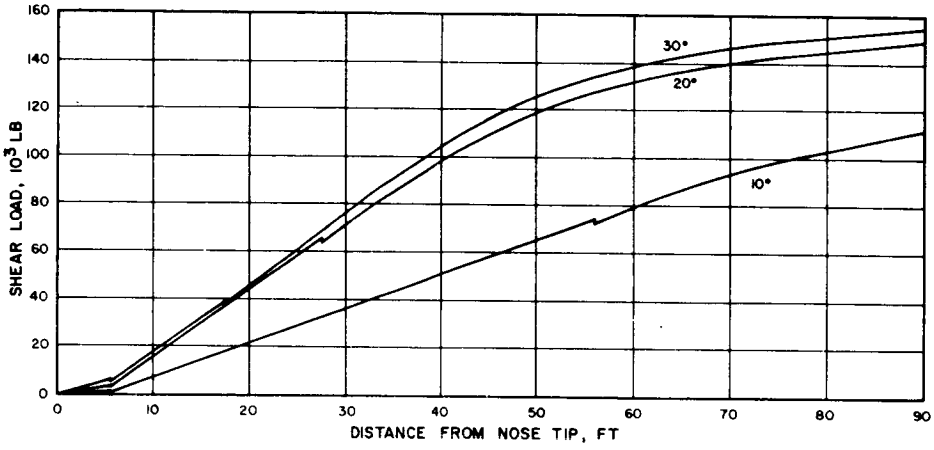

Figure 3-21. Combined Shear - Saturn V Launch Vehicle (Three-Stage)

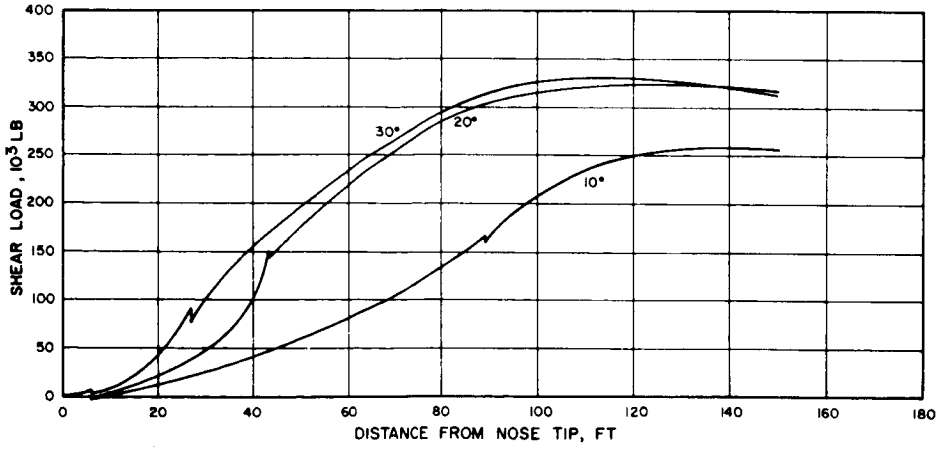

Figure 3-22. Combined Shear - Saturn V Launch Vehicle (Two-Stage)

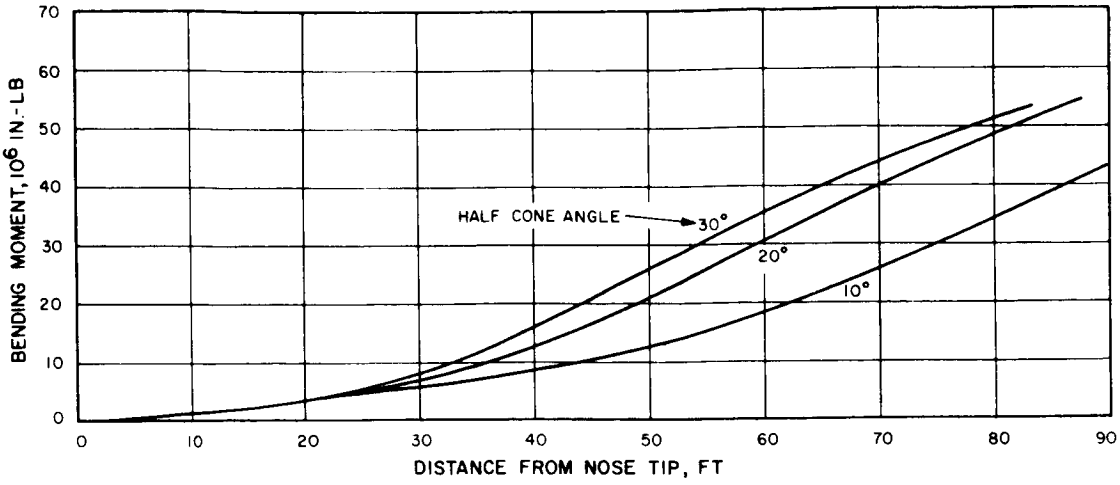

Figure 3-23. Bending Moment - Saturn IB Launch Vehicle

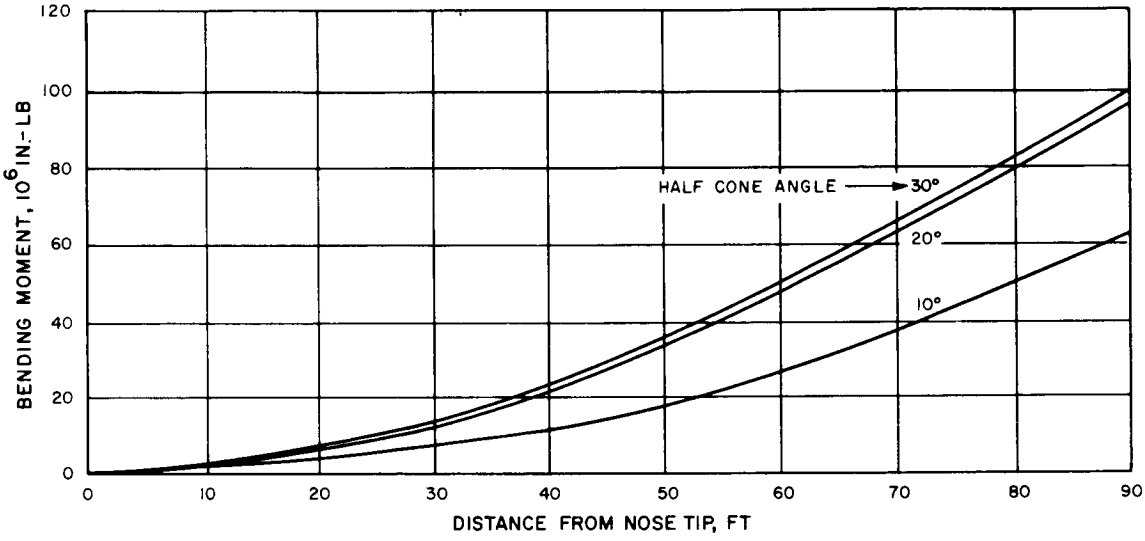

Figure 3-24. Bending Moment - Saturn V Launch Vehicle (Three-Stage)

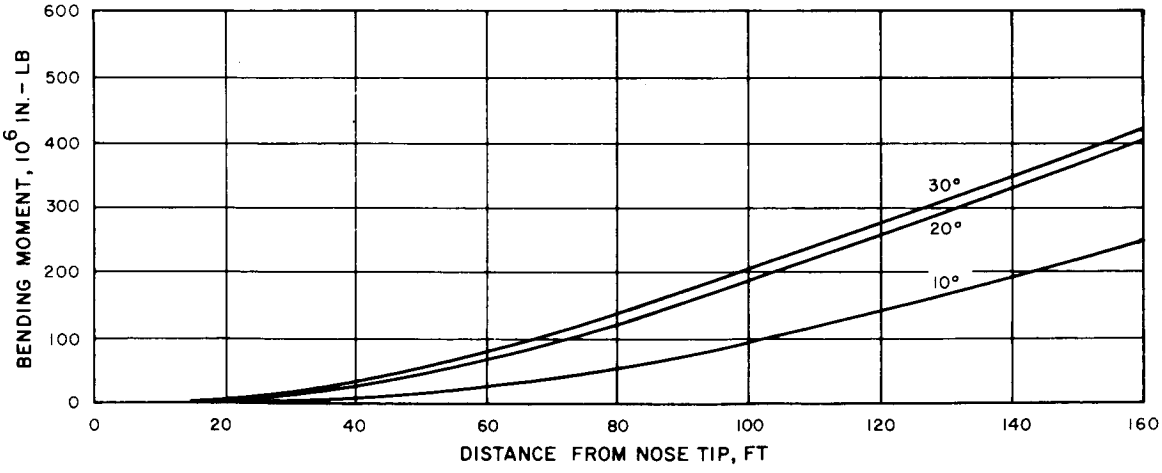

Figure 3-25. Bending Moment - Saturn V Launch Vehicle (Two-Stage)

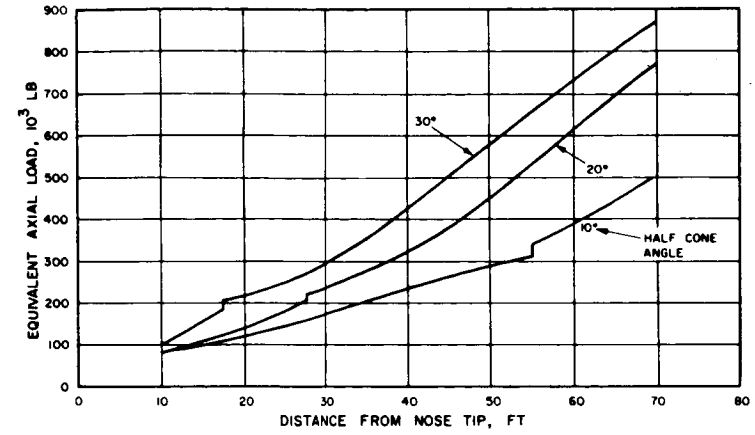

Figure 3-26. Equivalent Axial Load - Saturn IB Launch Vehicle

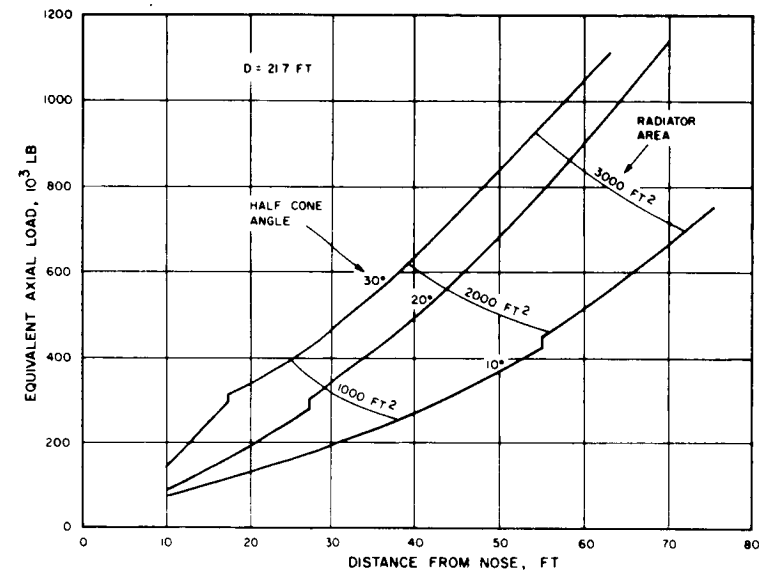

Figure 3-27. Equivalent Axial Load - Saturn V Launch Vehicle (Three-Stage)

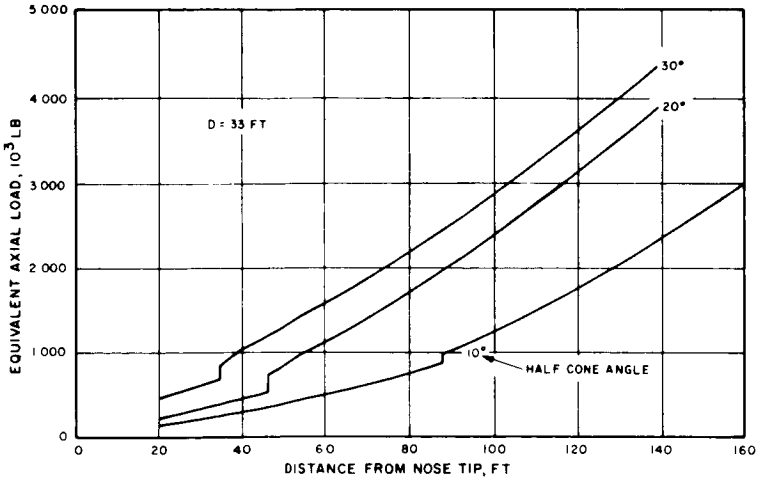

Figure 3-28. Equivalent Axial Load - Saturn V Launch Vehicle (Two-Stage)

which equals the structural capability of the S-IVB stage. For a given structural capability of the launch vehicle, therefore, there is a limiting combination of radiator size and scientific payload weight.

The structural capabilities of the Saturn launch vehicles for manned mission, as limited by the forward skirt sections of the upper propulsion stages are as follows:

Saturn IB	497×10^3 pounds
Saturn V, three-stage	823×10^3 pounds
Saturn V, two-stage	3070×10^3 pounds

The design loads for the S-IVB stage are from Reference 3-15, and for the S-II Stage from Reference 3-16. These stages are designed for manned missions, requiring a factor of safety of 1.40. The launch vehicle is capable of carrying a 12% higher load for unmanned missions, since for these missions a factor of safety of only 1.25 is required. These factors apply only to the launch vehicle and not to the payload section.

Using the launch vehicle structural capabilities for unmanned missions, and relating the allowable load on the radiator to radiator size (cone angle and length) by Figures 3-26, 3-27 and 3-28, the radiator area can be determined as a function of scientific payload weight. This relation is shown for the three launch vehicles in the upper right quadrants of Figures 3-29, 3-30, and 3-31. It can be seen that the largest radiator area is obtained seemingly contradictorily, with the smallest cone angle. This results from the greater length of powerplant permitted by the more favorable aerodynamic characteristics of the smaller angle.

The other three quadrants in Figures 3-29, 3-30, and 3-31 are graphical aids to relate the radiator area to electrical power, powerplant weight and the total payload launch weight. As an illustration, consider the following example for the three-stage Saturn V shown in Figure 3-30. Assuming that a scientific payload of 75,000 pounds is required, the maximum radiator area permitted by the launch vehicle structural capability is 3200 square feet with a 10° half-cone angle. The heat rejection rate from a $1200^{\circ}F$ radiator with a fin efficiency of 0.82 and an emissivity of 0.9 is 2.8 kW/ft^2, shown by the dashed line in the upper left quadrant. This shows that a maximum of 9.0 MW_t can be rejected. For a 11.5% system

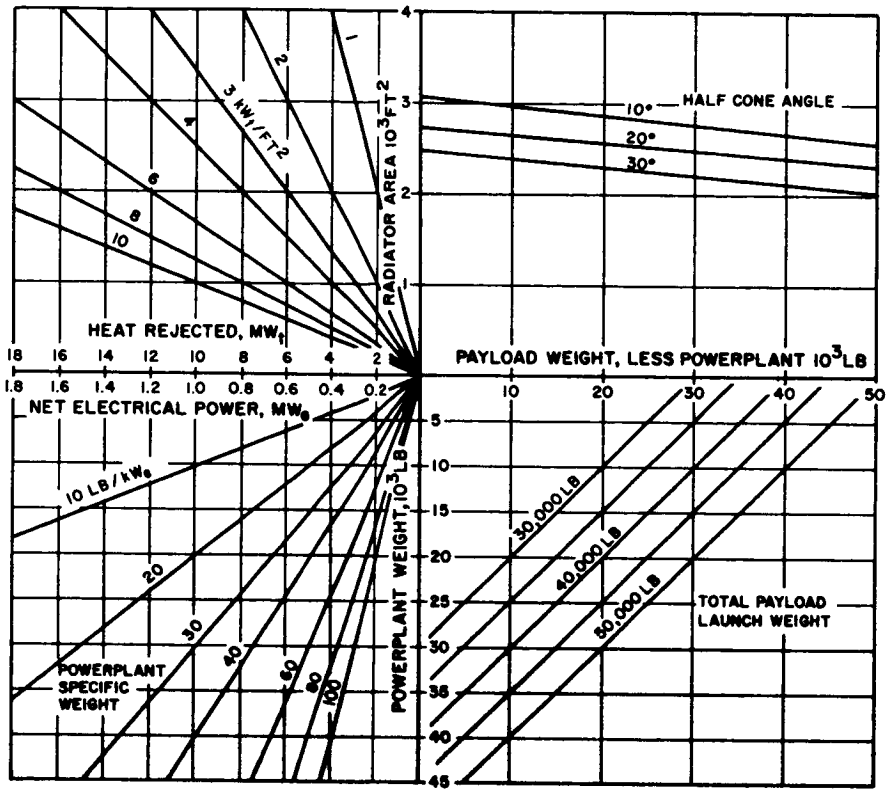

Figure 3-29. Radiator Area Capability of Saturn 1B

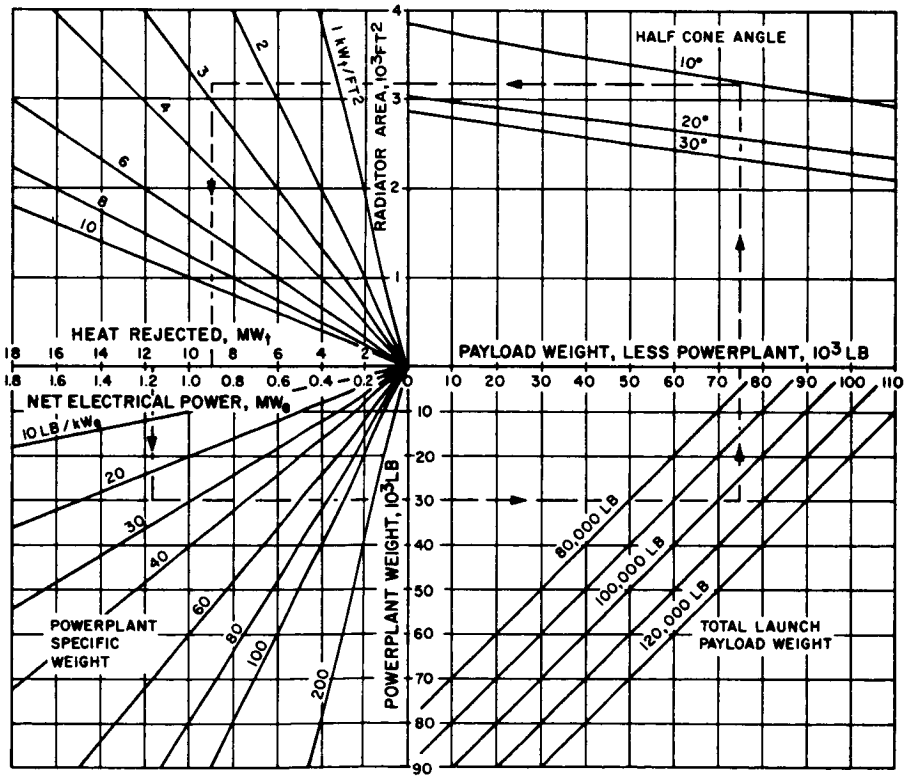

Figure 3-30. Radiator Area Capability of Three-Stage Saturn V

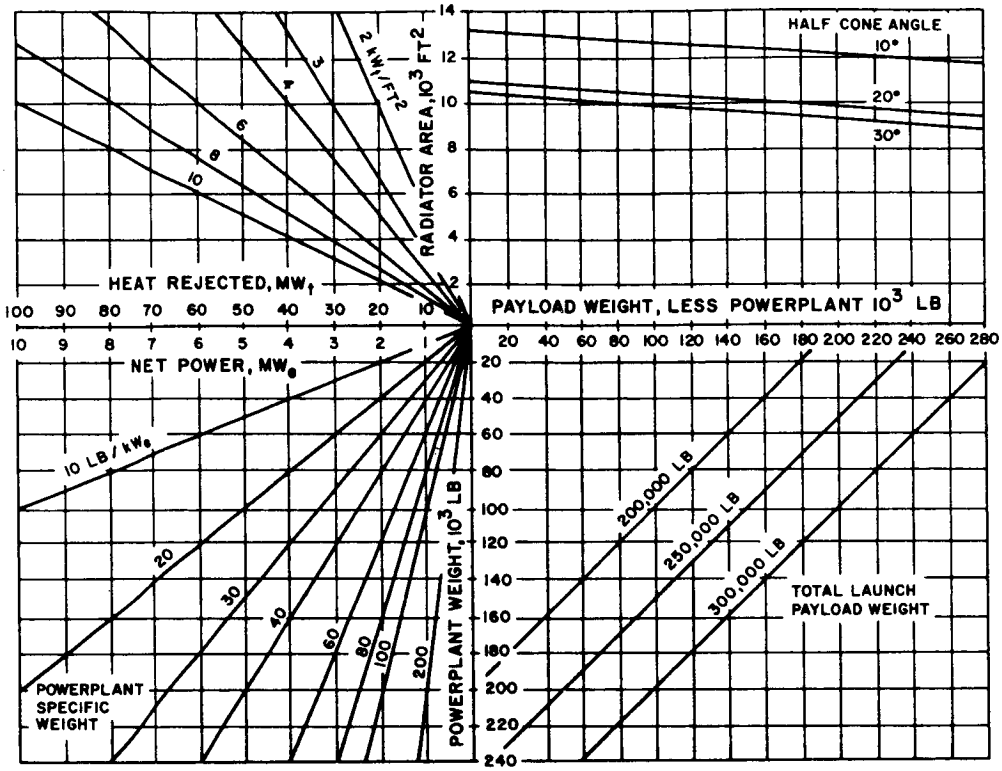

Figure 3-31. Radiator Area Capability of Two-Stage Saturn V

efficiency, the ratio of net electrical power to heat rejected is 0.13, therefore, by moving left on the horizontal scale by the factor 1.3, the net electrical power will be 1.17 MW_e. At a specific weight of 25 lb/kW_e, typical for a Potassium-Rankine system with beryllium radiator, the powerplant weight will be 29,000 pounds. Adding the 75,000 pound scientific payload, the total payload launch weight is 104,000 pounds. If the launch vehicle capability to the desired orbit is only 100,000 pounds, then the payload is weight limited and the scientific payload or the electrical power must be reduced. If the launch vehicle capability is 110,000 pounds, then the spacecraft is area limited and the effective temperature of the radiator must be increased (e.g. by increasing fin efficiency) or other sources of radiator area must be sought (e.g. upper stage utilization or deployment).

3.3 OTHER LOAD CONDITIONS

Although the major launch loads on the radiator occur at the maximum "$q\alpha$" condition, it was suggested earlier that other conditions may produce critical loads locally. The significance of these conditions can be determined only when the detail design of the radiator is

known. Of the many conditions, two warrant further discussion: the maximum axial acceleration condition, and the general category of dynamic response.

3.3.1 MAXIMUM AXIAL ACCELERATION CONDITION

Axial acceleration increases with flight time during launch, reaching a maximum at first-stage burnout. The condition is also known as "booster engine cut-off" (BECO). Figures 3-2 and 3-3 show that for the Saturn IB and Saturn V launch vehicles, the maximum accelerations are approximately 4.2 and 4.7 respectively. These accelerations occur at a time during the launch when dynamic pressure is negligible. At the altitude which has been reached by this time, lateral disturbances are greatly reduced so that attitude control oscillations and lateral accelerations are also insignificant.

Figures 3-29, 3-30, and 3-31 show the axial loads that result from the application of the maximum axial load factors to the mass distributions listed in Table 3-2. By comparing these loads with the corresponding equivalent axial loads in Figures 3-26, 3-27, and 3-28, it can be seen that the maximum "$q\alpha$" condition is the more critical.

The maximum axial acceleration condition is significant for structure which carries inertia loads only. Examples are the support structure for the power conversion equipment and scientific payload packages, and the support structure for the flat panel radiator.

For small payloads which are covered by an aerodynamic fairing, the maximum acceleration condition sometimes provides a basis for a qualification test to which the payload must be designed. This axial load factor may include additional factors to account for uncertainty and dynamic effects. A further conservatism often used is to specify a simultaneous lateral load factor based on the maximum lateral acceleration expected during launch. For large payloads, such as a typical nuclear powered spacecraft, this degree of conservatism would be intolerable.

3.3.2 VIBRATION RESPONSE

Significant loads in the radiator may result from response to dynamic excitation. The two sources of sustained excitation that are generally of major concern are aerodynamic buffeting and engine noise. Aerodynamic buffeting is of most concern when the payload shape is "dirty", as, for example, the Mercury and Apollo spacecraft, with their prominent escape towers.

The blunt nosed Gemini spacecraft was found to be equally efficient as a buffet generator (Reference 3-17). For configurations such as those assumed for a nuclear powered spacecraft, Figure 2-9, the aerodynamic shape is extremely "clean" and aerodynamic buffeting is not expected to be a major source of excitation.

Engine noise can be transmitted to the payload through the launch vehicle, and early in the launch, through the atmosphere. Being largely in the acoustic frequency range, the vibrations are rapidly attenuated. The significance of engine noise decreases with distance from the source so that it is not likely to be of major concern to the payload. In addition, the failure mode due to engine noise is fatigue. Unlike the sections of the launch vehicle which will expend part of their fatigue life during static firing tests, the payload will be subjected to engine noise only during actual launch.

Other sources of dynamic excitation are lift-off release loads, engine start, engine shutdown, stage separation, and fairing separation shocks. These impulses excite local, high-frequency responses. A typical amplitude-time measurement of this phenomenon would appear as a complex waveform composed of several high-frequency decaying sinusoids. Figure 3-32 shows the result of an analysis of the response to engine shutdown from Reference 3-18. It can be seen that the loads during the response do not exceed the peak acceleration at the time of engine shutdown.

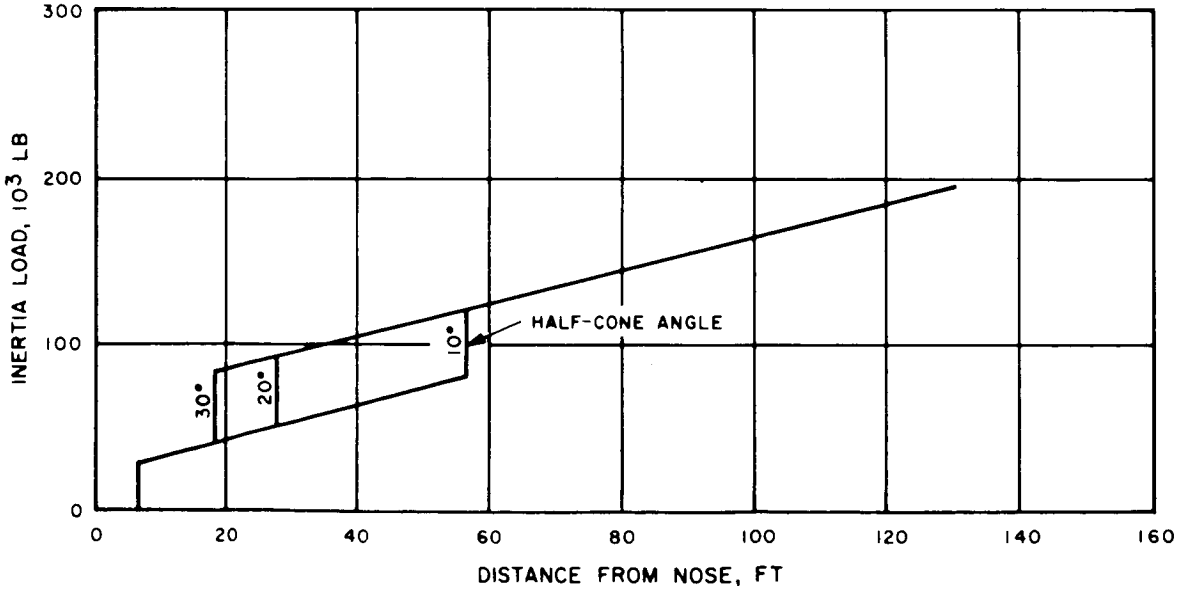

Figure 3-32. Axial Load at Engine Cut-Off - Saturn IB Launch Vehicle

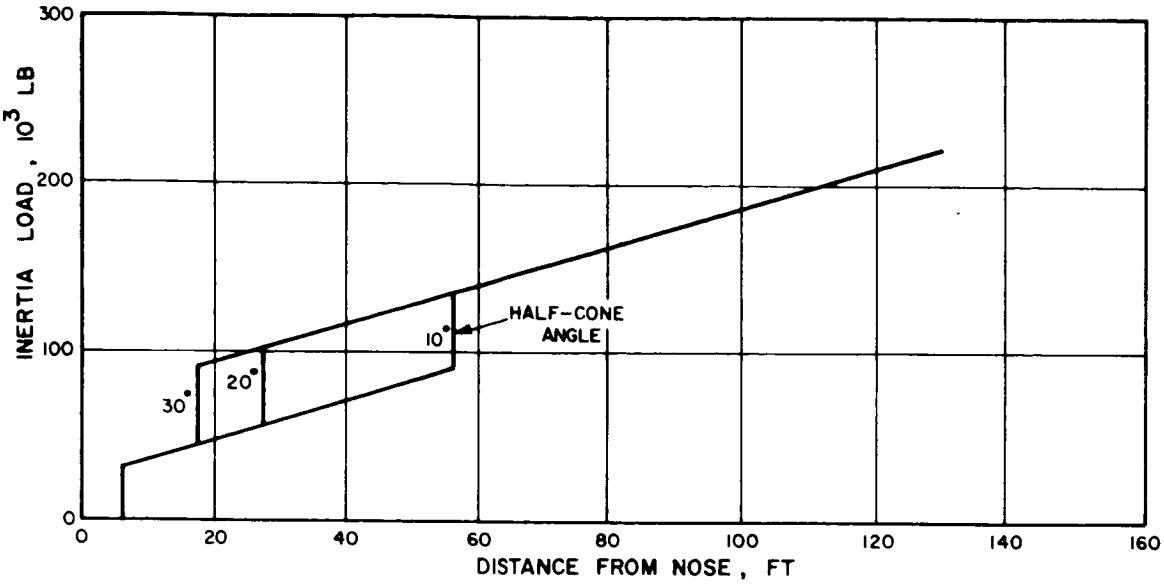

Figure 3-33. Axial Load at Engine Cut-Off - Saturn V Launch Vehicle (Three-Stage)

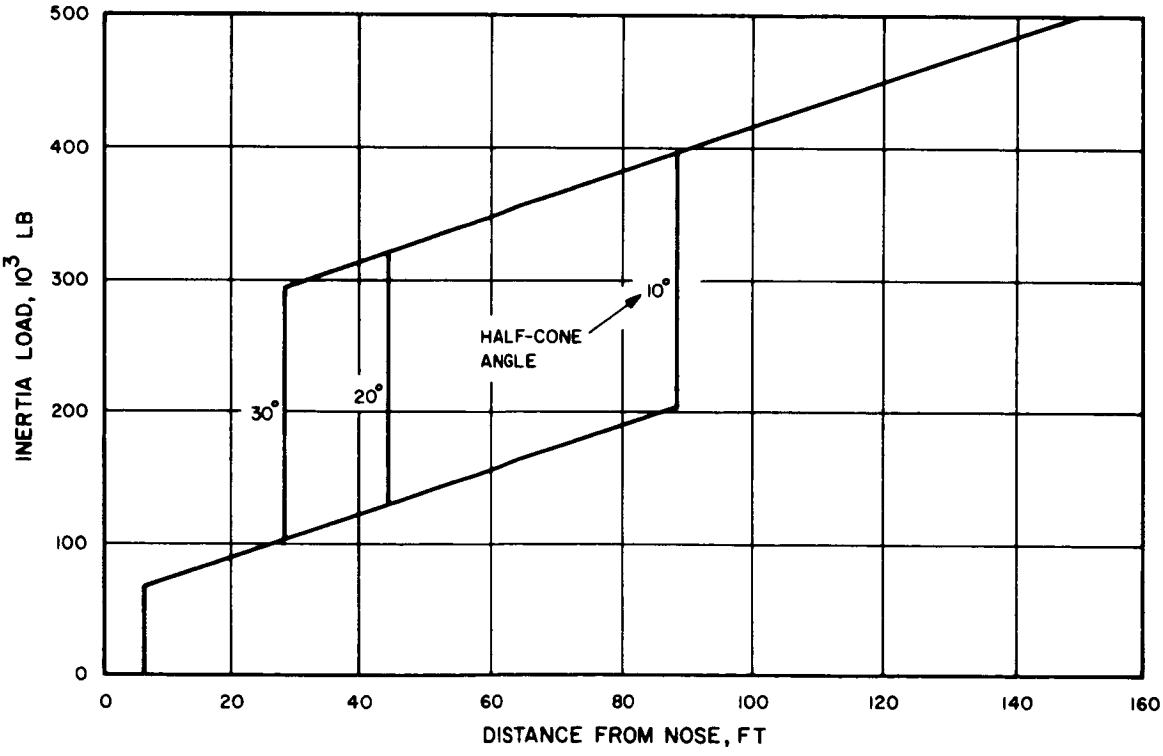

Figure 3-34. Axial Load at Engine Cut-Off - Saturn V Launch Vehicle (Two-Stage)

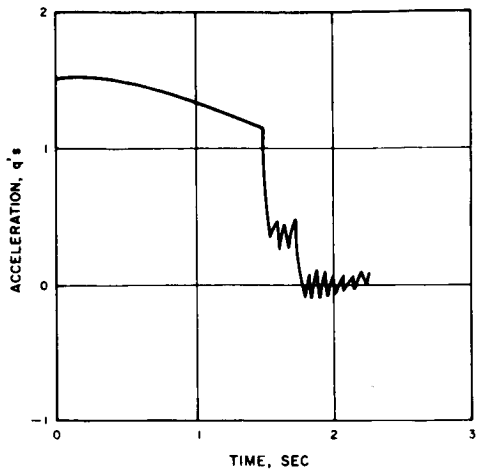

Figure 3-35. Centaur/Surveyor Interface Longitudinal Accelerations at Engine Shutdown

Aside from the actual dynamic environment that might be seen during launch, it is often necessary to design a payload to meet a dynamic environment as part of a qualification test. The levels for such a test are usually arbitrarily selected for convenience of test procedures, and conservatively envelope all conceivable environments that might occur during launch. In addition, the test duration is many times longer than anticipated periods of dynamic excitation during launch. Figures 3-33, 3-34, and 3-35 show the qualification levels for payloads mounted on the S-IVB stage, applicable to both the Saturn IB and three-stage Saturn V launch vehicles.

Having defined such an environment, there are several procedures for designing the payload structure to meet the requirements. The most convenient for design purposes is the static equivalent load concept (Reference 3-19). In this approach, an analysis of the system response behavior is used to determine a static equivalent load which will result in the desired lifetime. This approach was used to determine loads in a typical nuclear spacecraft configuration in Reference 3-20. A seven degree-of-freedom model as shown in Figure 3-36 was subjected to a longitudinal sinusoidal input, with appropriate assumptions as to damping coefficient. Figure 3-37 shows the transmissibility for mass m_1 (reactor and shield) as a function of frequency. Resonant modes can be identified at 65 cycles per second, 199 cycles per second, and 466 cycles per second. Peak response occurred at the first mode with a transmissibility of 23.1 for a median damping factor. The result was that critical loads

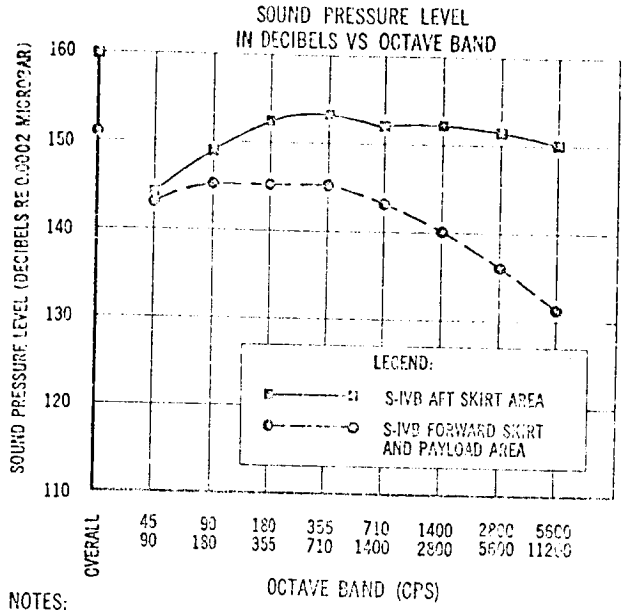

NOTES:
1. THE TIME DURATION IS ASSUMED TO BE EIGHTEEN MINUTES.
2. THE DIFFUSED SOUND FIELD OF RANDOM NOISE IS ASSUMED TO HAVE A GAUSSIAN AMPLITUDE DISTRIBUTION.

Figure 3-36. Design Specification for Acoustic Noise

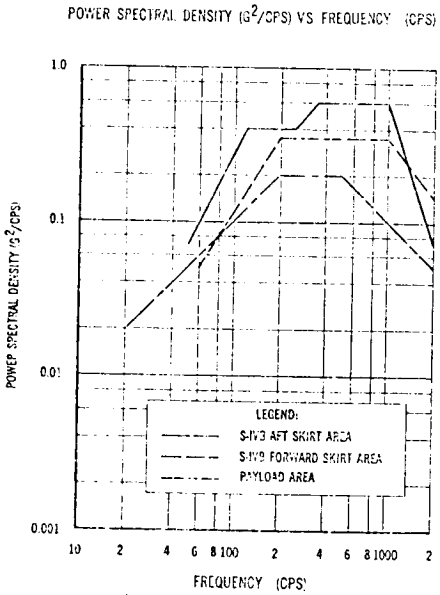

NOTES:
1. AMPLITUDE DISTRIBUTION IS ASSUMED GAUSSIAN.
2. DURATION IS ASSUMED TO BE TWELVE MINUTES FOR EACH OF THREE MUTUALLY PERPENDICULAR DIRECTIONS.

Figure 3-37. Design Specification for Random Vibration

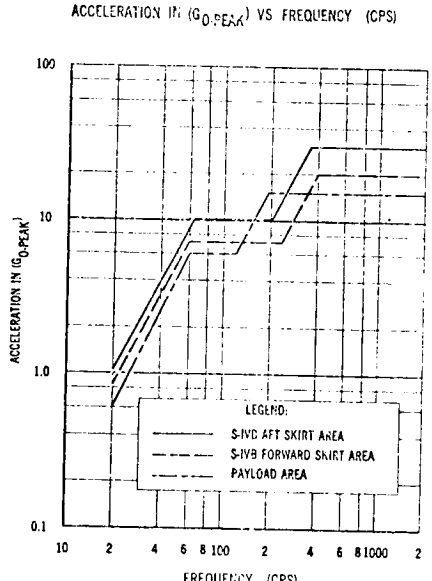

NOTES:
1. THE VIBRATION INPUT IS ASSUMED TO BE APPLIED IN EACH OF THREE MUTUALLY PERPENDICULAR DIRECTIONS.
2. THE LOGARITHMIC SWEEP RATE IS ASSUMED TO BE ONE OCTAVE PER MINUTE OVER THE FREQUENCY RANGE FROM 20 TO 2000 AND BACK TO 20 CPS.

Figure 3-38. Design Specification for Sinusoidal Vibration

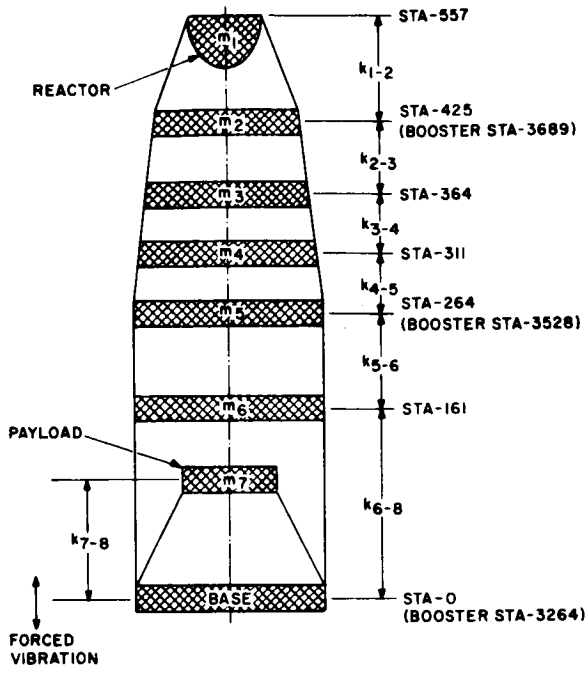

Figure 3-39. Seven Degrees of Freedom Dynamic Model

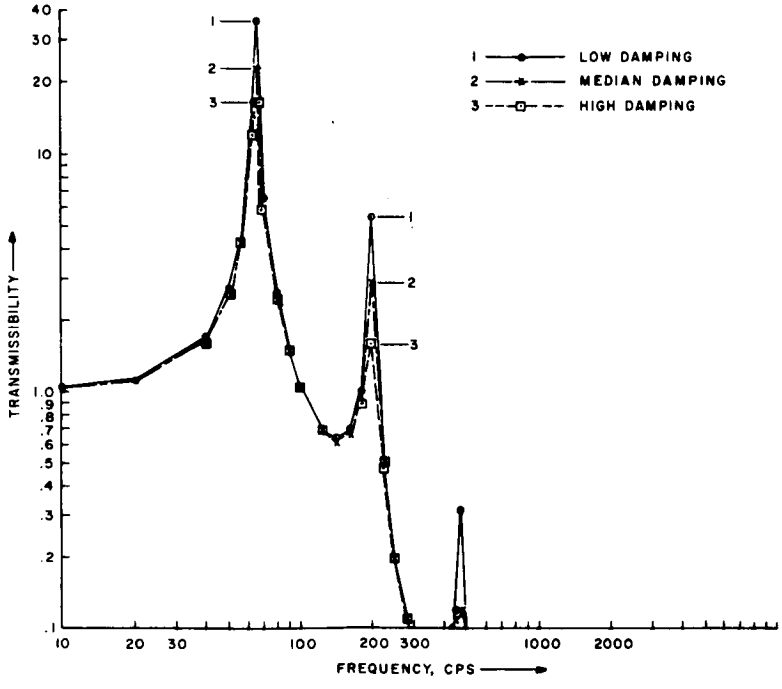

Figure 3-40. Transmissibility for m_1 of Seven Degrees of Freedom Model

were determined for the local support structure of the largest lumped mass (the reactor and shield) but the loads generally were less critical than the "static" launch loads at the maximum "q α" condition. The weakness in designing the payload to meet an arbitrary qualification dynamic environment is that it is overly conservative, and becomes increasingly unrealistic as the size of the payload becomes large with respect to the launch vehicle. The calculated response may unrealistically exceed the largest forcing function, the launch vehicle engine thrust. An enlightened test procedure is then to limit the shaker force during qualification test so that the payload response does not exceed a predetermined level, that level being the force that the launch vehicle is capable of exerting on the payload. Figure 3-38 shows the qualification test of the SNAP-10A system, as reported in Reference 3-21. Although the specified qualification level for the longitudinal axis between 9 and 400 cycles per second was 2.3g, the shaker input acceleration was reduced as each resonant frequency was approached. If the payload is designed conservatively to the static condition of maximum launch vehicle acceleration, critical loads will not be exceeded in such a dynamic test.

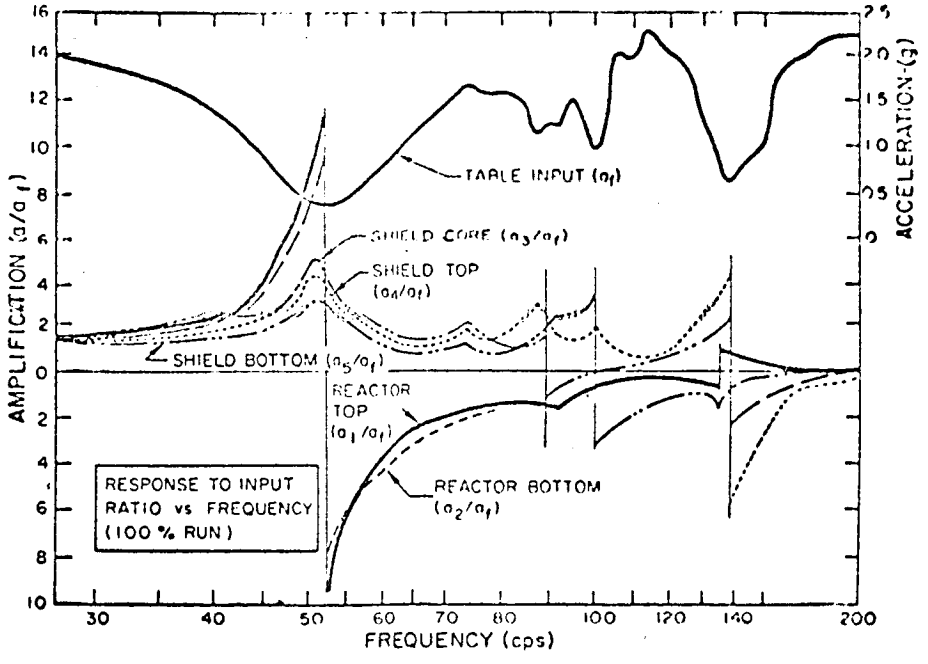

Figure 3-41. Qualification Test of SNAP-10A - Longitudinal Axis

For the design of local structure to a dynamic environment, the procedure is to avoid resonant frequencies where input levels are known to be high or where modes of the primary structure are excited. This detuning can often be accomplished only after a modal vibration test of the complete spacecraft has been conducted. The use of viscoelastic damping materials or fluid dampers may also be required.

However, these local concessions to the dynamic environment generally do not have a significant effect on the total spacecraft weight. The dynamic environment is often of concern when large flexible panels are present, not because of the stress level, but because of excessive deflections. Typical examples are the large solar array panels on Nimbus and Mariner spacecraft. Similar difficulties may arise with large, light weight, flat panel radiators.

For very large payloads, the practicality of designing to dynamic loads is limited by the facilities available for conducting a dynamic test to full design levels. Until recently, the largest vibration facility was the dual C-210 shaker installation at the General Electric Valley Forge Space Technology Center. This facility has a peak vector sine force of 50,000 pounds. It was used to test the Pegasus satellite, which, with its fixture, represented a mass of 10,700 pounds. At the time of this report, the Wyle Labs facility at Huntsville has shakers totaling 400,000 force-pounds which will be capable of testing a weight, including fixture, of 56,000 pounds. Maximum size capability is 33 feet in diameter and 60 feet in height. However, it can be seen that even this facility will not be capable of testing the largest payloads for the Saturn vehicles as a single unit.

It may be concluded that the loads due to dynamic response, although of major concern throughout the design and testing of a payload, do not lend themselves to parametric study for preliminary design purposes. If the radiator is designed to meet the maximum static load conditions, it will generally be adequate for the dynamic conditions.

3.3.3 PRELAUNCH LOADS

In addition to the loads occurring during launch, the radiator must be capable of withstanding the loads during transportation, handling and assembly. The usual philosophy is to make no compromise for prelaunch loads. Other than local fittings, the structure will be designed to mission associated environments only. This can be accomplished by requiring shock and vibration attenuating devices on the ground support equipment to limit the loads to those expected during launch.

A special case of prelaunch vibration loading which is frequently of concern is the on-pad ground wind condition. The phenomenon is that of launch vehicle bending in response to alternate vortex shedding by the vehicle in a lateral wind. Since the vehicle acts in a cantilever mode, large bending moments can occur at the base of the vehicle. The condition may be critical for structural design of the lower stages. Of primary concern to the payload are the large deflections that may occur, which must be accommodated by the umbilical tower swing arms. References 3-22 and 3-23 discuss how the problem has been resolved for the Saturn V launch vehicle by the use of external dampers.

3.4 REFERENCES

3-1. "Saturn IB Payload Planner's Guide," Douglas Report SM-47010, June, 1965.

3-2. "Saturn V Payload Planner's Guide," Douglas Report SM-47274, November, 1965.

3-3. "Study of Structural Bending Adaptive Control Techniques for Large Launch Vehicles - Summary Report," Autonetics, NASA CR 76055 and 76056, March 16, 1966.

3-4. Lovingood, J.A., Geissler, E.D., "Saturn Flight-Control Systems," Astronautics and Aeronautics, May, 1966.

3-5. Townsend, D., "A Method for the Determination of Control Law Effect on Vehicle Bending Moment," NASA TM X-53077.

3-6. Blair, J.C., Lovingood, J.A., Geissler, E.D., "Advanced Control Systems for Launch Vehicles," Astronautics and Aeronautics, August, 1966.

3-7. Klenk, W.J., "An Adaptive System for Load Relief and Accurate Control of Launch Vehicles," AIAA Paper 64-239, June, 1964.

3-8. Gates, Richard M., "A Study of Load Alleviating Control Systems for Large Launch Vehicles," The Boeing Company, Technical Summary Report, Contract NAS 8-11417, February, 1965.

3-9. Hoerner, Sighard F., "Fluid-Dynamic Drag," Published by the author, 1958.

3-10. Reese, H.B., "Results of an Experimental Investigation to Determine the Aerodynamic Loadings on Three Saturn Payload Shapes," NASA CR 74415, November 10, 1964.

3-11. Owens, R.V., "Aerodynamic Characteristics of Spherically Blunted Cones at Mach Numbers from 0.5 to 5.0," NASA TN D-3088, December, 1965.

3-12. Muraca, R.J., "An Empirical Method for Determining Static Distributed Aerodynamic Loads on Axisymmetric Multistage Launch Vehicles," NASA TN D-3283, March, 1966.

3-13. "Saturn IB Improvement Studies, Phase II," Douglas Report SM-51896.

3-14. "Saturn V Improvement Study - Final Summary Report," Boeing Report D5-13109, April, 1965.

3-15. Private Communication - H. Anderson, Douglas Missile and Space Systems Division, Huntington Beach, California.

3-16. Memo M-P and VE-SS-22, NASA-MSFC.

3-17. Callahan, J.A., "Structural Dynamic Aspects of the Gemini Program," AIAA/ASME Seventh Structures and Materials Conference, April, 1966.

3-18. Schuetti, R.H., et al., "Dynamic Loads Analysis of Space Vehicle Systems," NASA CR 76502, June, 1966.

3-19. Lifer, C.E., "An Analytical and Experimental Study of Procedures for Designing Structures for Vibration Environments," AIAA/ASME Seventh Structures and Materials Conference, April, 1966.

3-20. Larson, J.W., "Research on Spacecraft and Powerplant Integration Problems, Third and Fourth Quarterly Report," General Electric Document No. 64SD700, April, 1964.

3-21. "Structural Test on the Final SNAP-10A Prototype System (PSM-1A)," Atomics-International Report NAA-SR-9820, May, 1964.

3-22. Catherines, J.J. and Stephens, D.G., "Effectiveness of External Dampers for Attenuating Launch Vehicle Oscillations," Journal of Spacecraft and Rockets, December, 1966.

3-23. Jones, G.W. and Farmer, M.G., "Wind-Tunnel Studies of Ground-Wind Loads on Saturn Launch Vehicles," AIAA/ASME Seventh Structures and Materials Conference, April, 1966.

4. UPPER STAGE UTILIZATION

The analysis of launch loads in Section 3. has shown that for each launch vehicle there is a maximum radiator area limit for a non-deploying, cone-cylinder configuration. One approach to obtain more radiator area beyond this limit is to extend the radiator aft of the payload-launch vehicle interface. By utilizing the surface area of the upper stages, radiator area can be gained without increasing the overall launch vehicle height.

This section will discuss concepts for utilizing the upper stages of three launch vehicles; Saturn IB, three-stage Saturn V, and two-stage Saturn V. Since this study is related to large nuclear systems for missions in the next decade or later, detailed definition of these launch vehicles at this time is speculative. There are significant differences among the various launches of the same designation of launch vehicle, even for the presently defined Apollo Program. Post-Apollo Saturn launch vehicles will be tailored to specific mission requirements, and will likely be "uprated," "modified," or "improved" versions of the vehicles presently defined. The various Saturn improvement studies (References 4-1 and 4-2) indicate many possible choices for improvement. For the purpose of this study, standard Saturn launch vehicles as defined for the Apollo Program were assumed. For details that differ from one launch to another, a specific launch configuration was assumed as being typical. For example, the type, number and placement of antennas was based on vehicle SA-204 (Reference 4-3).

Since missions utilizing the Saturn V two-stage launch vehicle have yet to be planned, an Instrument Unit (IU) for this launch vehicle does not yet exist. However, it is reasonable to assume that a unit similar to the present IU will be used, designed to match the 33-foot diameter of the S-II stage. Externally, the differences will include elimination of the access door, since access is already provided in the forward skirt of the S-II. Umbilical connections for the 33-foot IU can be added to the swing arm on the Mobile Launcher (ML) that presently services the S-II forward skirt.

Two concepts for utilizing the area of the upper stages will be discussed:

a. Sheath type

b. Integral radiators

A sheath type radiator is one which fits down over the outside of stage aft of the payload, so that the stage can be used without modification. An integral radiator is one in which the functions of stage structure and radiator are combined. This may necessitate a major redesign and requalification of the stage, depending on how much of the stage structure is utilized.

4.1 SHEATH TYPE RADIATOR

The objective of a sheath type radiator is to gain additional radiator area aft of the payload interface on the launch vehicle without disturbing the launch vehicle stages. Ideally, any changes to the launch vehicle stages that might be required as a result of the influence of the radiator would be minor to the extent that requalification of the stage would not be necessary.

There are several problems inherent to the use of a sheath type radiator that can be discussed independently of the stage that is being covered.

Aerodynamically, the sheath type radiator has several adverse features. Because the radiator protrudes beyond the normal envelope of the launch vehicle, aerodynamic drag and normal loads will be increased. As an indication of the magnitude of this effect, a sheath extending 10 inches from the side of a 260-inch diameter stage increases the cross-sectional area by 16 percent. In addition, a protuberance in an otherwise undisturbed area will introduce flow separation, changing the local pressure distribution and possibly aggravating buffet conditions on the launch vehicle aft of the protuberance. To fair-in the protuberance requires conical flare sections on the forward and aft ends. Since these flare sections are poorly suited to radiator construction, some precious area is lost to non-radiating or inefficiently radiating surfaces.

Since the sheath radiator is part of the payload assembly, the radiator must slip down over the launch vehicle stage as the payload is mated to the launch vehicle. Similarly, the stage must slip out of the sheath when the payload separates in orbit. To perform this separation cleanly (without damage to the radiator feed lines and headers) some guidance device will be required in the event that relative rotations are induced by separation. An excessive mass penalty for missions beyond the initial earth orbit would be imposed if the stage were not separated in orbit. Additionally, the materials presently used in launch vehicle construction (aluminum, fiberglass, organic adhesives and insulation) are not compatible with the high

temperature environment that would occur when the radiator is operating. These problems all point to the desirability of removing the stage from the sheath before operating the radiator.

The sheath radiator will cover the separation plane between the payload and launch vehicle. Since the separation device is an explosive charge, the radiator must be protected from possible blast debris. In addition, there is a potential hazard, since the explosive charge must be installed prior to mating of the payload.

The most prominent protuberances on the launch vehicle that must be cleared by a sheath type radiator are the antennas. Further, rf transparency through the sheath must be provided Since these areas of transparency are lost as radiator surface, it is desirable to keep them to a minimum. The sheath radiator drawings optimistically show only a local area of transparency. As a general rule, any metallic object with a surface dimension greater than one-quarter wavelength located within three wavelengths of the antenna is considered objectionable. For telemetry systems operating at 250 MHz three wavelengths would be approximately 12 feet. However, reflecting objects at an angle to the direction of polarization could possibly be tolerated at closer distances. Radar and command system antennas, operating at higher frequencies, would have less critical requirements.

The transparent area, for minimum antenna power loss, would ideally be a completely open area. This is intolerable aerodynamically, so that a panel of rf transparent material is required. A conventional material for the panel, such as fiberglass, would be incompatible with the high temperatures occuring during operation of the radiator. Temperature resistant, rf transparent materials (e.g., glass) would be significantly heavier. An acceptable solution might be to use a fiberglass panel which is ejected during launch after peak aerodynamic pressures have been reached but prior to high temperature operation of the radiator.

Structurally, the sheath radiator is not part of the primary load path. In fact, care must be taken in designing the fit and stiffness of the sheath to ensure that it does not provide a redundant load path. The aerodynamic loads on the sheath are carried in tension and bending to the payload adapter section. To avoid a complete cantilever, some lateral support must be provided at the aft end of the sheath. The conical flare section which serves to fair-in the sheath aerodynamically, can be contacted with a ring on the stage to provide lateral support

through compression. The axial stiffness of this flare section can be designed so that significant axial loads are not transferred. The location of the lateral support on the stage is chosen at a station where lateral stiffness is reinforced, i.e., by an internal stiffening ring.

In mating the sheath to the launch vehicle, two procedures may be used. The clean approach is to assemble the sheath radiator with the payload, load the coolant, and check out the complete system before transporting the payload to the vehicle assembly area. However, since the sheath must fit over the upper stage of the launch vehicle, additional clearance must be provided by the derrick (used to lift the payload onto the launch vehicle). For Saturn V vehicles assembled in the Vehicle Assembly Building (VAB), the length of the payload above the interface may be close to the limit height of the existing facility, and additional clearance may not be available. The alternative is to mate the sheath to the launch vehicle separately. This would require loading of the coolant and making the feed line connections after mating. If the sheath does not cover the IU, as shown in some concepts, prior mating of the sheath would be mandatory.

4.1.1 INSTRUMENT UNIT SHEATH RADIATOR

The Instrument Unit (IU) is the "nerve center," containing the guidance system, control systems, and instrumentation for the launch vehicle. Its environmental control system provides cooling during ground operations and flight for the electronic equipment in both the IU and the forward skirt section of the S-IVB stage. On the Saturn IB and three-stage Saturn V vehicles, the IU is 260 inches in diameter, 36 inches high and mounted on top of the S-IVB stage. For the two stage Saturn V, the IU is assumed to be a similar 36-inch high section, mounted on top of the S-II stage. In all cases, the payload interfaces with IU and any radiator extending aft of the payload interface must first contend with the IU.

Figure 4-1 shows a concept for a sheath type radiator extending over the IU and forward skirt of the S-IVB. The feed lines and headers are located behind the radiator in order to obtain the maximum radiator area for the protuberance required, and to provide meteoroid bumper protection for the feed lines and headers. A 30 degree conical flare is used as an aerodynamic fairing between the sheath radiator and the basic launch vehicle diameter. The feed lines also penetrate the primary load carrying shell in this section.

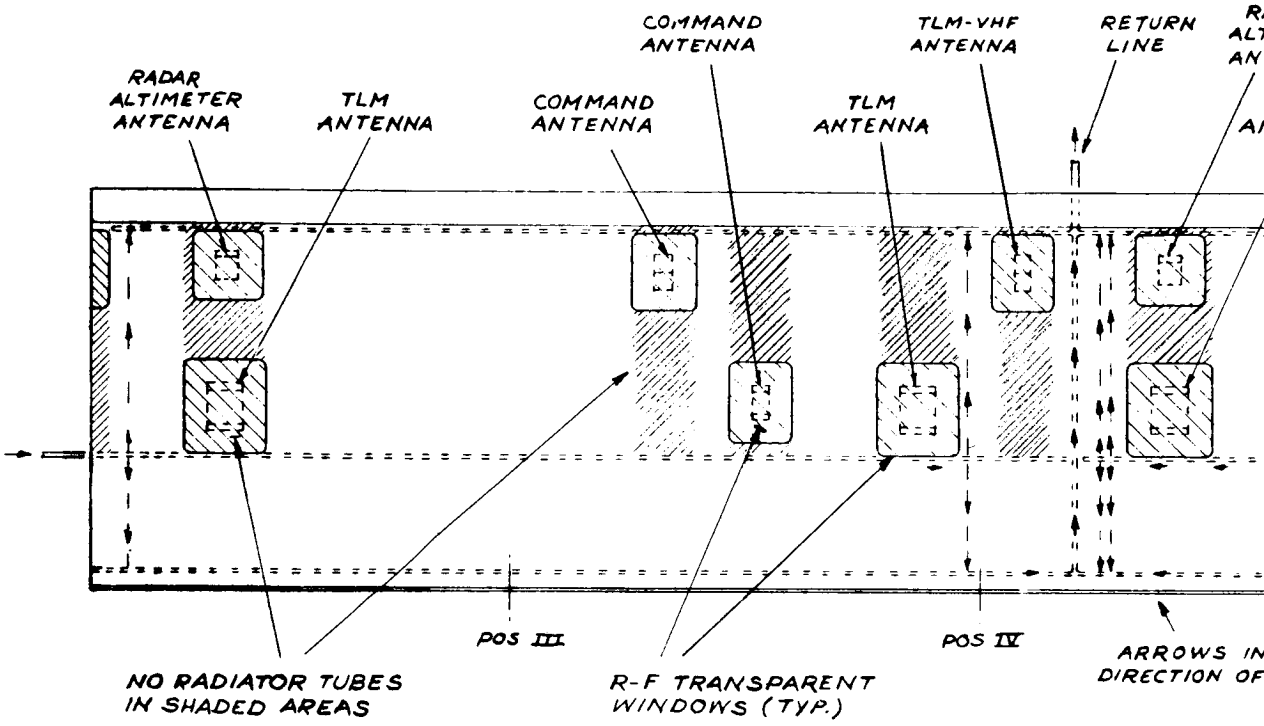

DEVELOPED VIEW OF RAD

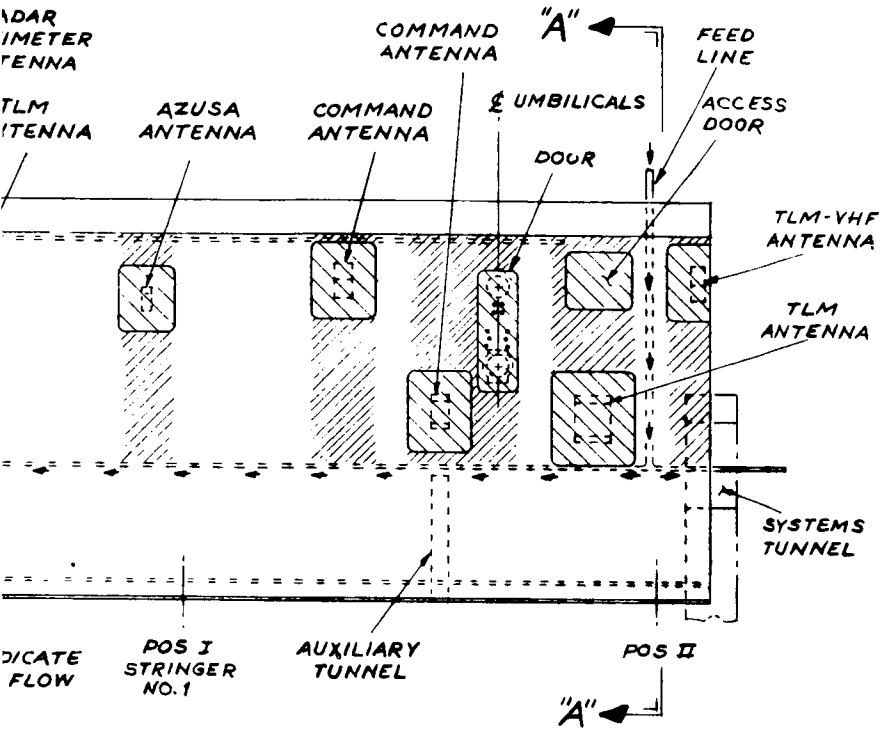

IATOR

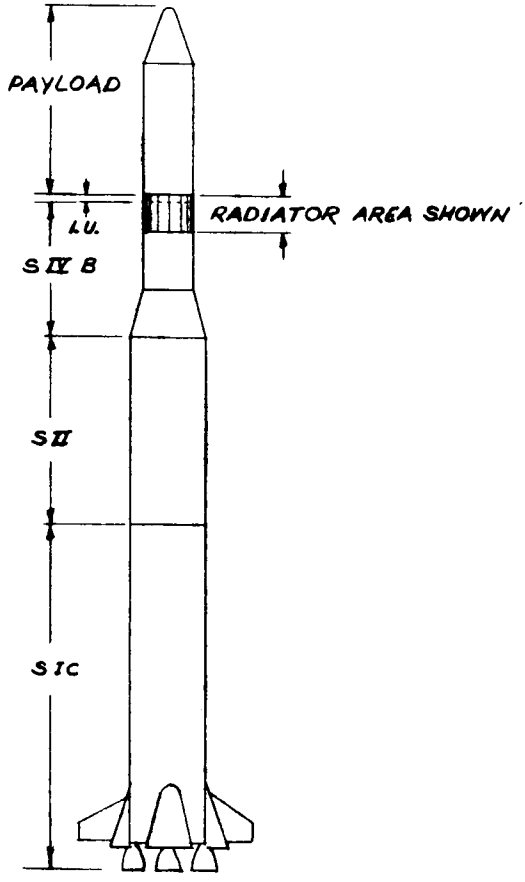

Figure 4-1. Sheath Radiator Extending Over the IU and the Forward Skirt of the S-IVB

Area is lost on the sheath radiator to provide rf transparency for the various antennas and to provide access to the umbilical area. The door which normally covers the umbilical area after removal of the swing arm is mounted on the sheath, rather than on the IU. An access door must be provided in the sheath in order to gain entry to the IU and S-IVB forward skirt areas, after the sheath has been mated to the IU. This access is required to torque the bolts at the payload interface, and can be used for general access to the interior of the payload section. A small hole must be provided in the sheath opposite position IV on the IU. This is to permit optical alignment of the guidance reference gyro. A clear line of sight must be available at all times up to lift-off.

Because of the number and size of the antennas on the IU, a large part of the area on the sheath radiator is not available as radiating surface. The gain in area is small considering the problems that are introduced. Therefore, on the other layouts of sheath radiators, the sheath has been shown starting aft of the IU. In general, this will permit the sheath to fit closer to the stage.

4.1.2 SATURN S-IVB STAGE SHEATH RADIATOR

The S-IVB is the final propulsion stage on both the Saturn IB and the three stage Saturn V. Layouts of radiators on the S-IVB are based on the Saturn V vehicle stations, but the concepts shown would also apply to the Saturn IB vehicle.

Figure 4-1 shows a sheath radiator covering the IU and forward skirt of the S-IVB. The sheath extends far enough from the side of the vehicle to clear the systems tunnel fairing as well as all antennas. Transparent panels are provided at each antenna location. An open area in the sheath is required for access of the swing arm to the umbilical area. In each of these locations, there are no radiator tubes and the area is lost as a radiating surface. Lateral support at the aft end of the sheath is provided by butting the flare section against a ring located at the station of one of the forward skirt stiffening rings. (See Figure 4-2).

If the sheath is continued aft to cover the tank area, additional area can be obtained with the same concept and without introducing any new problem areas. Figure 4-4 shows the sheath extended to Saturn V Station 2826.5 which is a convenient support point. Beyond this station, the sheath would have to clear three ullage motors, two auxiliary propulsion system modules, the aft umbilical panel, and the fairing of the liquid hydrogen feed line.

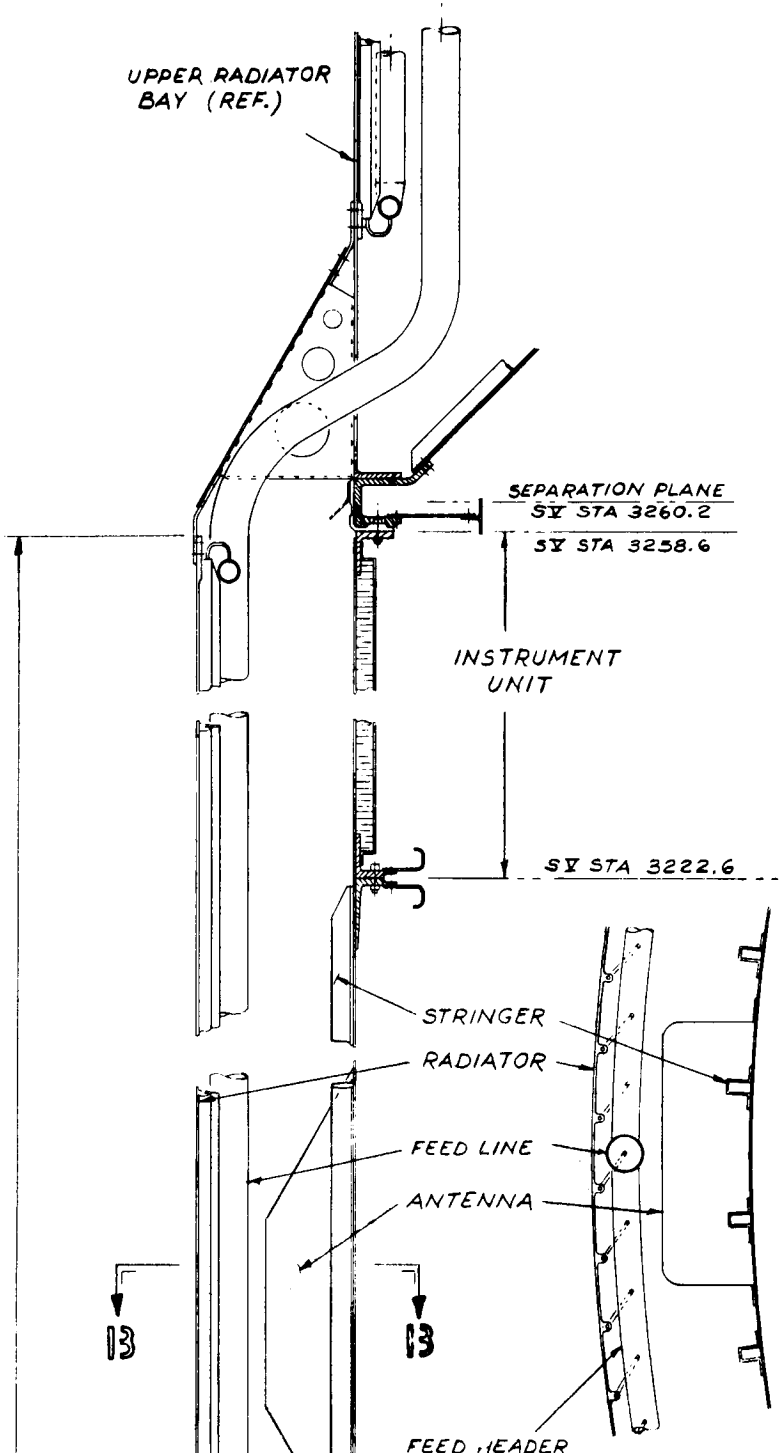
UPPER RADIATOR BAY (REF.)
SEPARATION PLANE
SV STA 3260.2
SV STA 3258.6
INSTRUMENT UNIT
SV STA 3222.6
STRINGER
RADIATOR
FEED LINE
ANTENNA
B
B
FEED HEADER

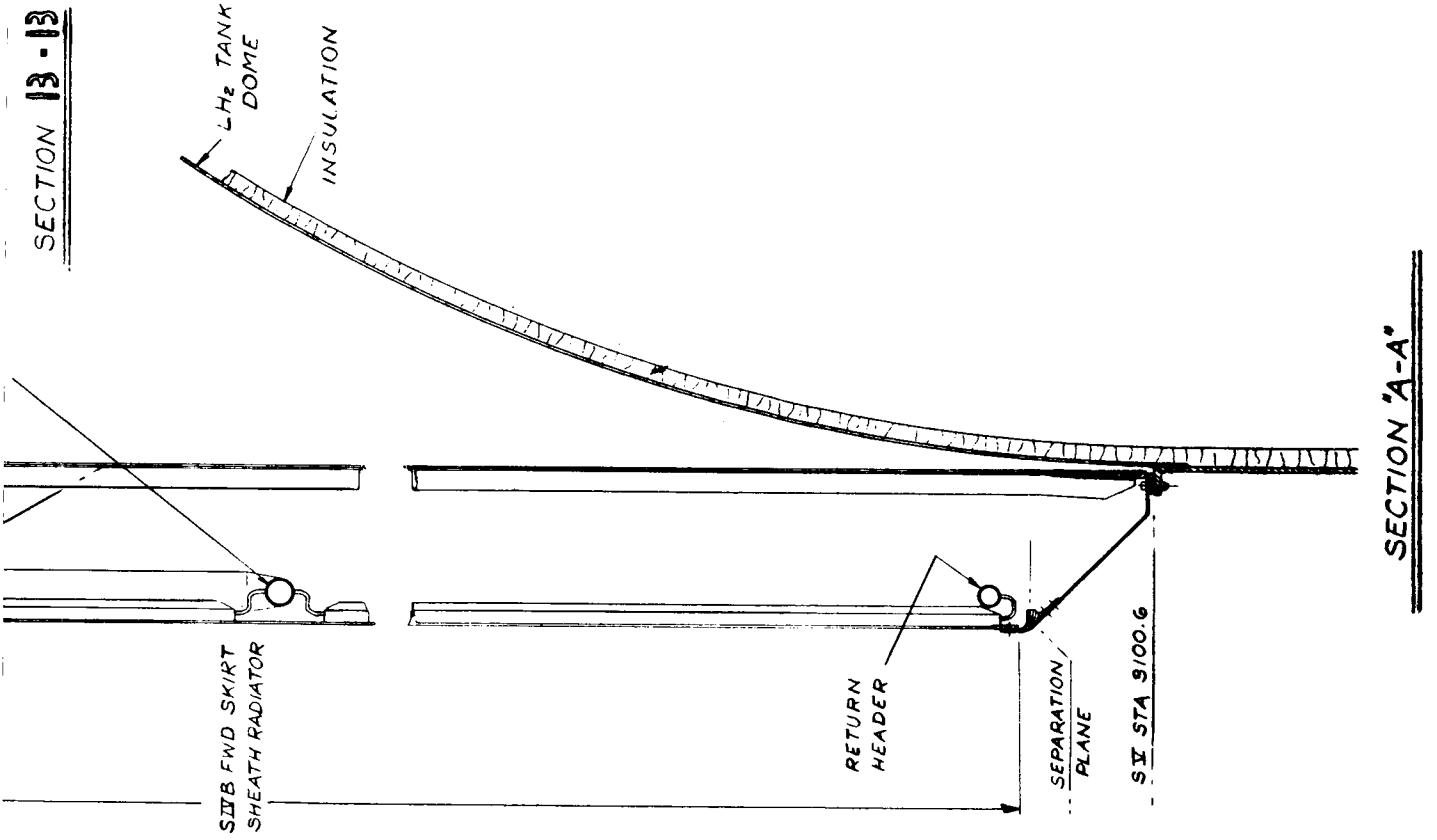

Figure 4-2. Section Through Sheath Radiator Over IU and the Forward Skirt of the S-IVB

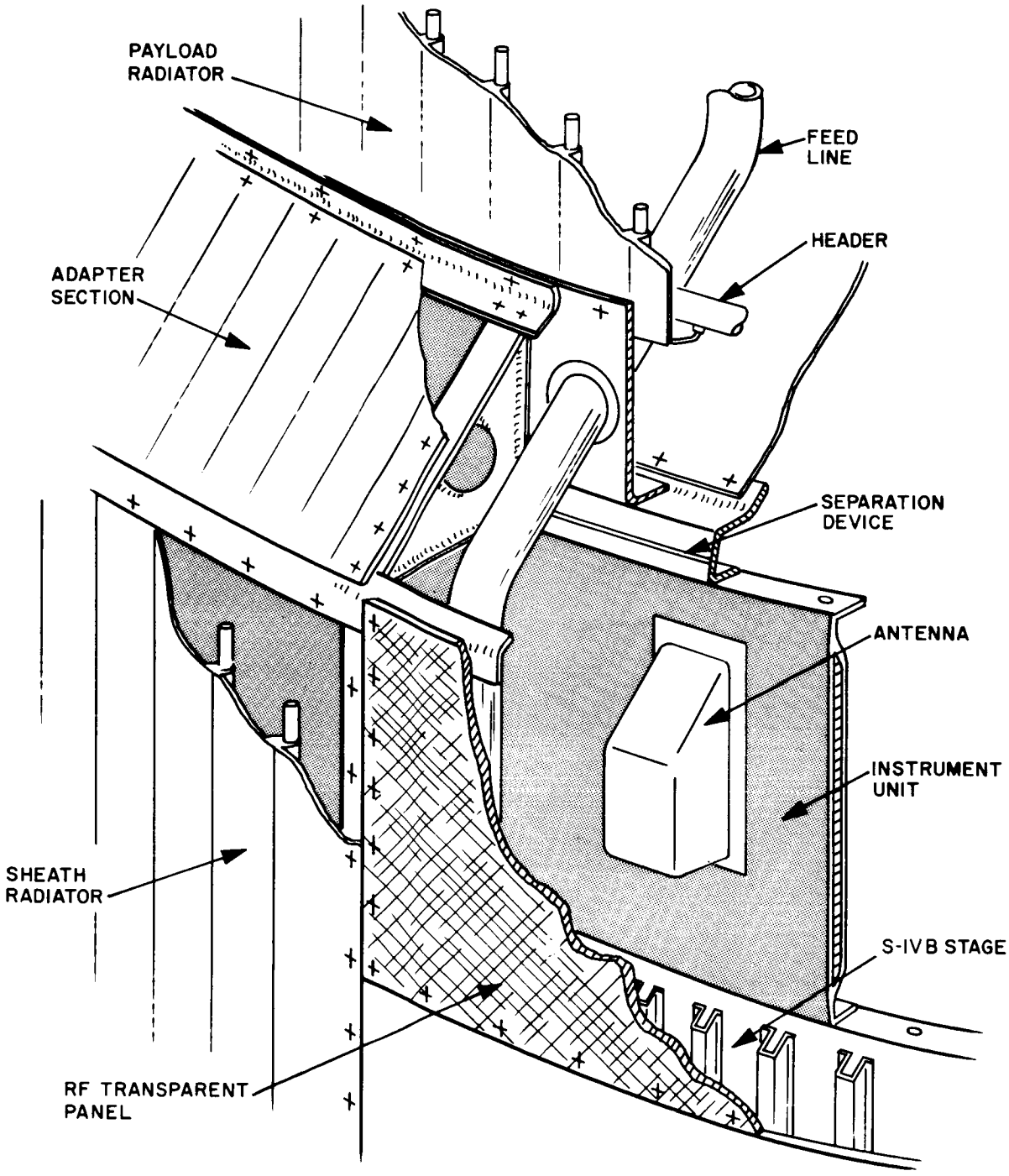

Figure 4-3. Detail of Sheath Radiator over IU

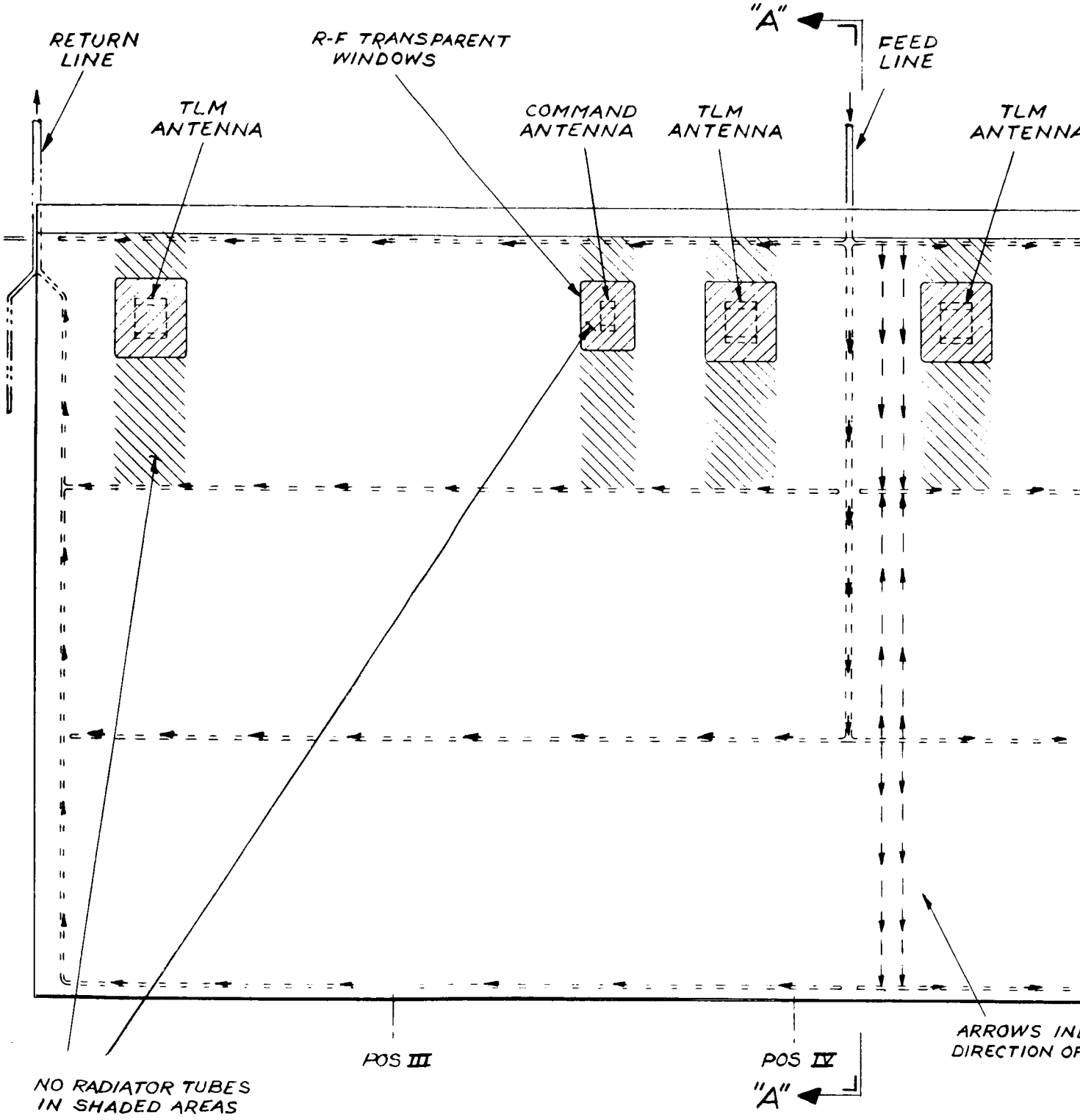

DEVELOPED VIEW OF RADIAT

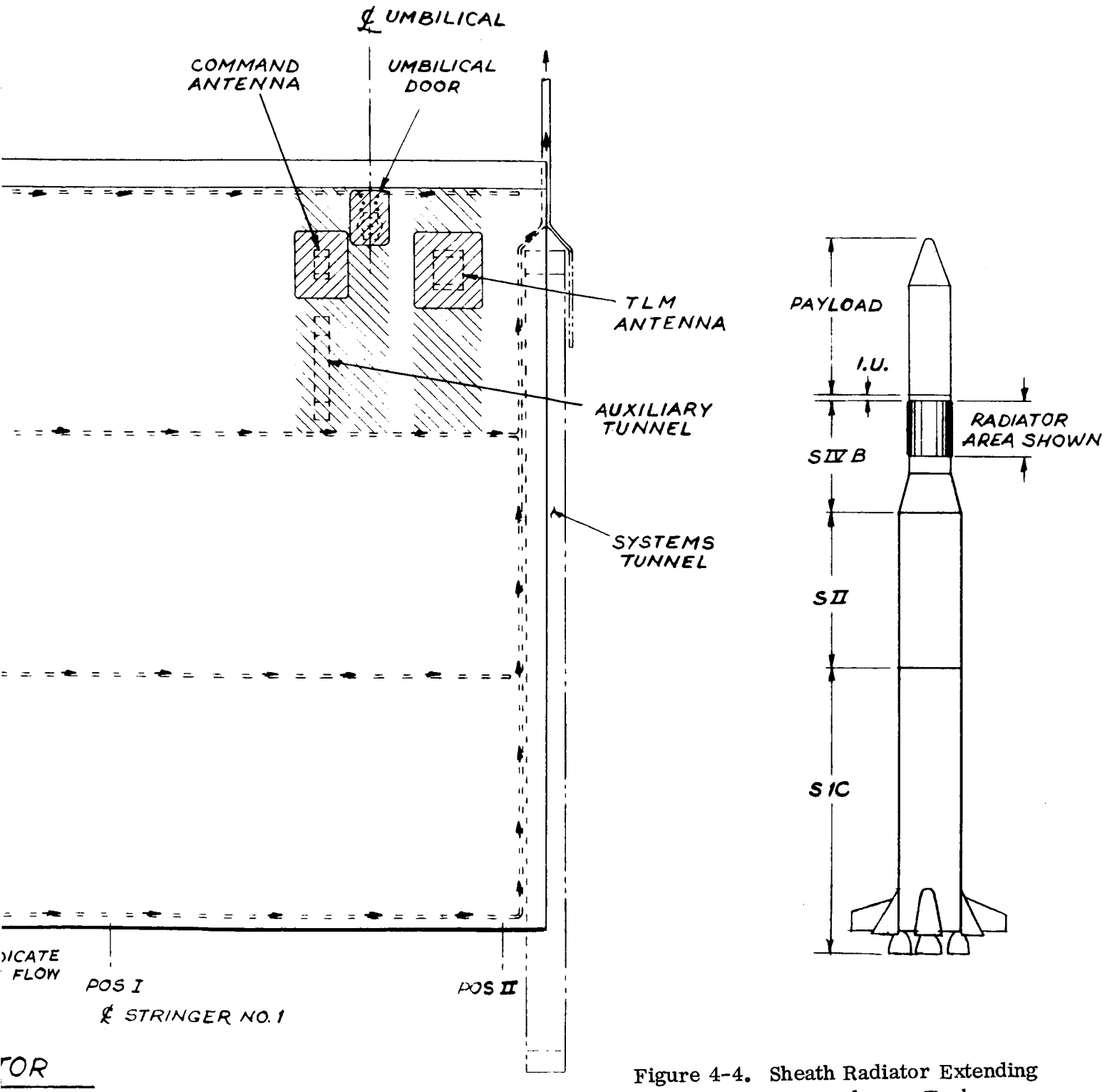

Figure 4-4. Sheath Radiator Extending over S-IVB Hydrogen Tank

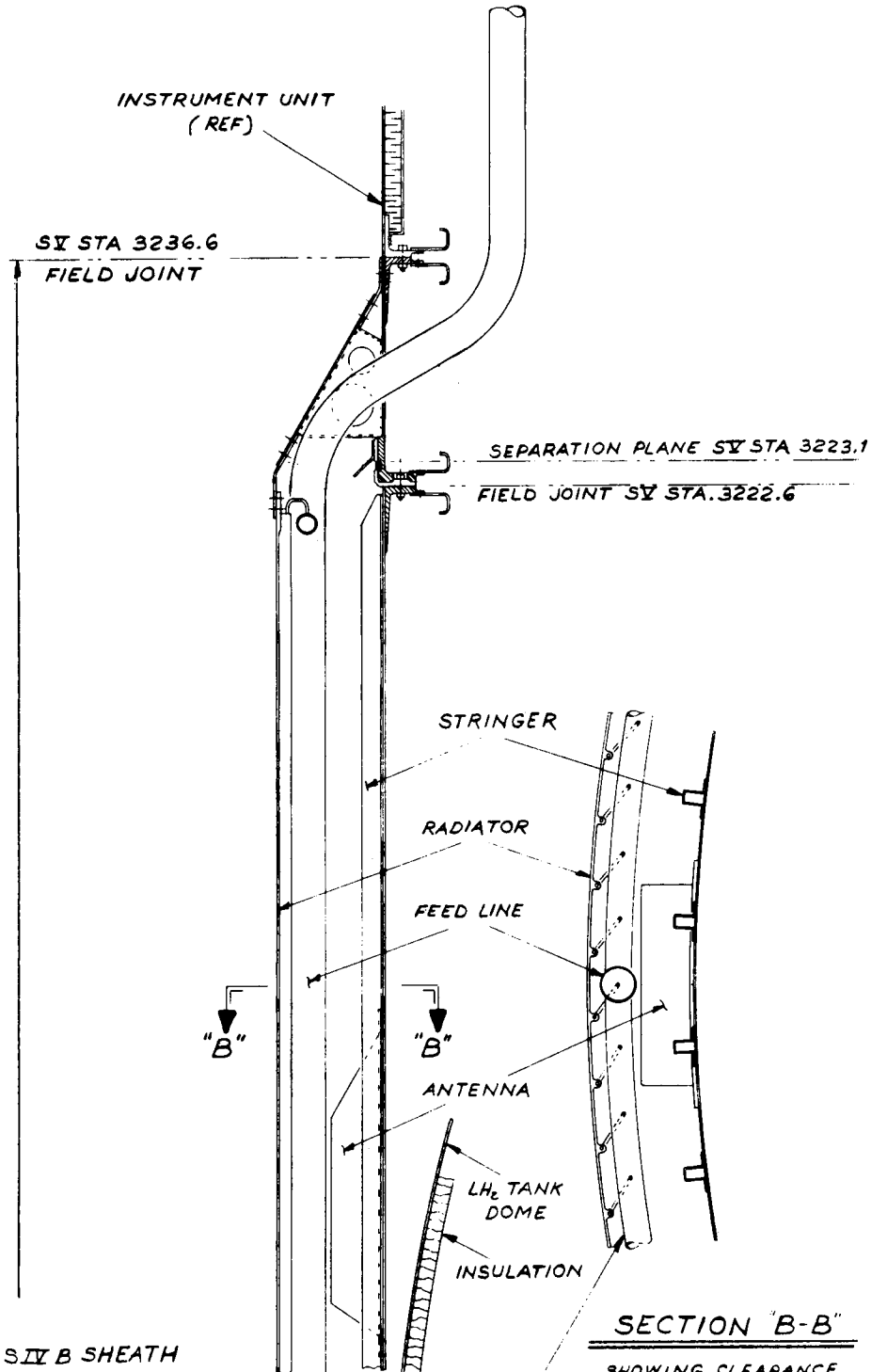

SECTION "B-B"

SHOWING CLEARANCE

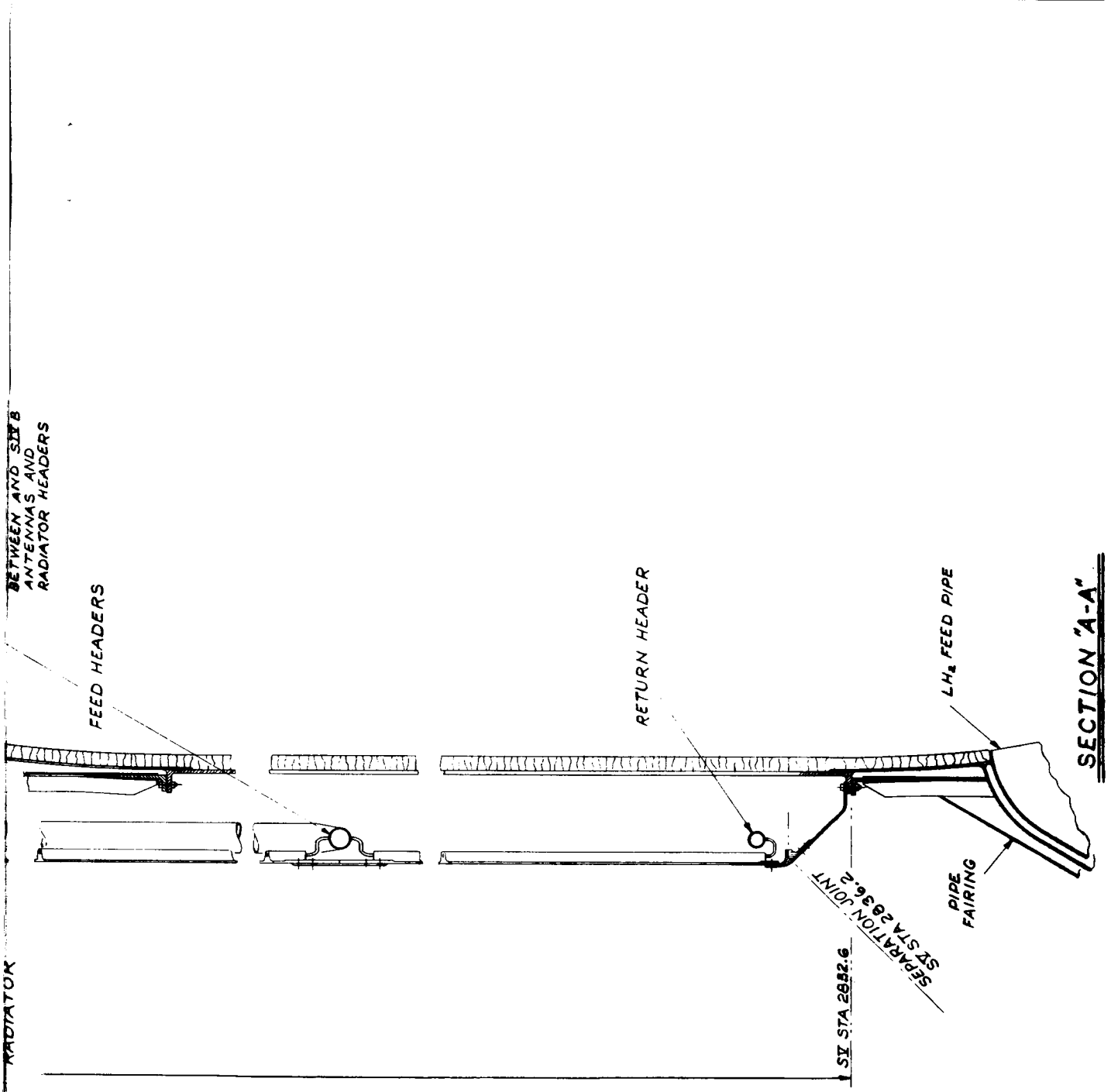

Figure 4-5. Section Through Sheath Radiator over S-IVB Hydrogen Tank

4.1.3 SATURN S-II STAGE SHEATH RADIATOR

In the two stage version of the Saturn V, the S-II becomes the upper stage. The S-II then mates with a 33-foot diameter IU which in turn mates with the payload.

Figure 4-6 shows a sheath radiator fitting over the forward skirt of the S-II. In this concept, the sheath is shown beginning below the IU. A variation of this same concept would be a sheath covering both the IU and the S-II; however, in this case the sheath would have to be larger in diameter to clear the antennas on the IU. Since the antennas on the forward skirt of the S-II are flush mounted, the sheath is a closer fit on the S-II than a similar sheath on the S-IVB. Critical clearance is between the radiator headers and the hot section stringers on the forward skirt. The aft end of the sheath is supported by a ring attached to the forward skirt stringers at the station where the external insulation begins. (See Figure 4-7).

If the sheath is extended farther aft, as shown in Figure 4-8, to cover the tank area, the sheath must be larger in diameter to clear the insulation band at the forward dome to cylindrical section joint. Because three additional bays have been added, larger diameter feed lines are shown. No additional cutouts are required other than those in the forward skirt and for the systems tunnel. Lateral support for the sheath is provided by a ring bonded to the insulation at Station 1972, where an existing internal stiffening ring is located. To extend the sheath farther aft would require an increase in diameter to clear the fairings on the liquid hydrogen fill lines (four places), the recirculation line, fill and drain lines, as well as the intermediate umbilical panel.

4.2 INTEGRAL RADIATOR

The objective of the integral radiator is to make use of the stage structure as radiator. In addition to saving the weight of a separate radiator structure, the integral radiator avoids some of the interference problems of the sheath type radiator. The disadvantage of the integral radiator is that it may necessitate redesign and requalification of the stage.

Some of the problems inherent to the integral radiator will be discussed before examining specific examples.

If only the forward skirt area of one of the propulsion stages is utilized as an integral radiator, the tank structure will remain intact and redesign of the stage will be minor. The principal

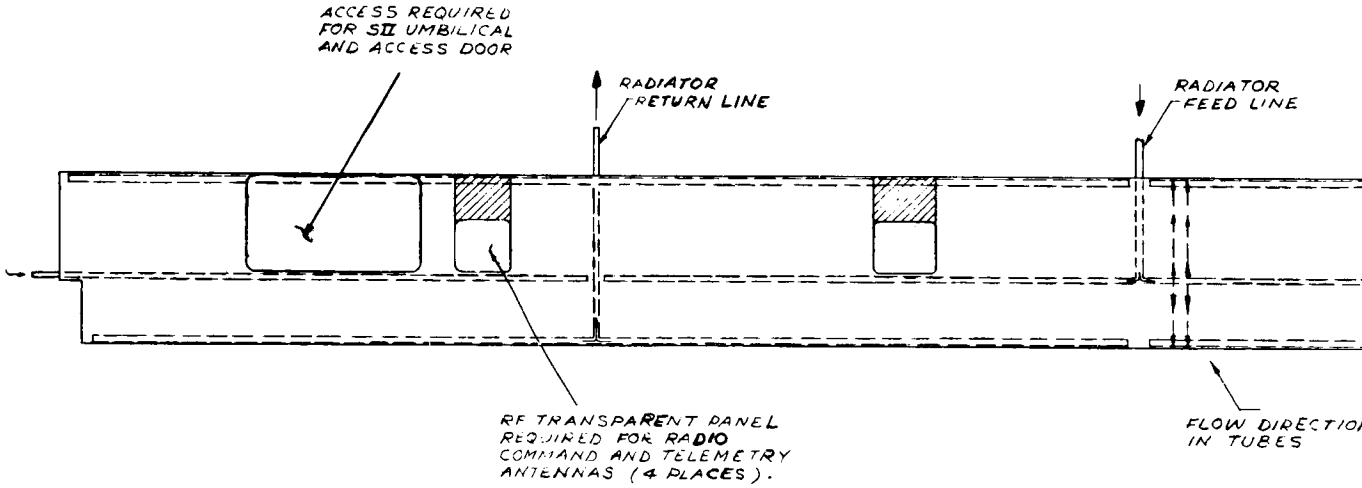

DEVELOPED VIEW OF RADIA

NOTE: TUBES ARE OMITTED IN CROSS HATCHED A

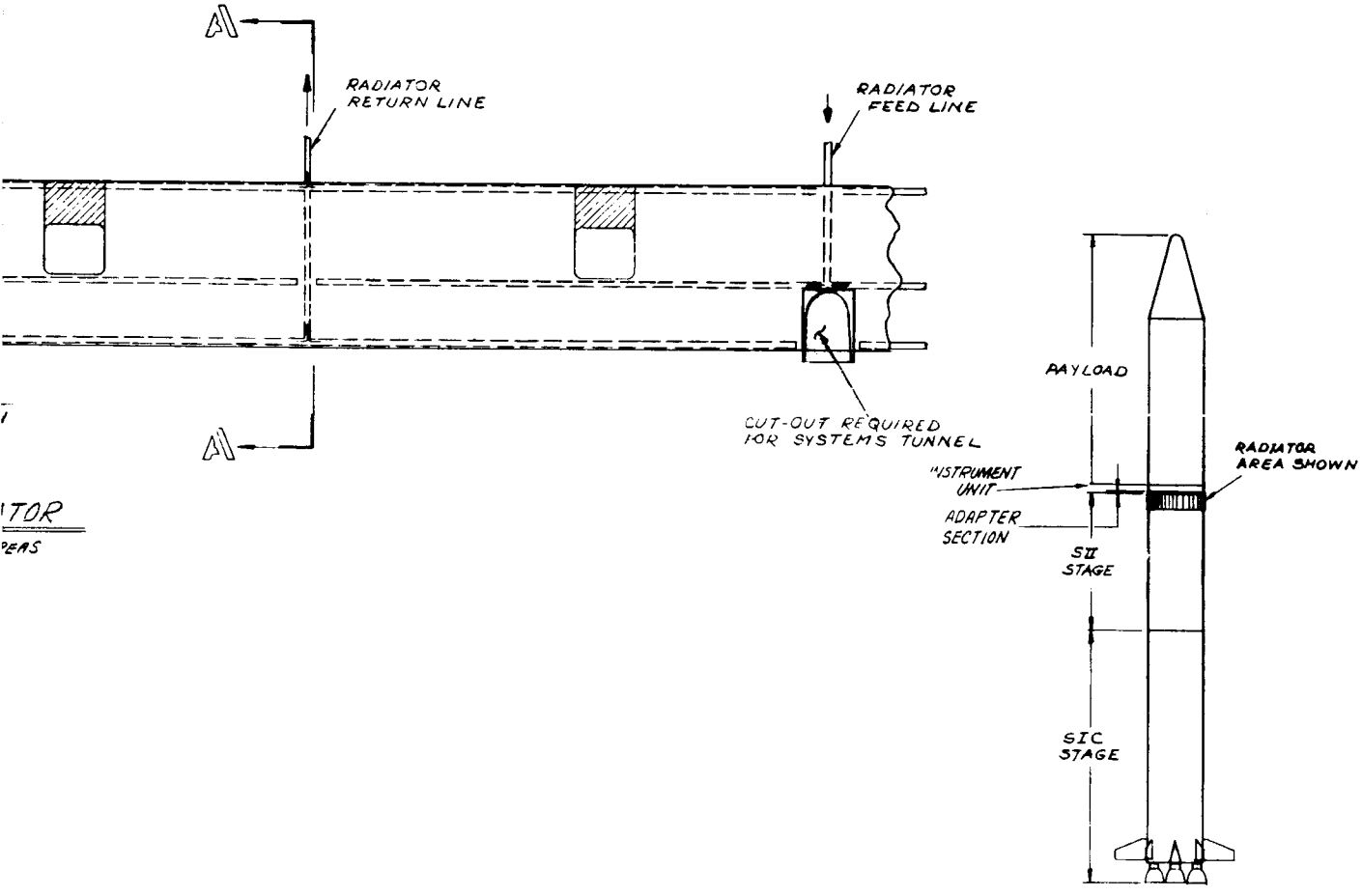

Figure 4-6. Sheath Radiator Extending over S-II Forward Skirt

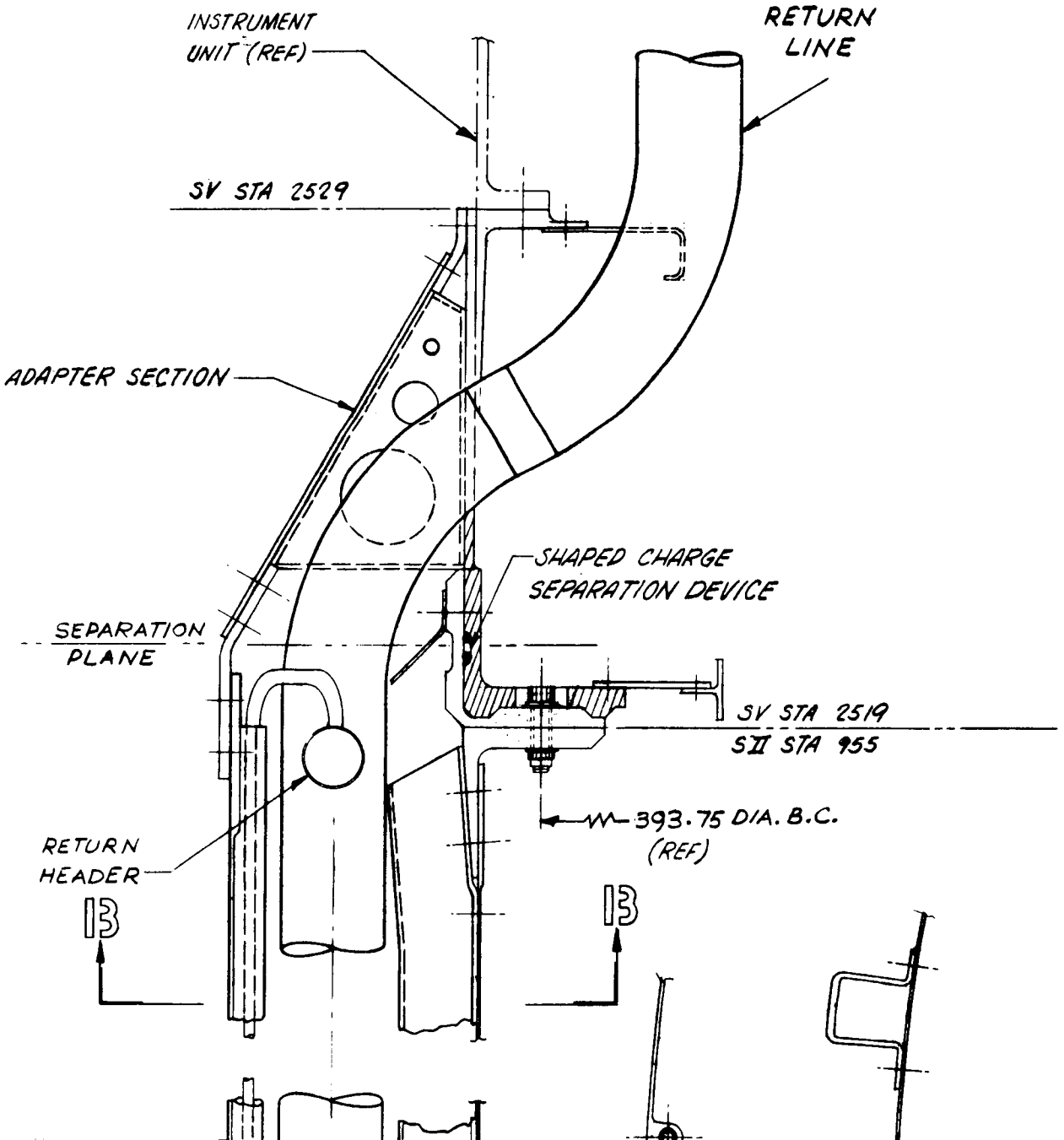
INSTRUMENT UNIT (REF)
RETURN LINE
SV STA 2529
ADAPTER SECTION
SHAPED CHARGE SEPARATION DEVICE
SEPARATION PLANE
SV STA 2519
SII STA 955
393.75 DIA. B.C. (REF)
RETURN HEADER
13
13

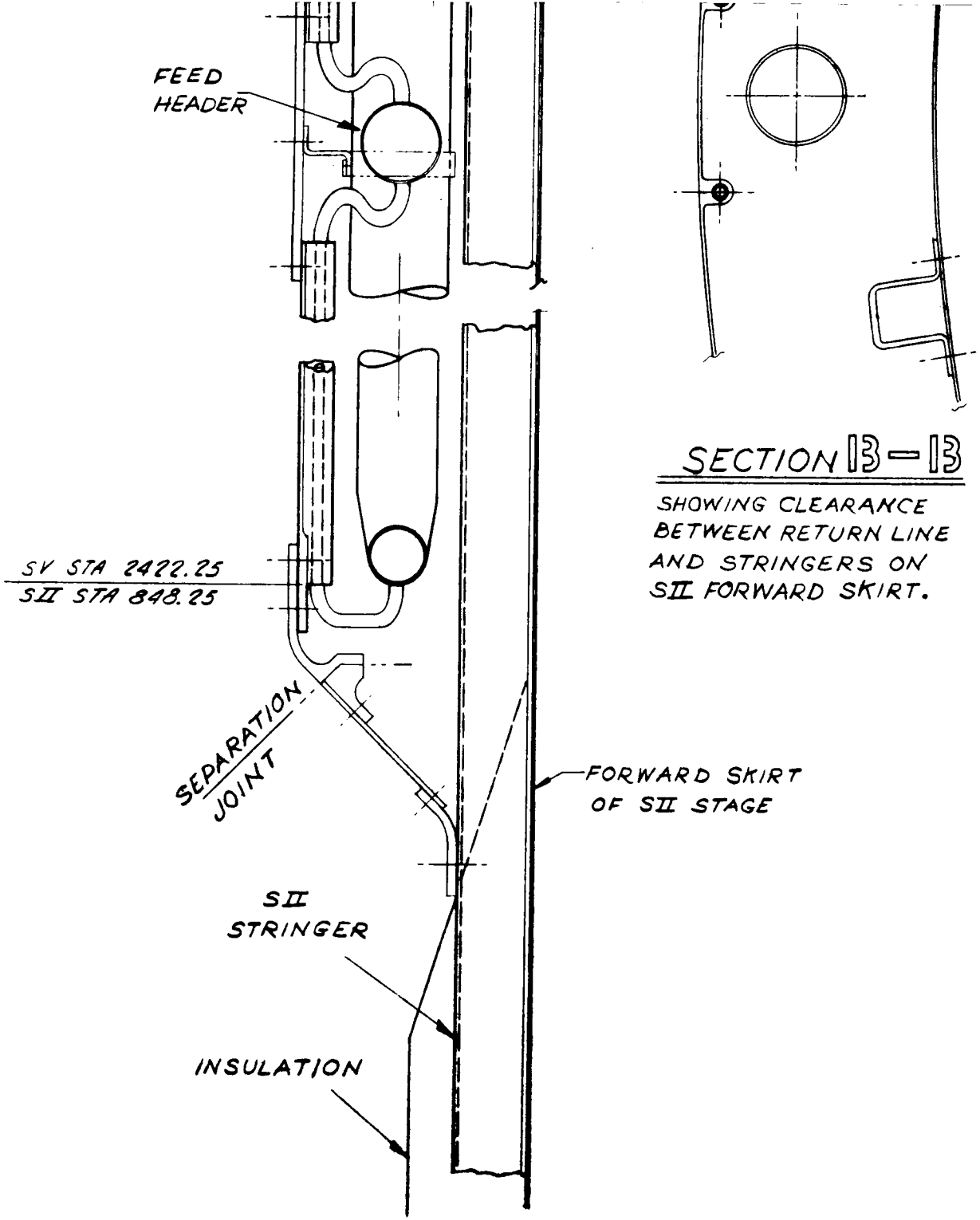

Figure 4-7. Section Through Sheath Radiator over S-II Forward Skirt

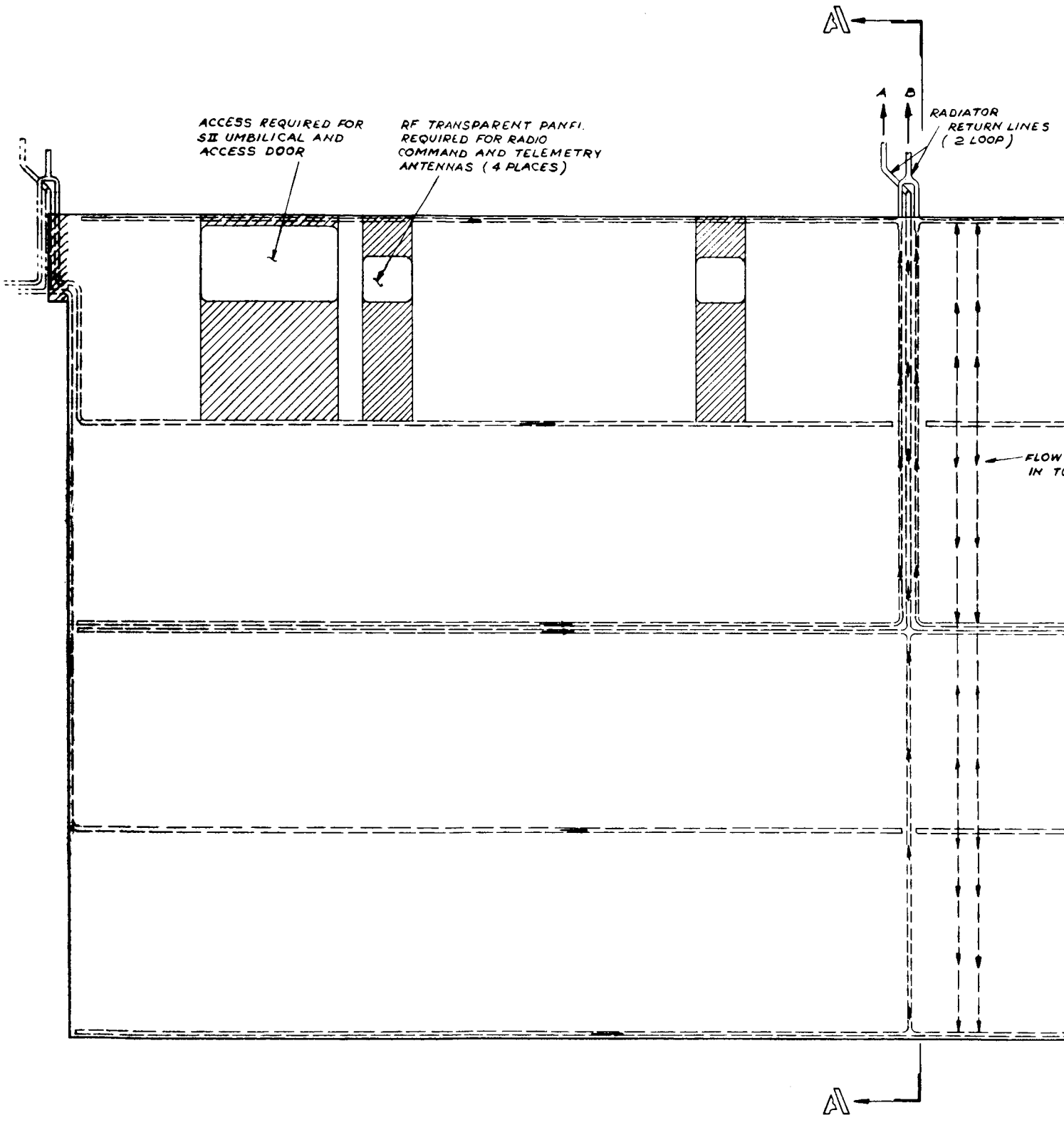

DEVELOPED VIEW OF RADIATOR

NOTE:— TUBES ARE OMITTED IN AREAS SHADED

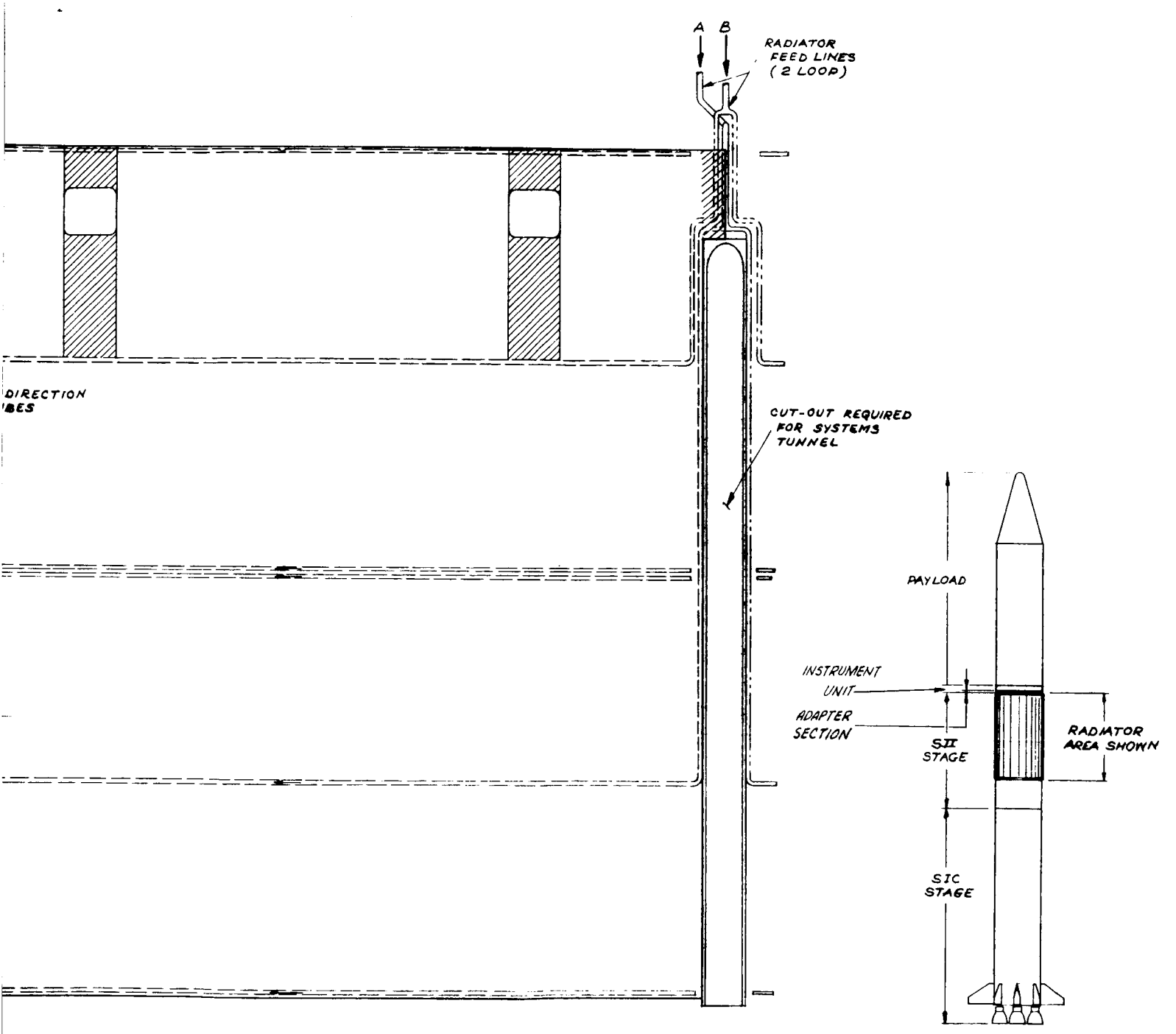

Figure 4-8. Sheath Radiator Extending over S-II Hydrogen Tank

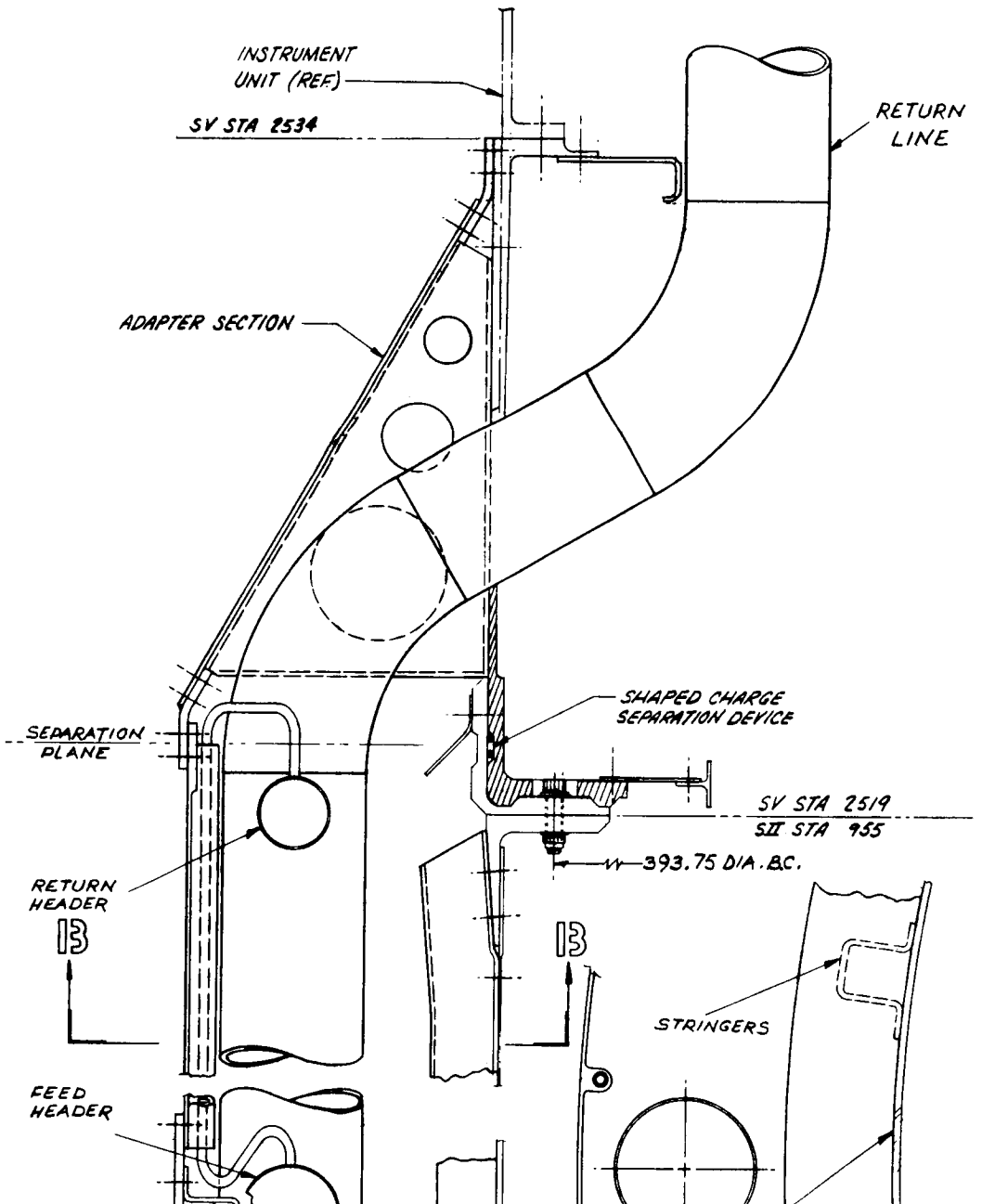
INSTRUMENT
UNIT (REF.)
SV STA 2534
RETURN
LINE
ADAPTER SECTION
SHAPED CHARGE
SEPARATION DEVICE
SEPARATION
PLANE
SV STA 2519
SII STA 955
393.75 DIA. B.C.
RETURN
HEADER
13
13
STRINGERS
FEED
HEADER

Figure 4-9. Section Through Sheath Radiator over S-II Hydrogen Tank

concern is for the components mounted in the forward skirt area. If the position of these components is left unchanged, separation of the forward skirt from the remainder of the stage will require a disconnect from all services that run to the aft skirt section via the systems tunnel. One solution would be to gather all of these services into a single, explosively actuated disconnect panel. However, the components would then remain with the payload, imposing a mass penalty if the payload is subsequently propelled to a higher orbit or beyond escape. The components would have to be made from materials that could withstand the high temperature environment during operation of the radiator. In addition, the interface between payload and stage Contractors would be more complex. A less troublesome solution would be to relocate these components so that they remain with the spent stage after separation. This could be accomplished by providing a conical framework fitting close to the forward dome of the liquid hydrogen tank as shown in Figure 4-10.

If the radiator is integral with the tank structure of the propulsion stage, major redesign of the stage would be necessary. This may require development of new fabrication methods, new tooling and measuring devices, and new ground support equipment, as well as the necessity to perform static and dynamic structural tests to requalify the stage.

One item of concern when the radiator is made integral with the tank wall is the propellant dispersion system. This system destroys the vehicle on command in an abortive launch by severing the propellant tanks with linear shaped charges. For the hydrogen tank, on both the S-II and S-IVB stages, the charge is located in the systems tunnel. The problem arises after a normal launch and the dispersion system has not been fired. Before the radiator can be operated at high temperature, the charges must be disposed of without risk of damage to the radiator. If the radiator does not extend the full length of the hydrogen tank, the charge normally in the systems tunnel could be relocated to a station aft of the separation plane. Recent studies have shown that these charges constitute a hazard on the Saturn V vehicle because they are installed while the vehicle is in the VAB (Reference 4-4). Proposals have been made to replace the linear charges with fixed-position charges which would result in mixing of the propellants and slow burning, rather than catastrophic destruction. If this concept is adopted, conflict with the integral radiator will be eliminated.

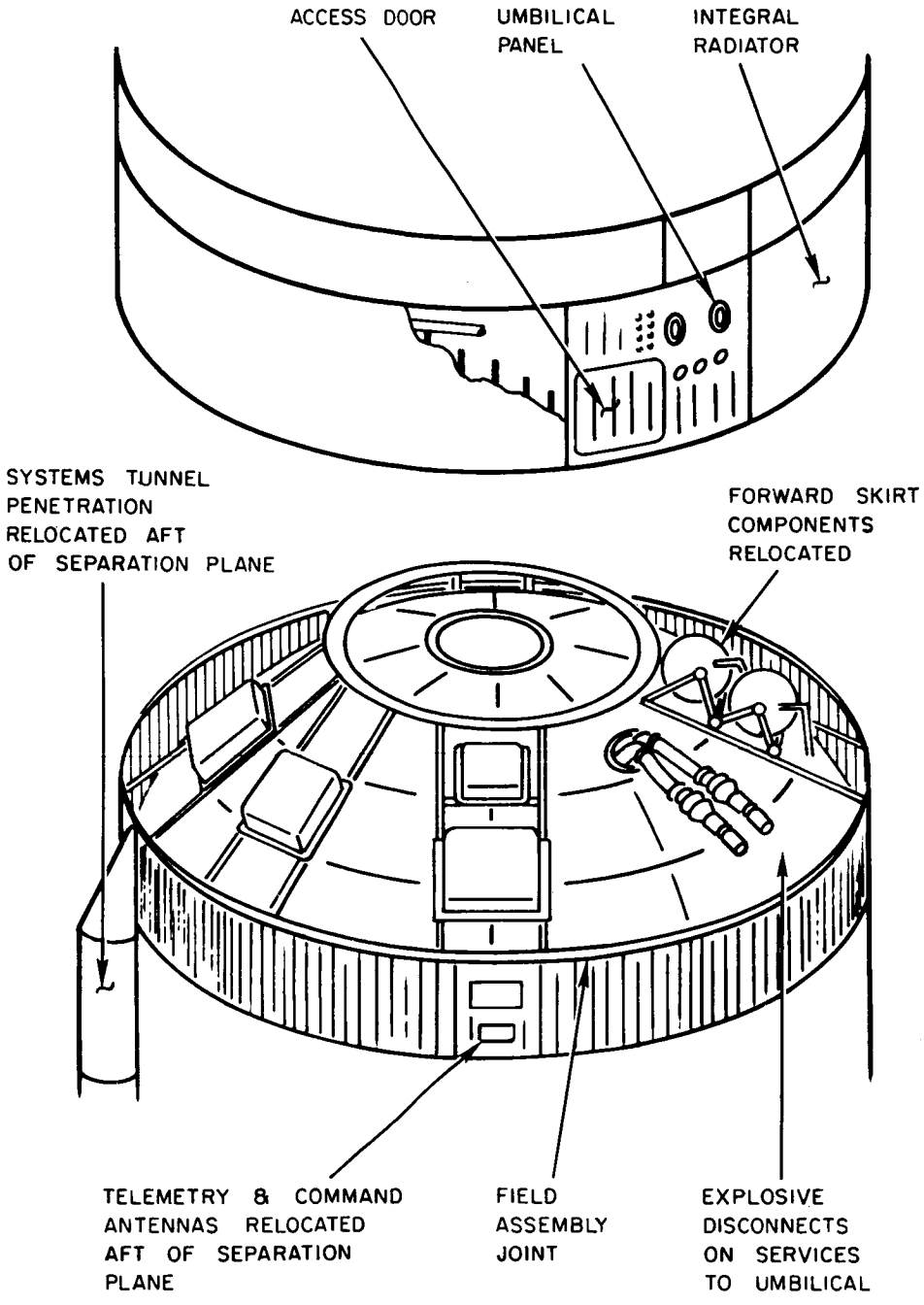

Figure 4-10. Equipment Changes in Forward Skirt Area for Integral Radiator

4.2.1 INSTRUMENT UNIT INTEGRAL RADIATOR

Figure 4-11 shows a concept for a radiator integrated with the structure of the IU in conjunction with a radiator integral with the forward skirt of the S-IVB. Except for the umbilical area, the entire IU surface functions as a radiator. The antennas on the IU are mounted externally; the only penetration of the radiator required is for the connector which can be located between tubes. Similarly, the window for optical alignment of the guidance reference gyro and the exhaust from the environmental control system can be located between tubes.

Not shown in Figure 4-11 is the equipment mounted internally in the IU. This equipment would remain in approximately the same position, only the details of support from the radiator would be different from the present IU.

Although the present IU power is supplied by batteries, post-Apollo IU's could use radioisotope thermoelectric generators. These generators would require radiators for waste heat rejection. This would strengthen the argument for using an integral radiator, since the radiator would be necessary for all launches. For nuclear powered missions, this same radiator area could be utilized after launch by switching the heat load from the generator to the nuclear powerplant. The materials used for an integral radiator in the IU may not be consistent with the primary heat rejection requirements of the nuclear powerplant. However, secondary cooling requirements, for pumps, bearings, etc. may be a suitable match for the IU generator cooling requirements.

Since integration of a radiator with the IU will require a complete redesign of the IU structure, the possibility arises of redefining the boundaries of the IU. This is particularly appropriate in considering the two stage Saturn V, since the IU is not presently defined for this vehicle. It is technically feasible to eliminate the IU as a separate section by relocating its components in the skirt areas of the propulsion stages or by incorporating it into the payload. However, from the viewpoint of checkout and launch operations, there are several compelling reasons for maintaining the IU as a separate component. The components of IU have been developed to be in fixed location with respect to one another and with respect to their precise environmental control system. Checkout of the IU is a complex procedure that should be carried out without interference from other systems or any concern for their test schedules. Certainly there will be other missions for post-Apollo Saturn launch vehicles for which an IU

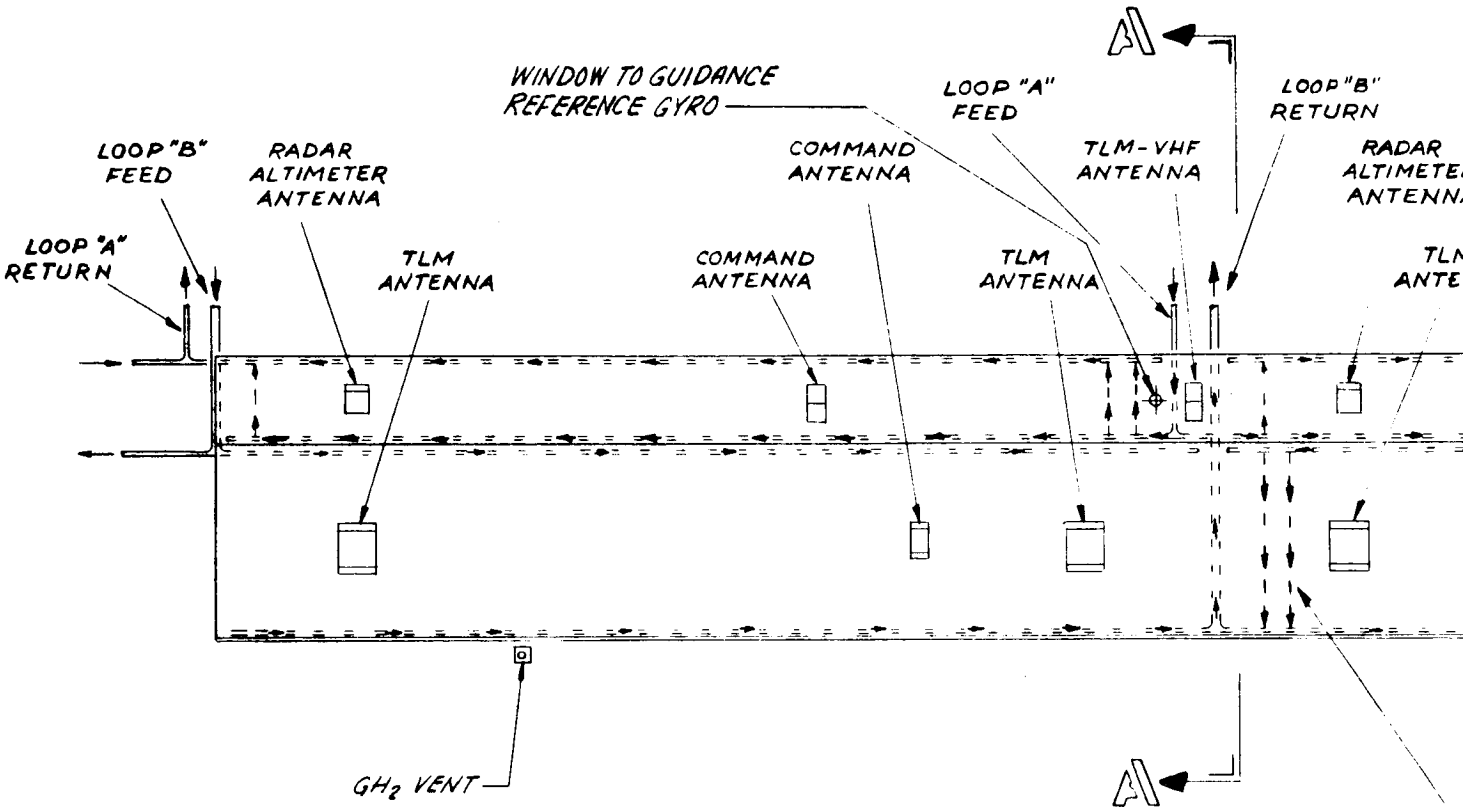

DEVELOPED VIEW OF RADI

NOTE: TUBES OMITTED IN CROSS HATCHED

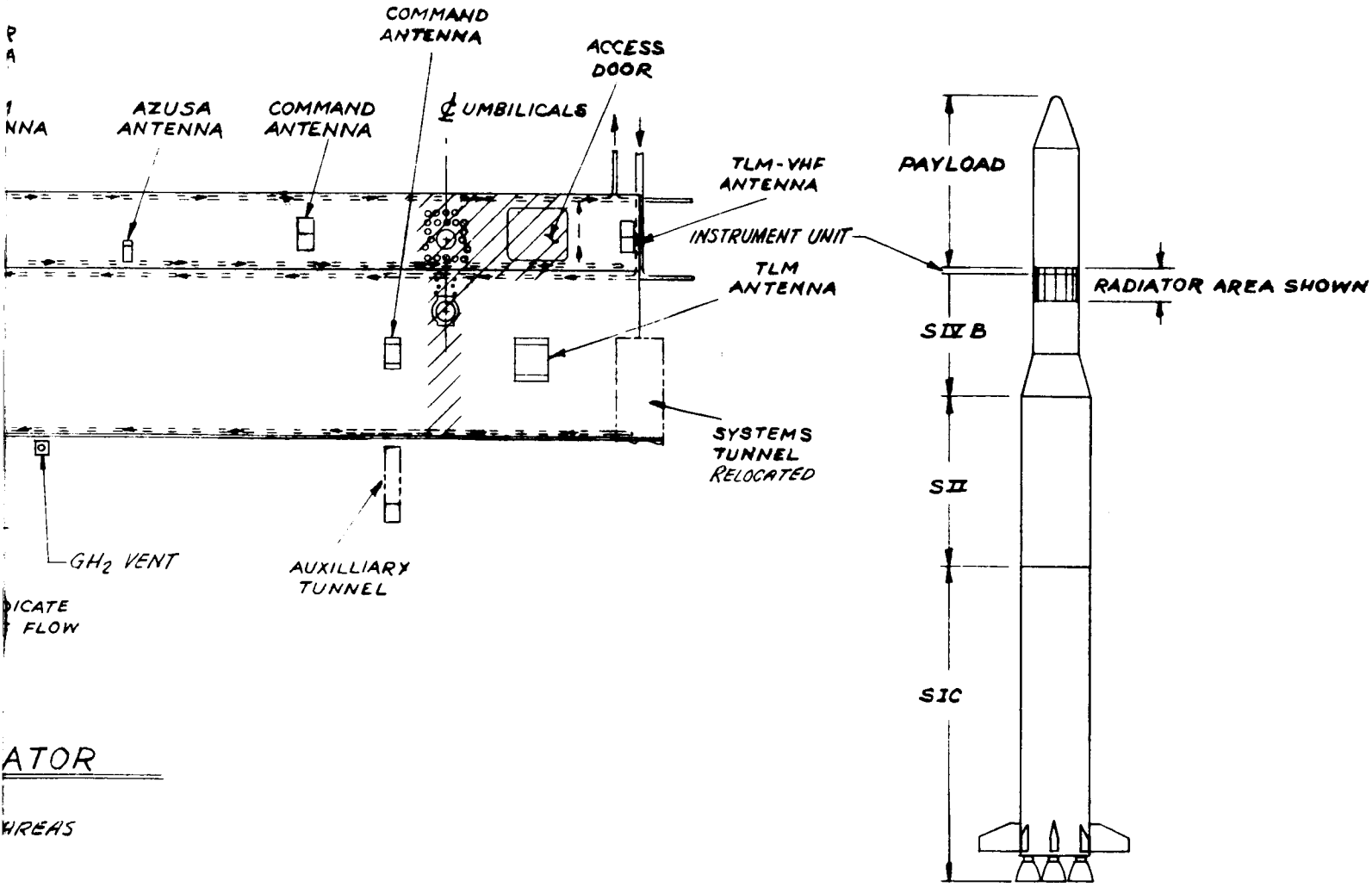

Figure 4-11. Radiator Integrated with IU and S-IVB Forward Skirt

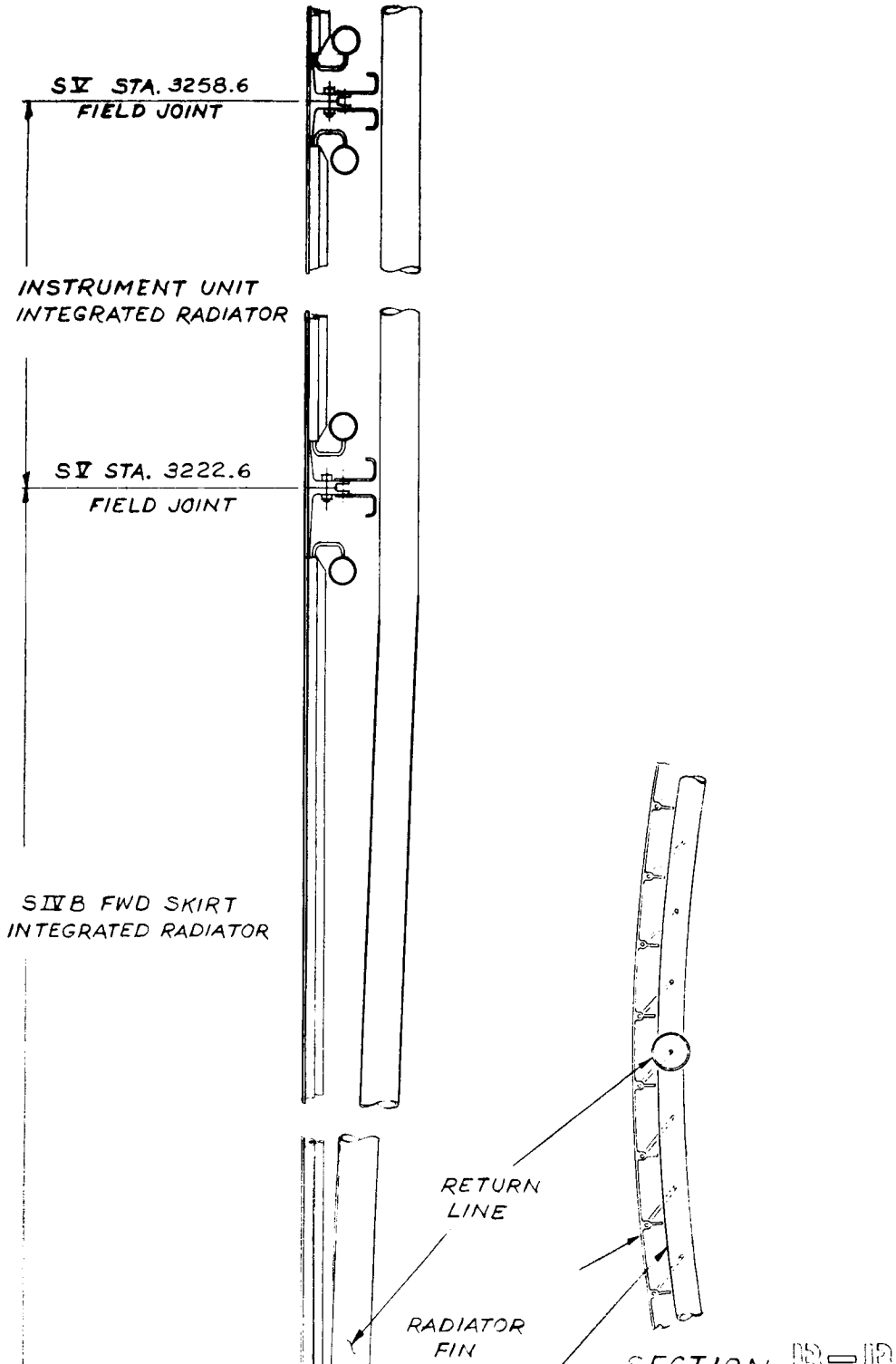
SV STA. 3258.6
FIELD JOINT
INSTRUMENT UNIT
INTEGRATED RADIATOR
SV STA. 3222.6
FIELD JOINT
SIVB FWD SKIRT
INTEGRATED RADIATOR
RETURN
LINE
RADIATOR
FIN

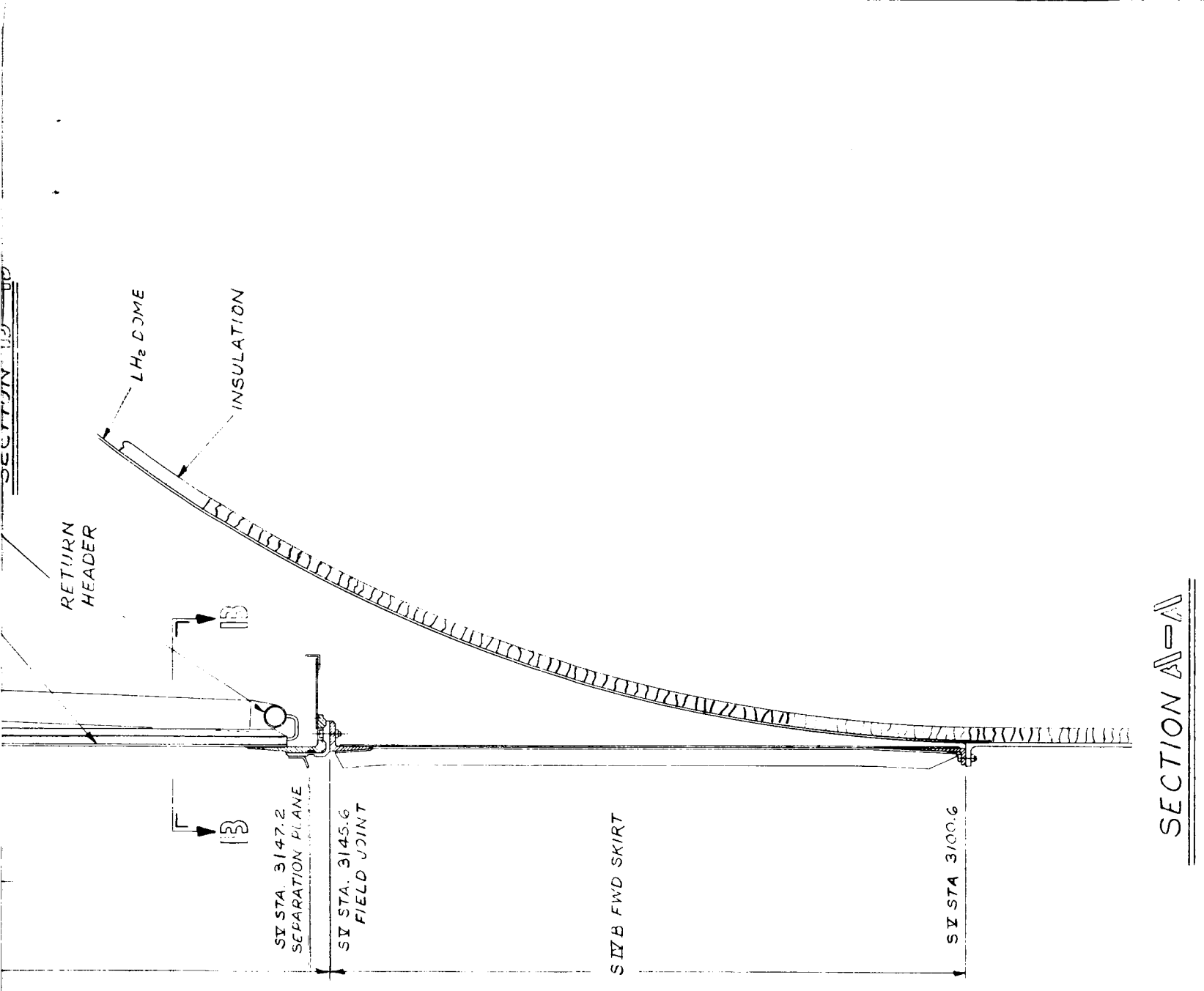

Figure 4-12. Section Through Radiator Integrated with IU and S-IVB Forward Skirt

will be required, and it would be highly advantageous to define a single IU configuration suitable for all missions. For these reasons, the IU has been maintained as a three-foot section in the layouts discussed.

4.2.2 SATURN S-IVB STAGE INTEGRAL RADIATOR

Figure 4-11 shows a radiator integrated with the forward skirt of the S-IVB stage. The only areas in which tubes are omitted is at the umbilical. The separation plane is at Station 3047.2, just forward of the point of tangency between the forward tank dome and the cylindrical section. Sufficient clearance is provided between the forward skirt and the tank dome to allow access for installation of the bolts at the field joint between the forward skirt and the integral radiator. Sufficient room is provided between this joint and the field joint to the cylindrical tank section at Station 3045.6 to permit penetration of the skirt by the services in the systems and auxiliary tunnels. The hydrogen tank vents have also been relocated to this part of the skirt to avoid the necessity of disconnects when the tank separates from the skirt.

If the tank area is integrated with the radiator, as shown in Figure 4-13, several new problems are encountered. As well as the umbilical and systems tunnel cutouts, radiator area is lost at the auxiliary tunnel. The feed header for the radiator section in the forward skirt has been located as far aft as clearance with the tank dome will allow. This leaves a band of non-radiating surface between the skirt section and the next station aft at which a header can be located in the tank cylindrical section. A short tunnel is required to carry the feed line from the point where it penetrates the skirt section to the feed header in the tank section. The return header for this bay is located in the existing systems tunnel. The headers in the tank area are internal so that penetrations of the load carrying shell are required in only two places. To isolate the headers from the liquid hydrogen, the headers are covered with insulated tunnels. The insulation concept for the hydrogen tank follows the existing S-IVB concept, except that in the radiator areas the insulation tiles are long strips fitting between the tubes, rather than square tiles in the milled waffle recesses. After launch, as the radiator is brought up to operating temperature, the polyurethane foam will decompose and outgas. After separation, the bottom of the tank will be open and the outgas products will be free to pass out of the tank. Redeposition on the exterior surfaces of the payload may be of some concern, if, for example, optical surfaces become clouded or thermal control coatings are

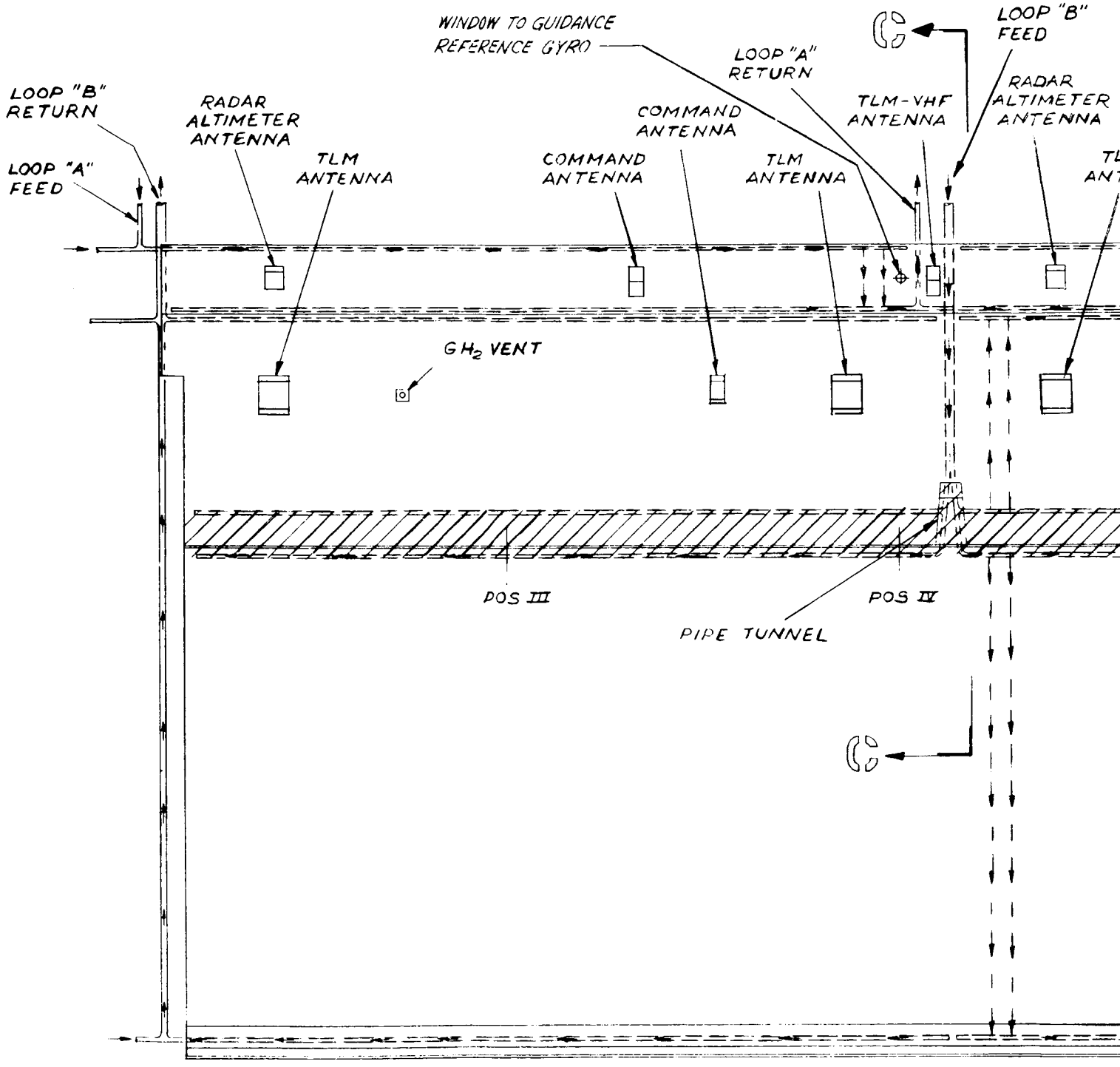

NOTE: TUBES OMITTED IN C

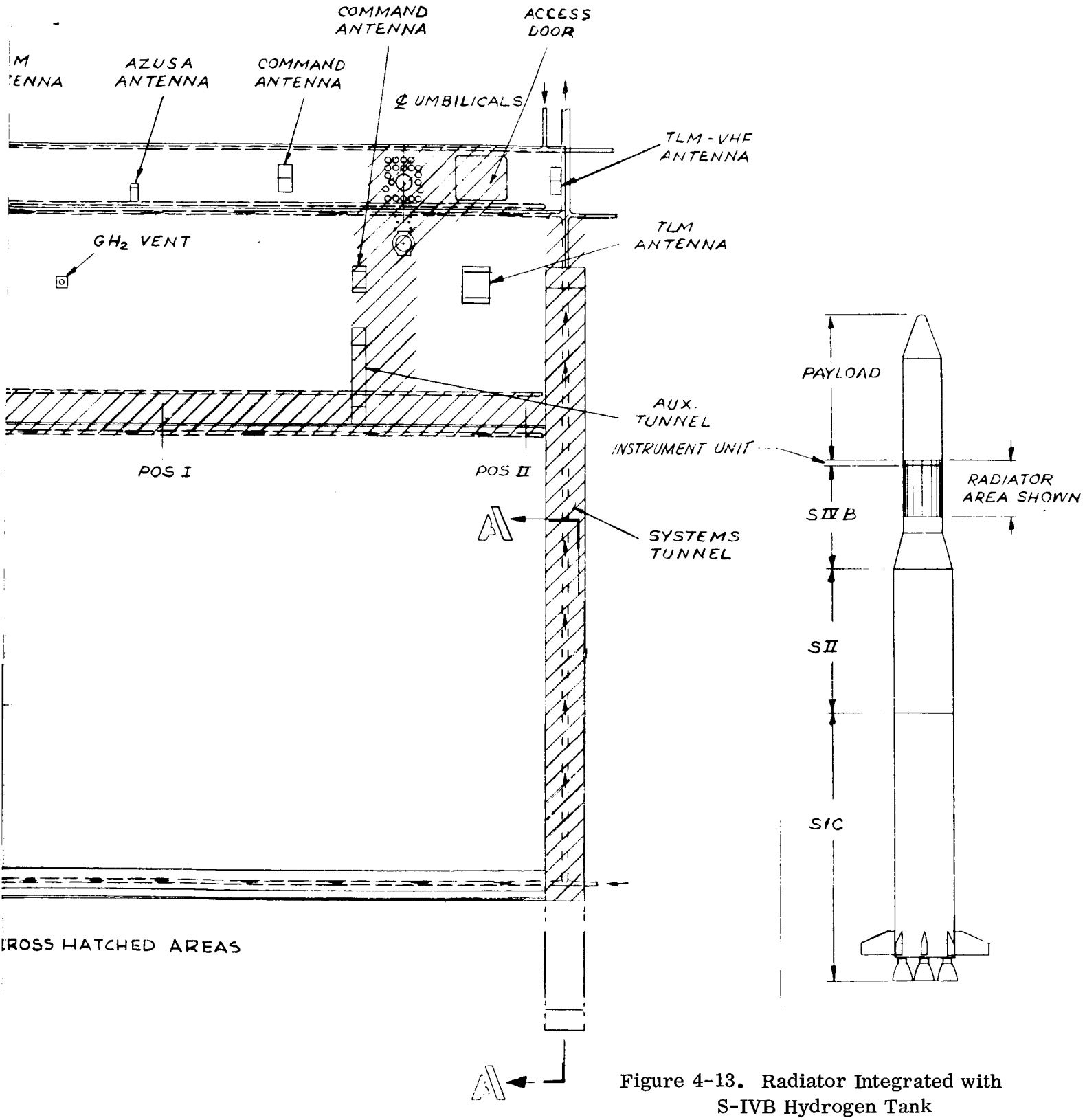

Figure 4-13. Radiator Integrated with S-IVB Hydrogen Tank

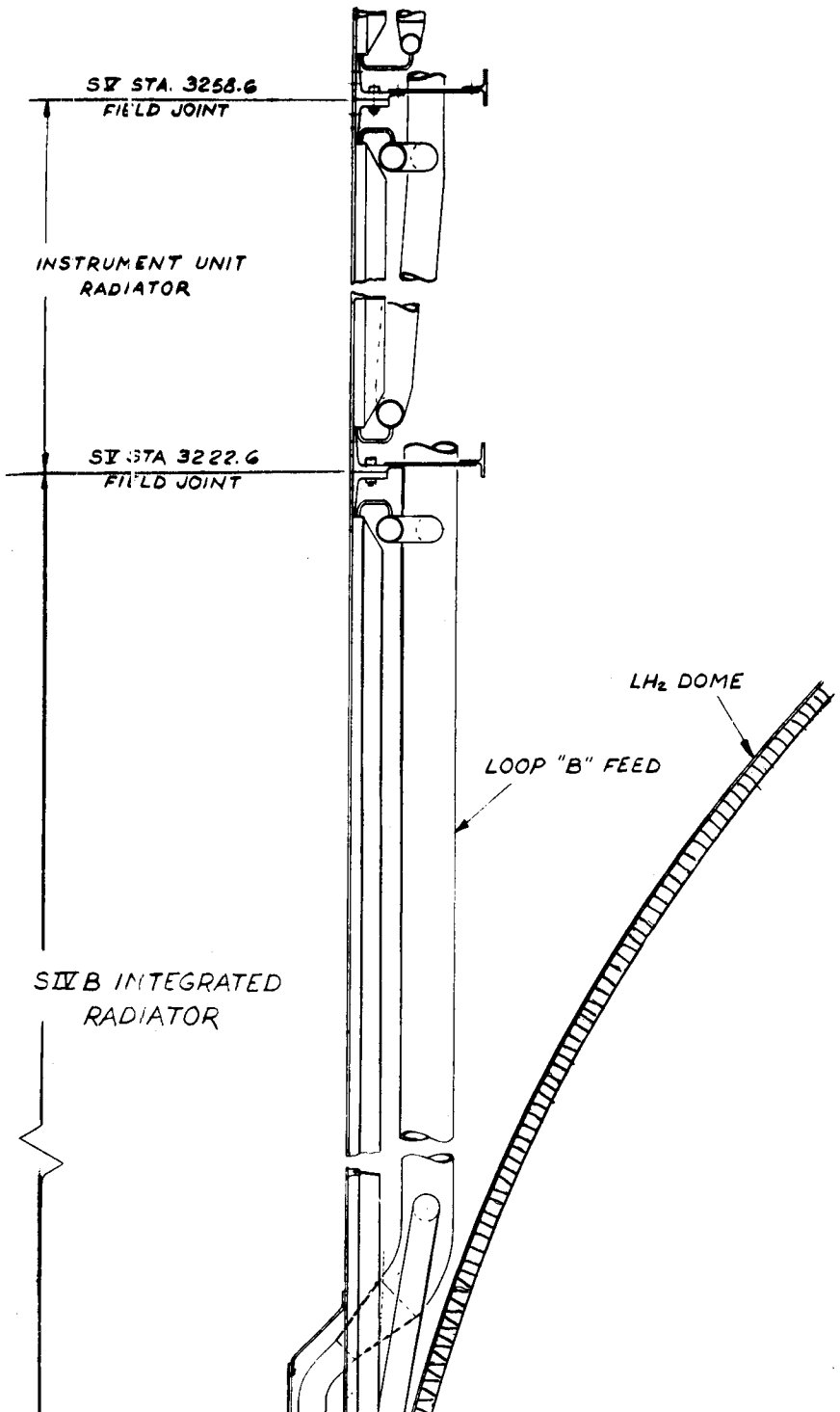
S-IV STA. 3258.6
FIELD JOINT
INSTRUMENT UNIT
RADIATOR
S-IV STA 3222.6
FIELD JOINT
S-IV B INTEGRATED
RADIATOR
LH2 DOME
LOOP "B" FEED

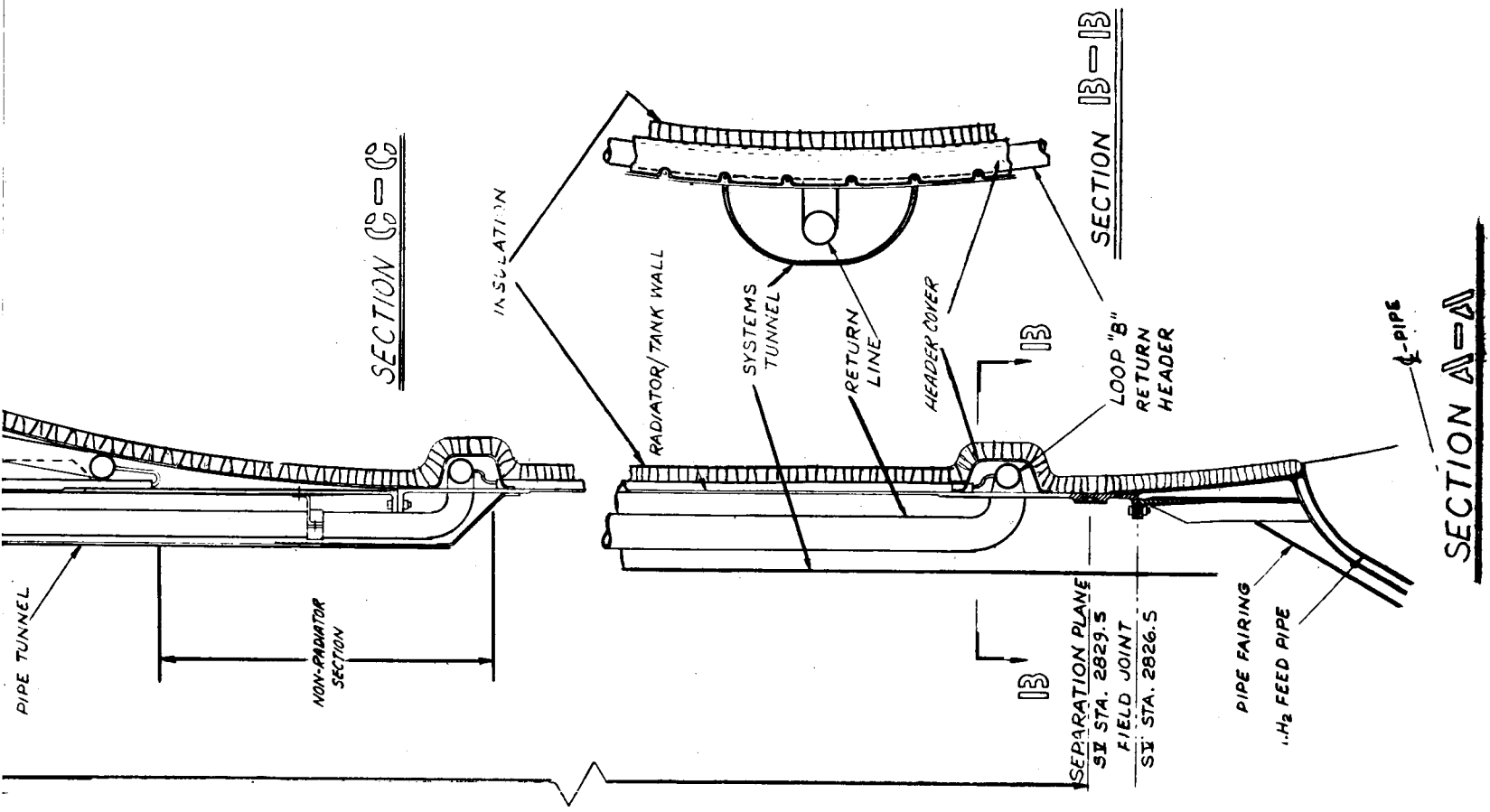

Figure 4-14. Section Through Radiator Integrated with S-IVB Hydrogen Tank

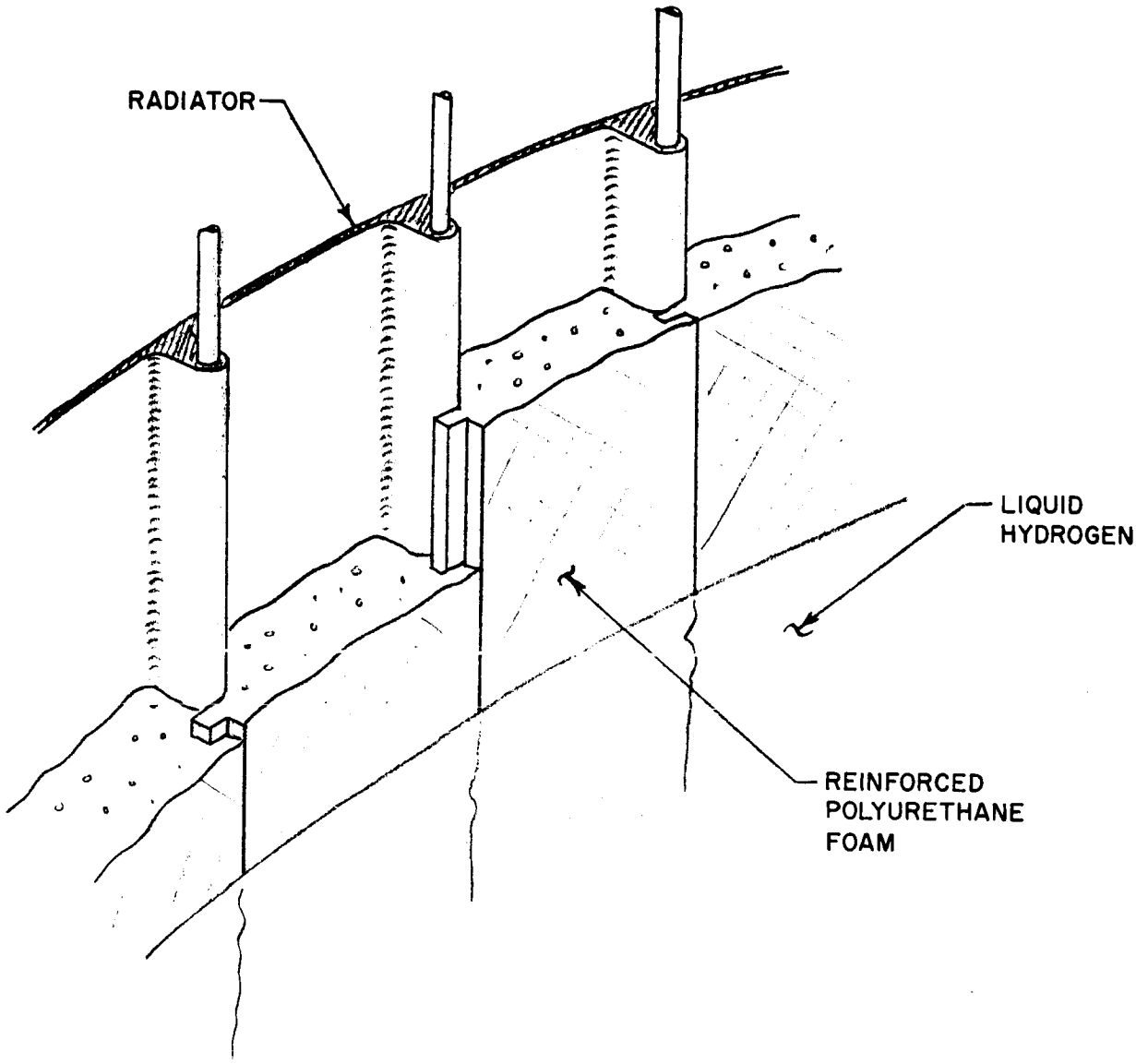

Figure 4-15. Detail of Radiator Integrated with S-IVB Hydrogen Tank

degraded. The residue that remains on the interior surface of the radiator is likely to be of less concern.

The separation plane is located immediately forward of the field joint at Station 2826.5. This joint and all structure aft is unchanged from the existing S-IVB. Since the separation device severs the hydrogen tank wall, it is feasible for this system to double as part of the propellant dispersion system. The problems of the propellant dispersion system were discussed in Section 4.2.

As with the sheath type radiator on the S-IVB, extension of the radiator farther aft than the field joint to the aft skirt results in conflict with the ullage motors, auxiliary propulsion system modules, aft umbilical panel, and the fairing on the liquid hydrogen feed line. The gain in radiator area that could be obtained by extending to the separation plane in the aft skirt does not justify the complexity that it would entail.

4.2.3 SATURN S-II STAGE INTEGRAL RADIATOR

Figure 4-16 shows a radiator integral with the forward skirt of the S-II stage. Since the S-II does not have externally mounted antennas, such as the IU and S-IVB stages, a cutout in the skirt skin is required to the full size of the antenna. To avoid this lost area when the skirt is used as a radiator, the command and telemetry antennas have been relocated aft of the separation plane. Their relative positions have been reversed so that the telemetry antenna, which requires a greater interior clearance, is located to take advantage of the wider space available between the skirt and the tank dome. The services in the systems tunnel are relocated to penetrate the skirt skin aft of the separation plane, and the fairing on the systems tunnel is shortened. Figure 4-10 shows some of the internal changes that must be made. To avoid disconnects to each of the components in the forward skirt area, they have been relocated to a framework mounted above the tank dome. This permits the components to remain with the tank after separation. Explosive disconnects are required on all services to the umbilical panel. Similarly, if the S-II makes use of the cooling loop in the IU as the S-IVB does on three stage S-V vehicles, disconnects will be required on these coolant lines.

Separation of the forward skirt takes place at Station 2459.5. Sufficient clearance is provided between the skirt and the tank dome to enable access to the field joint immediately aft of the separation plane. The removable work platforms in the forward skirt area must be redesigned

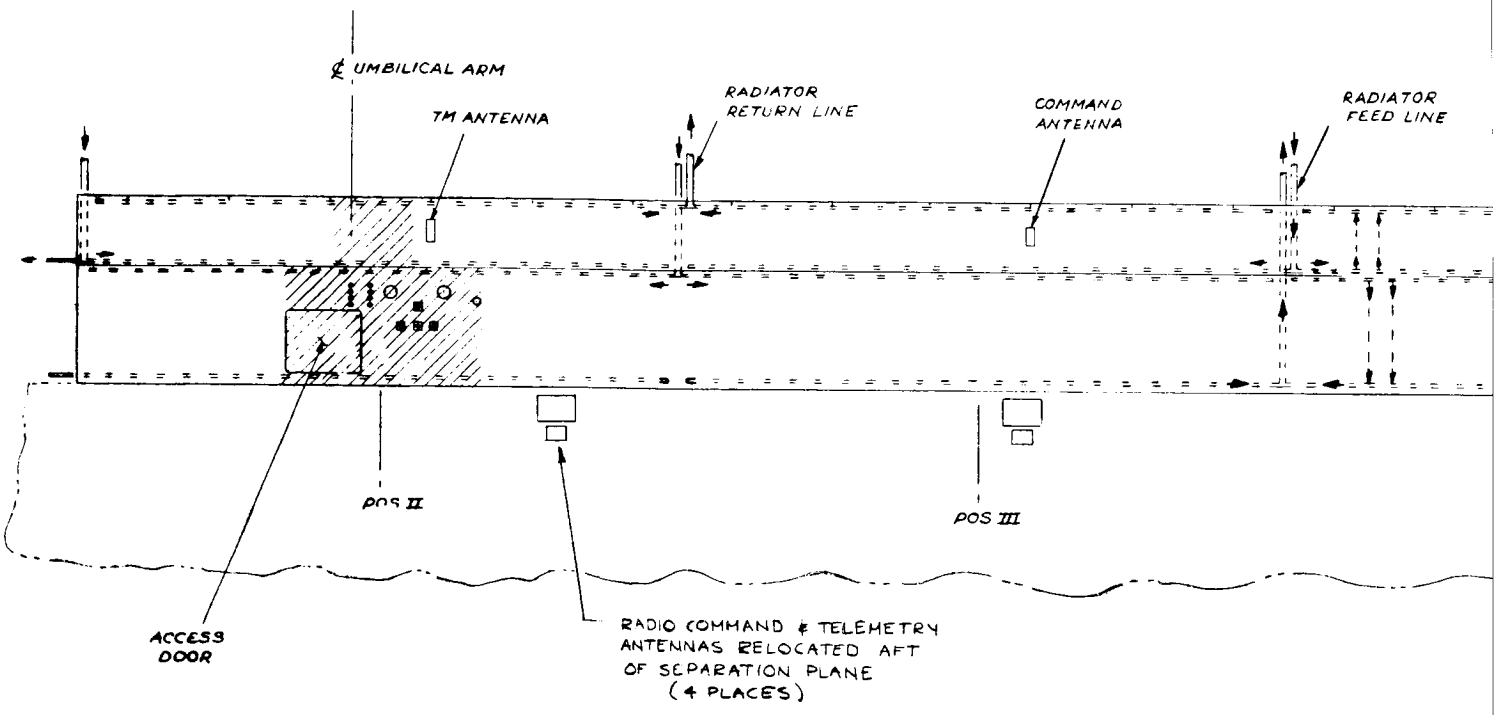

DEVELOPED VIEW OF SII

NOTE : TUBES ARE OMITTED IN HATCHE

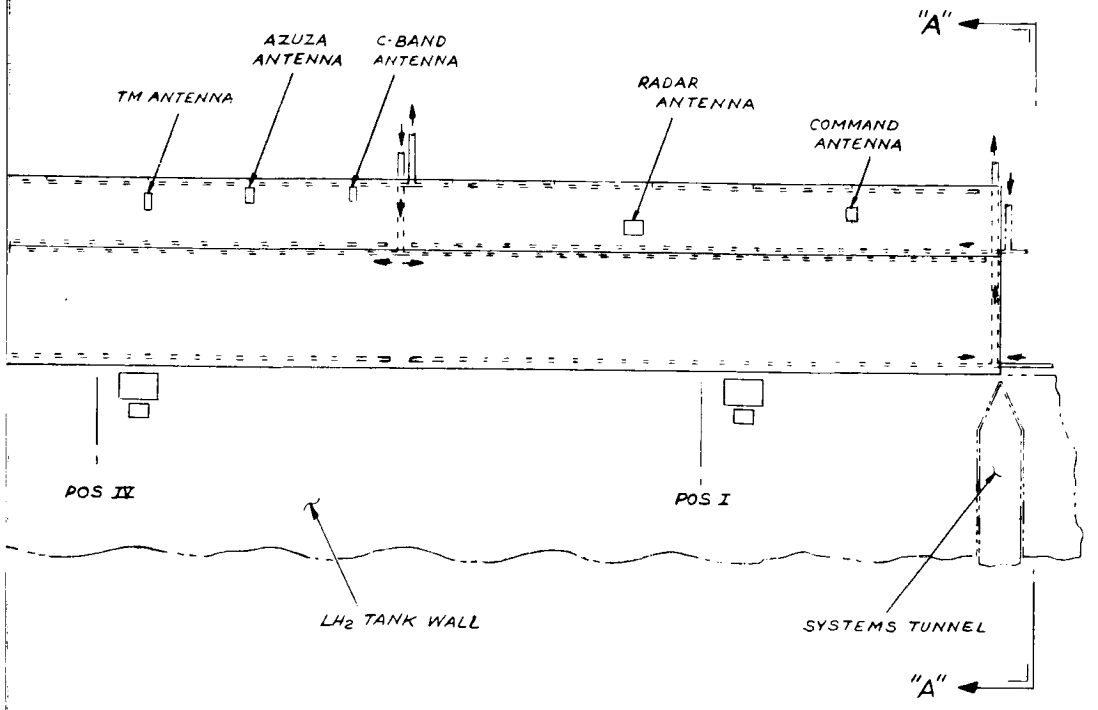

RADIATOR
D AREA

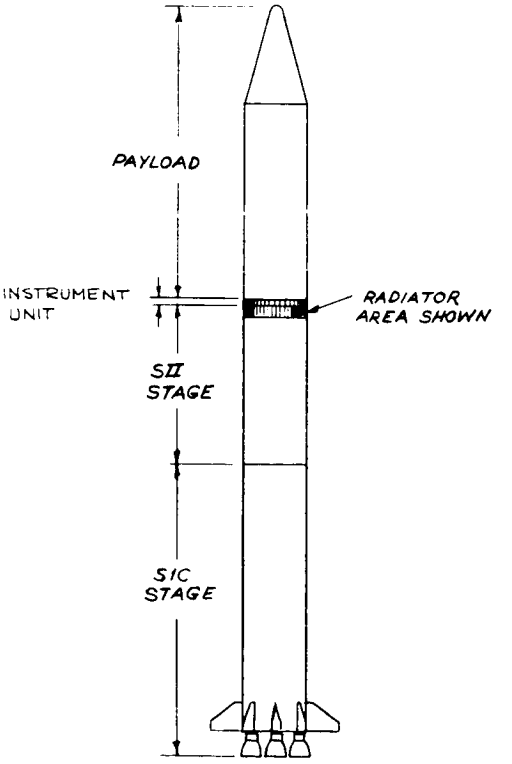

Figure 4-16. Radiator Integrated with S-II Forward Skirt

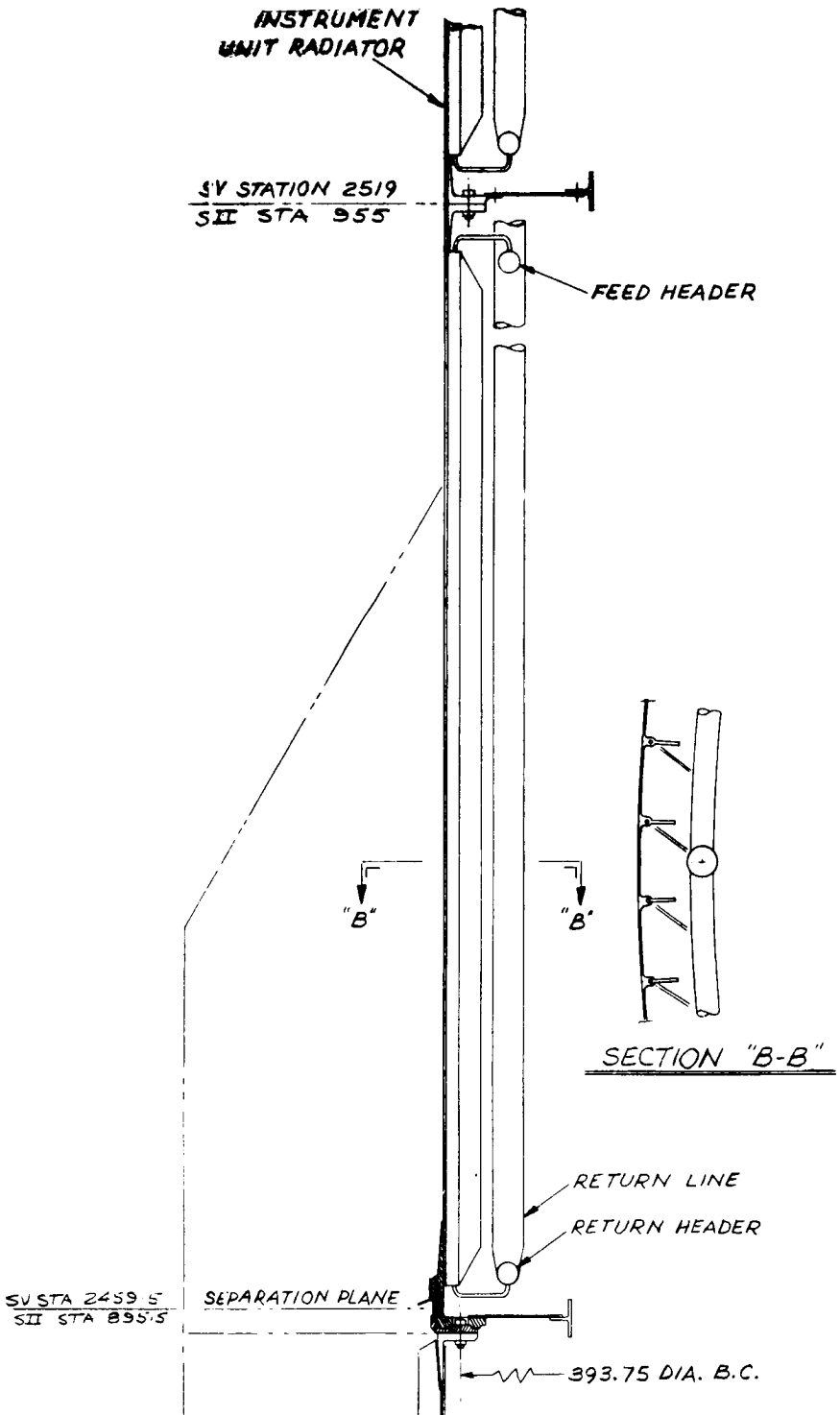
INSTRUMENT
UNIT RADIATOR
SV STATION 2519
SII STA 955
FEED HEADER
"B"
"B"
SECTION "B-B"
RETURN LINE
RETURN HEADER
SV STA 2459.5
SII STA 895.5
SEPARATION PLANE
393.75 DIA. B.C.

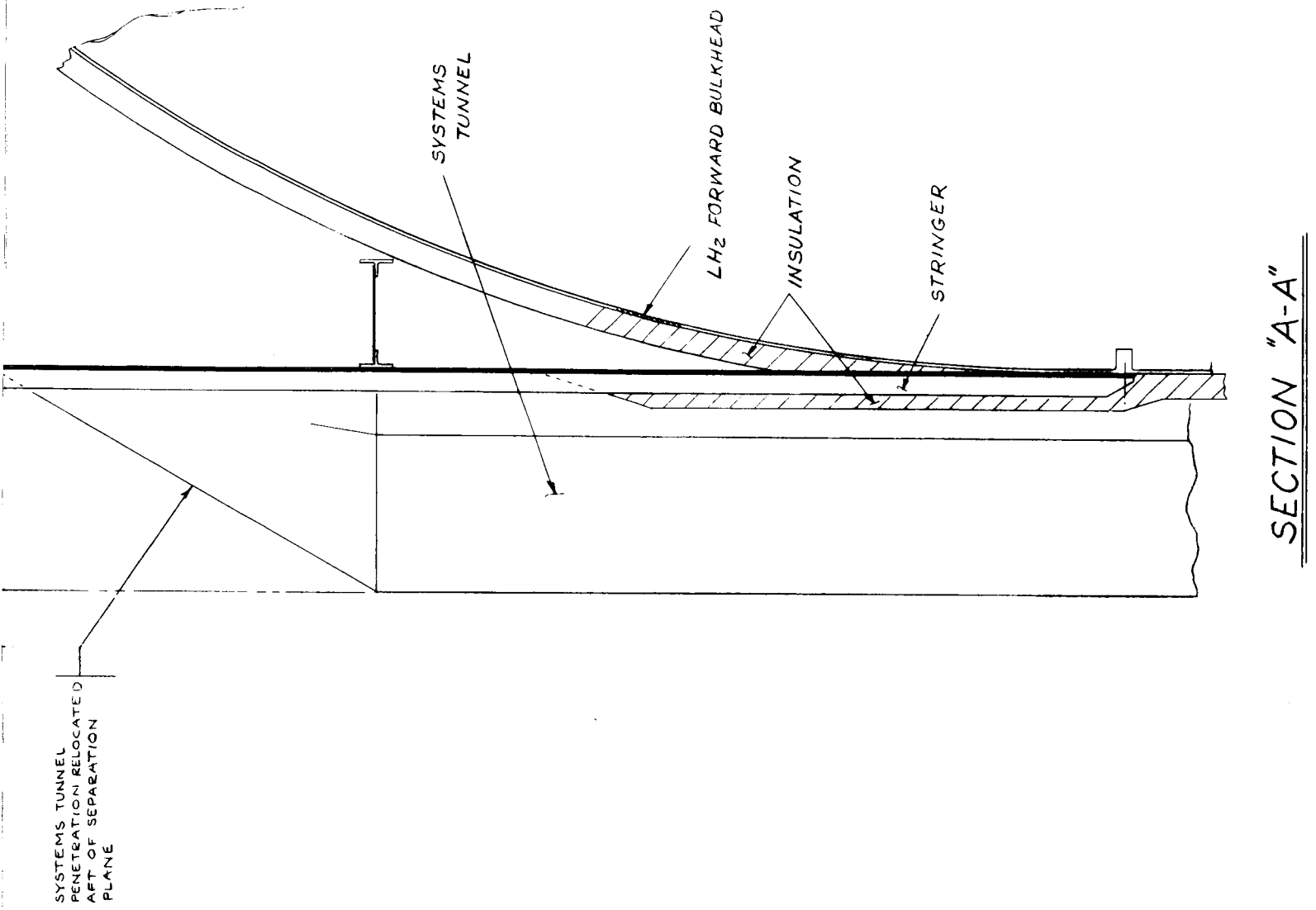

Figure 4-17. Section Through Radiator Integrated with S-II Forward Skirt

since most of the servicing in the forward skirt area will now be done at below the normal floor level. This awkwardness is part of the price paid for increased radiator area.

To utilize the tank surface of the S-II stage for radiator area, a completely different concept for tank construction must be used. Unlike the S-IVB stage, the S-II stage has external insulation, which makes the task of integrating the tank wall with a radiator much more difficult. Internal insulation is degraded by seepage of the liquid hydrogen, and must have sufficient density to withstand the compressive load imposed on it by tank pressurization. The S-II, having a much larger hydrogen tank than the S-IVB, is less able to afford these penalties. However, by using internal insulation, a radiator concept similar to that shown in Figure 4-13 could be used for the S-II.

A second approach would be to use external but jettisonable insulation. Based on Centaur experience, this could be accomplished for a weight of approximately 800 pounds (Reference 4-5). However, this would mean that the radiator would be launched at cryogenic temperature. Material selection must be compromised to obtain a material suitable for high temperature operation as well as cryogenic service. Thermal expansion problems between launch and radiator operation temperatures would be further aggravated. No experience is available for the use of bimetallic joints, as required for radiator construction, at cryogenic temperatures. Further, start-up of the radiator would be more difficult because the radiator would first have to be heated above the coolant freezing temperature. When the insulation is internal, freezing of the coolant is of less concern since aerodynamic heating during launch will maintain the radiator at elevated temperature.

The solution chosen for illustration is to use a double wall construction for the hydrogen tank, as shown in Figure 4-18. The radiator shell becomes the primary structure, carrying the aerodynamic and inertia loads from the payload. The inner shell then carries only the inertia loads of the tank itself, and the internal pressurization. Insulation is located between the two walls. (See Figures 4-19 and 4-20.)

Cutouts in the radiator are required for the command and telemetry antennas in the forward skirt as well as for the systems tunnel. The radiator extends aft to Station 1942, where an external field joint is used to join the radiator to the tank. Since the tank diameter is smaller than the radiator, it must make a transition aft of this joint to match the 33-foot diameter of

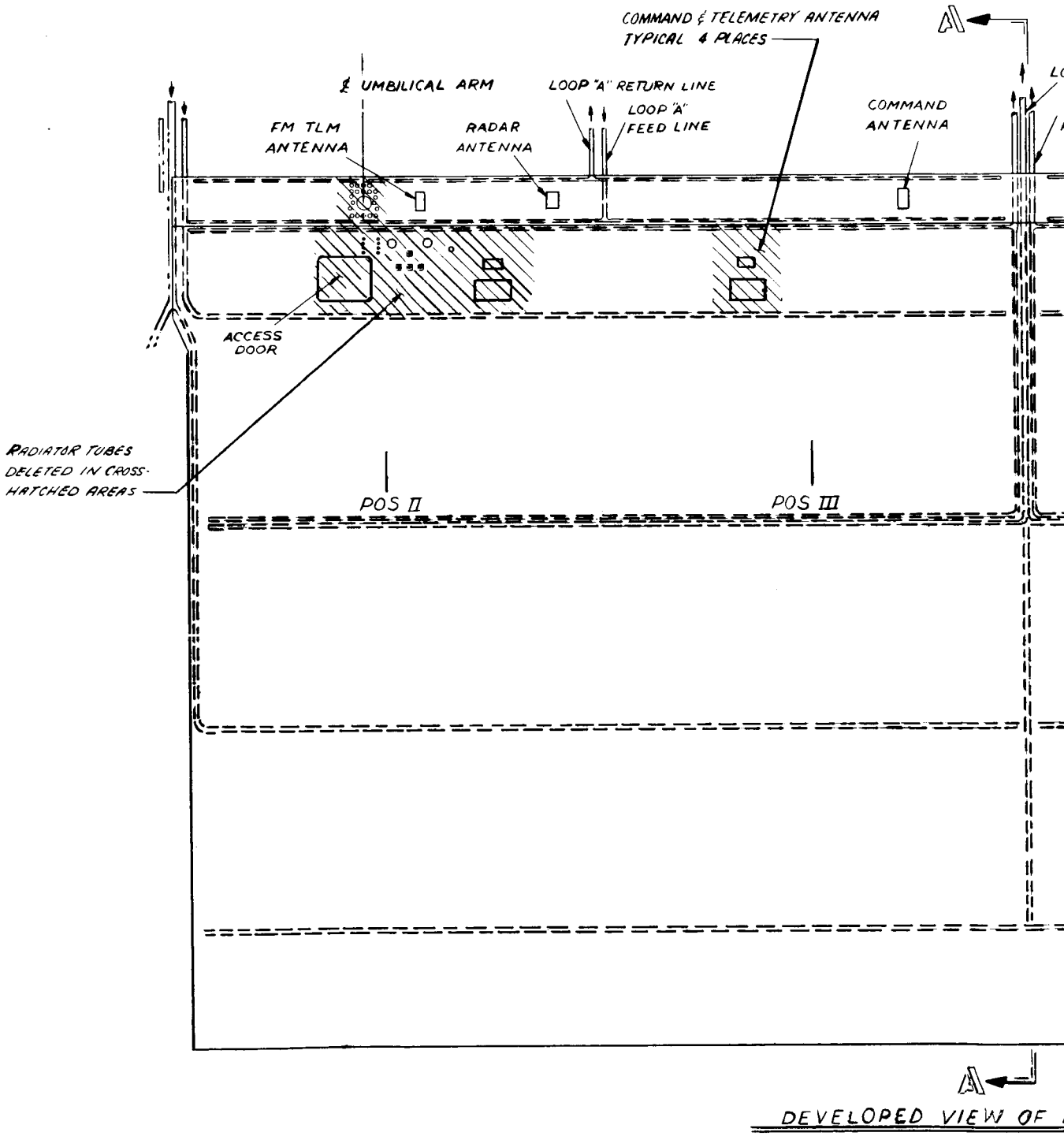

DEVELOPED VIEW OF

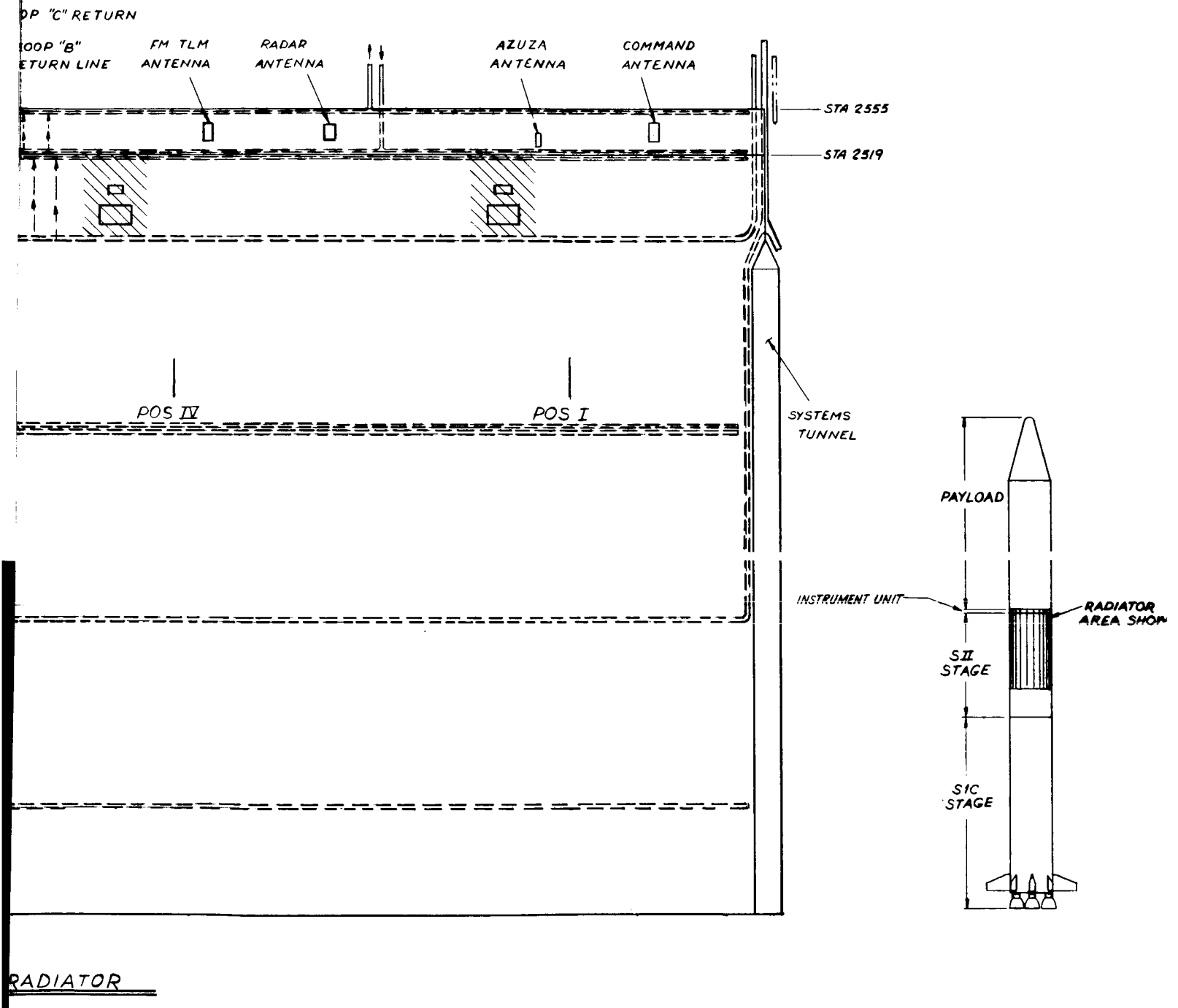

Figure 4-18. Radiator Integrated with S-II Hydrogen Tank

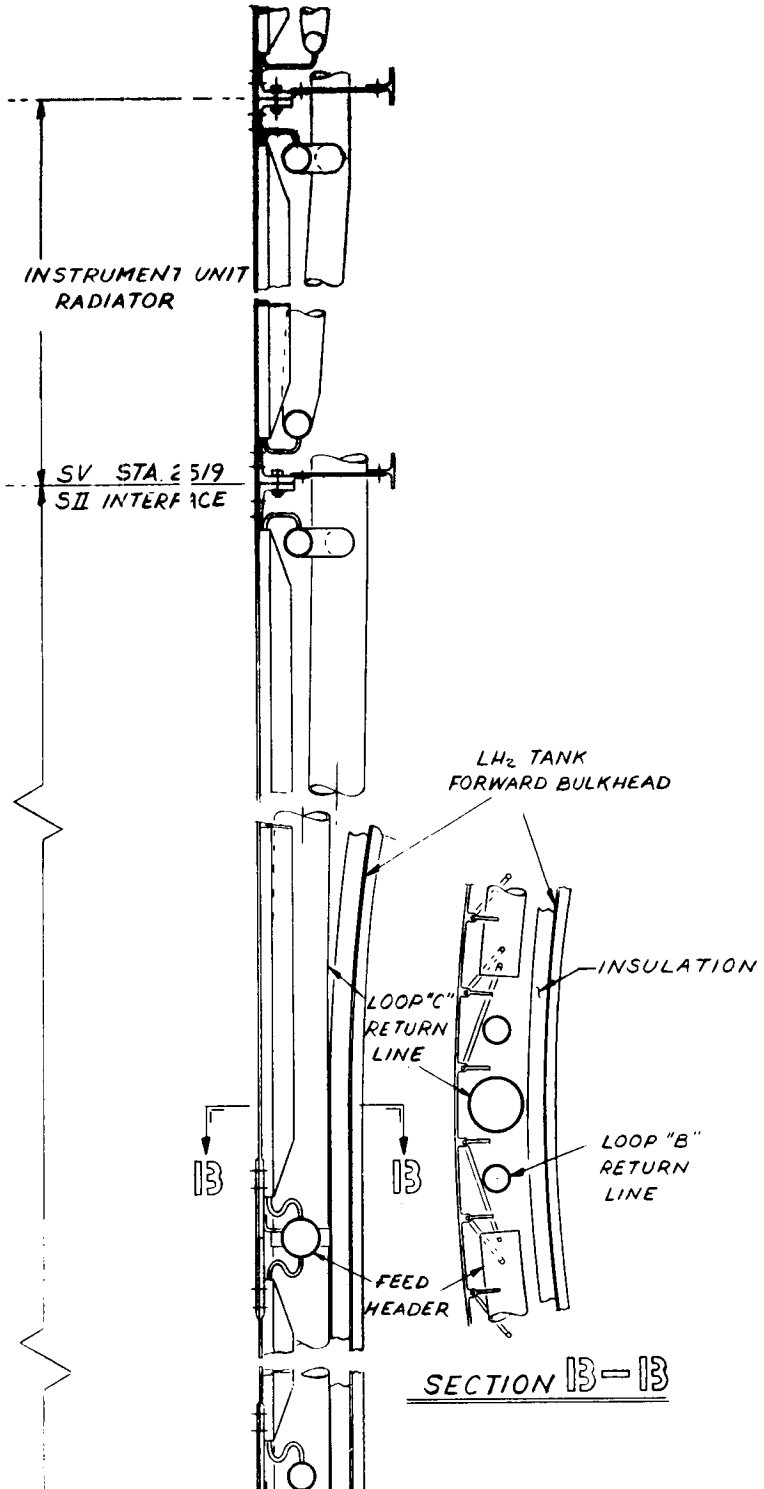

SECTION 13-13

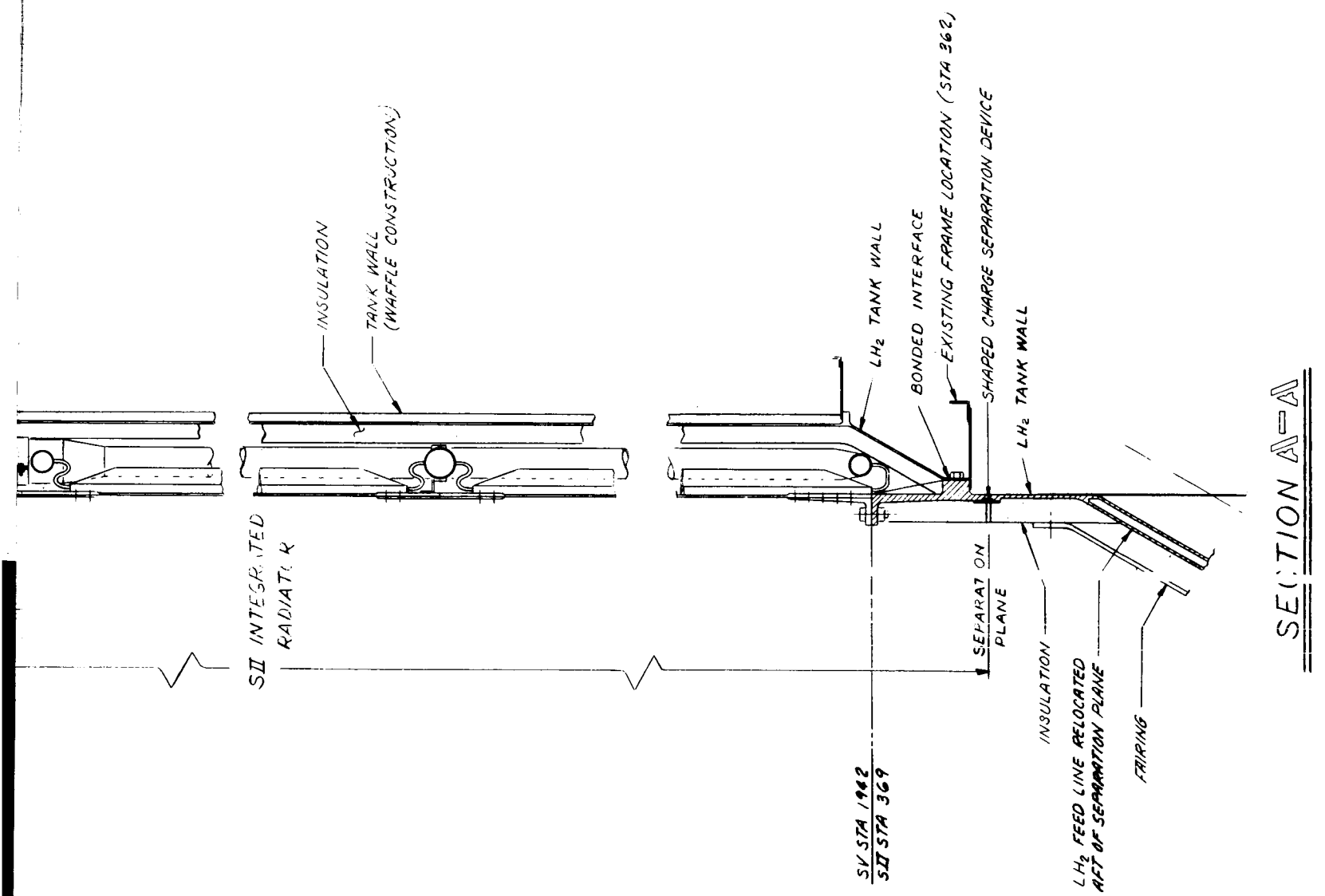

Figure 4-19. Section Through Radiator Integrated with S-II Hydrogen Tank

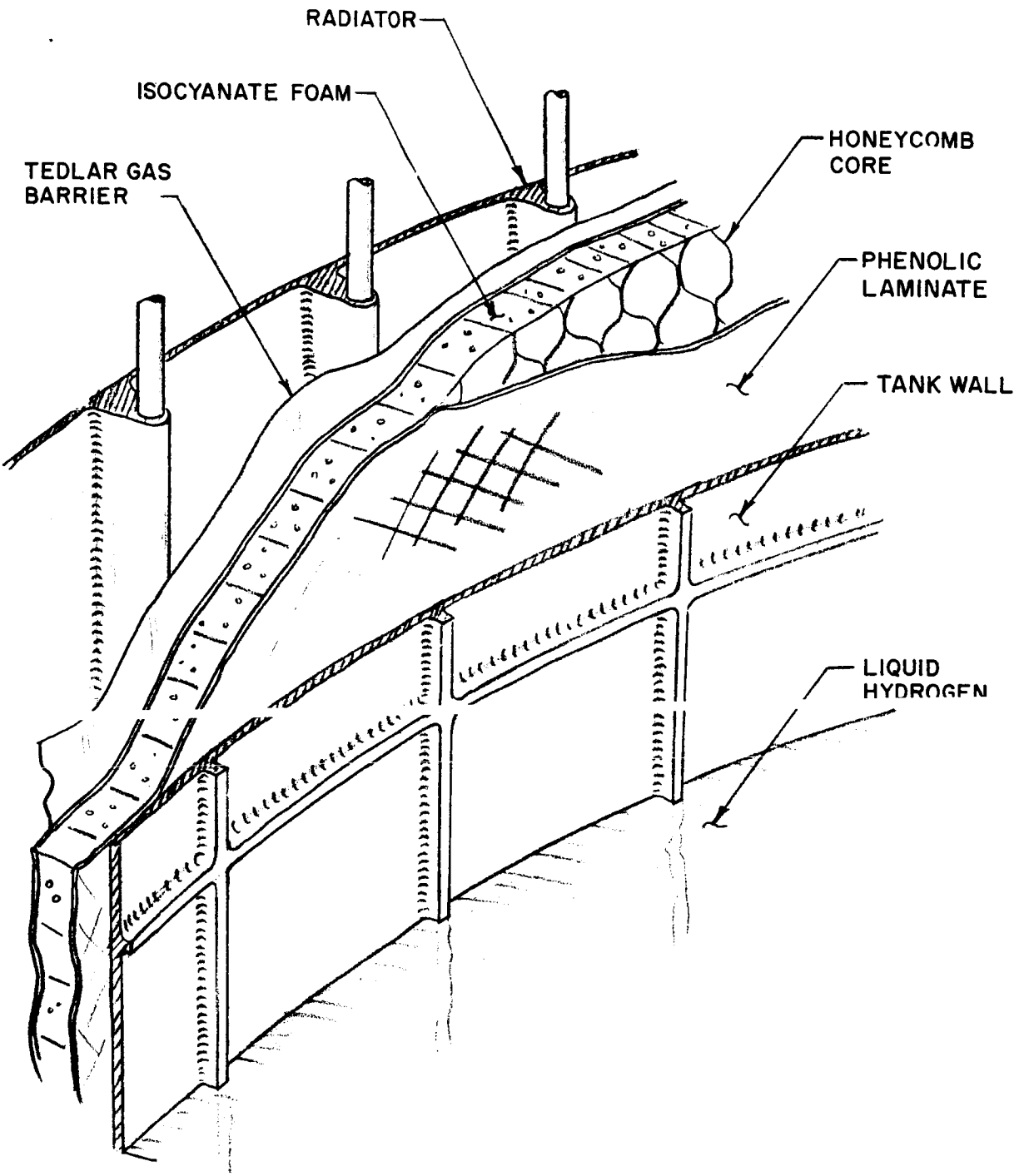

Figure 4-20. Detail of Radiator Integrated with S-II Hydrogen Tank

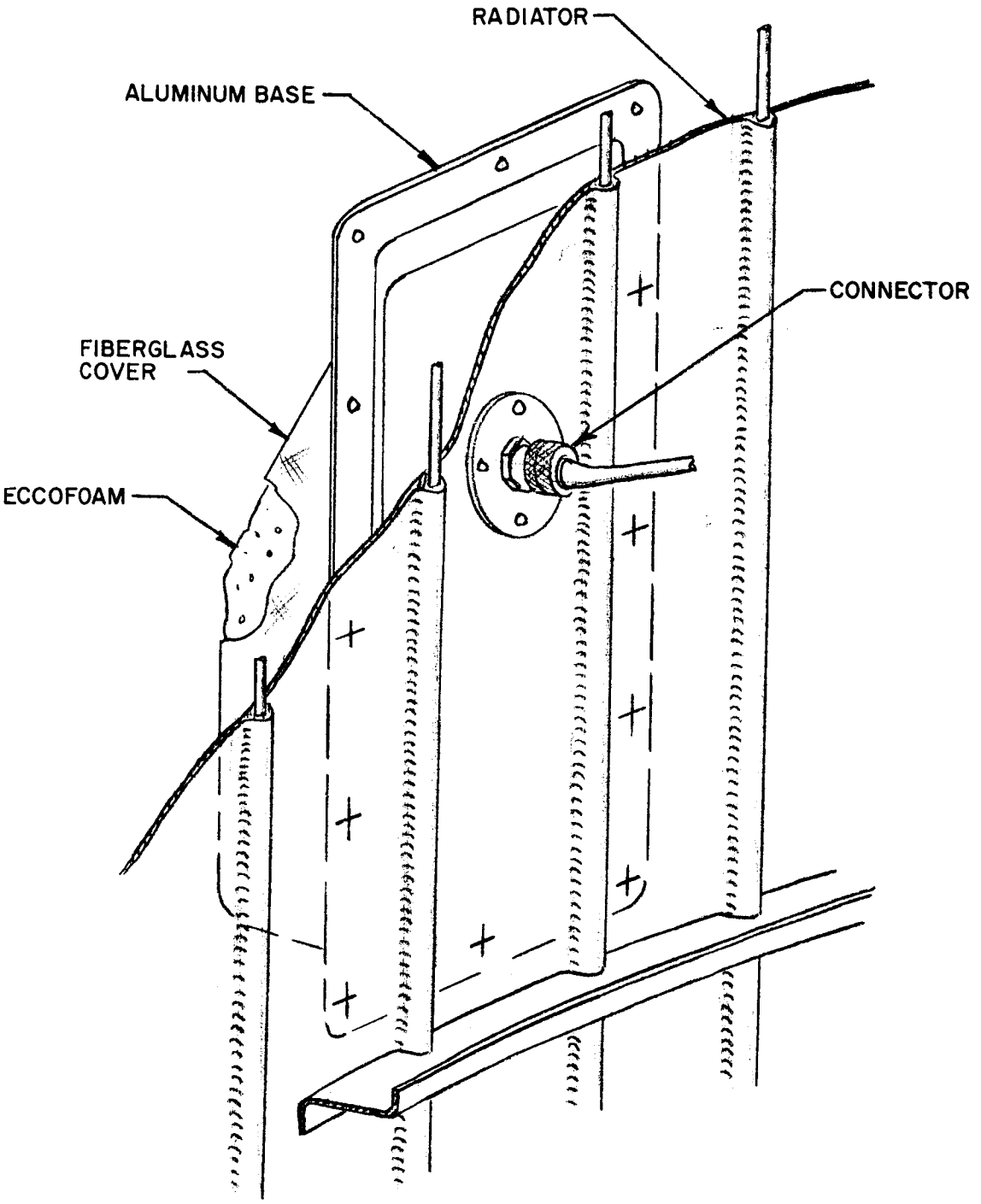

Figure 4-21. Typical Antenna Installation on Integral Radiator

the load carrying shell. Separation then takes place below this transition so that the inner tank shell remains with the radiator. The liquid hydrogen feed lines are relocated aft of the separation plane to avoid the need for explosive disconnects. Similarly, the liquid hydrogen recirculation, fill and drain lines, and the wiring for the engine cutoff sensor, and all associated external fairings are relocated to the short section of hydrogen tank between the separation plane and the bolting ring to the oxygen tank.

As shown, most of the hydrogen tank remains with the radiator after separation. Since the materials presently used for insulation (tedlar, phenolic laminate, isocyonate foam) will not withstand the radiator operating temperatures, new materials will be required. An alternative would be to permit decomposition, sublimation, and outgassing of this material by providing vents and by locating all equipment that might be adversely affected by the outgassing material away from the vents. If the radiator operating temperature is high enough, even the aluminum used in the tank construction may not be stable. A typical radiator temperature for a potassium Rankine nuclear power system is 1250^{o}F. Disposal of the aluminum as the radiator temperature rises is much more conjectural. Sublimation rates below the melting temperature (1200^{o}F) are negligible, while the behaviour of liquid aluminum at zero "g" in a vacuum is unknown. It is feasible, that with sufficient temperature drop through the insulation and a sufficiently large radiating surface of the tank (through the opening made by separation), the aluminum can be maintained below its melting temperature. If it is necessary to use a material for the tank that is capable of withstanding higher temperatures, (e.g., stainless steel) a bimetallic joint must then be made between the hydrogen tank inside the radiator and the section aft of the radiator, which will presumably be aluminum. This is shown in Figure 4-19 as a "bonded" joint. The actual process could be either adhesive bonding or a process such as "A1-Fin." *

A more reasonable approach, although mechanically more complex, would be to dispose of the entire hydrogen tank at separation. This would require moving the separation plane to just aft of the field joint at Station 1942, and providing a device for guiding the tank as it is extracted from the radiator. Separation devices would then be required for all services to the umbilical Panel.

---

*Proprietary method for joining aluminum and steel, A1-Fin Corporation, Bethel, Connecticut.

4.3 FACILITY LIMITATIONS

4.3.1 SATURN IB FACILITIES

The facilities for assembly and launch of the Saturn IB vehicle are of interest in this study in that they establish a maximum length which cannot be exceeded. The major facilities for the Saturn IB are Complex 34 and Complex 37. (See Figure 4-22.)

Assembly of the vehicle takes place on the launch pedestal installation, each stage being lifted by a derrick on top of the service structure. The service structure of Complex 37 is the taller of the two and so establishes the maximum height limitation.

The derrick maximum hook height is 350 feet above pad level. Since the vehicle rests on the launch pedestal installation 35 feet above the pad level, the maximum vehicle height that can be accommodated, with a six-foot sling clearance, is 309 feet. This would permit a payload length of 167 feet, measured from the top of the Instrument Unit (IU-Vehicle Station 1698.8). The service structure is designed so that an additional 30 feet can be added to the top, if needed.

4.3.2 SATURN V FACILITY

The height limitation for the Saturn V is established by the door on the Vehicle Assembly Building (VAB). The vehicle is assembled on the base of the Mobile Launcher inside the VAB. The Mobile Launcher (ML), with the vehicle, is then lifted from its pedestals and removed from the VAB by the Crawler-Transporter. The door opening on the VAB is 406 feet from the reference plane at the base of the ML, which is 10 feet above the bottom of the vehicle. Allowing six feet for clearance, this permits a maximum vehicle of 400 feet above the ML base, or a total of 410 feet overall. This limitation was used as a ground rule for the Saturn V Improvement Studies.

The 410-foot limitation permits a payload length of 128.8 feet measured from the top of the IU (Vehicle Station 3258.6). For two stage versions of the Saturn V (eliminating the S-IVB stage), the top of the IU would be at Vehicle Station 2555, permitting a payload length of 187.4 feet.

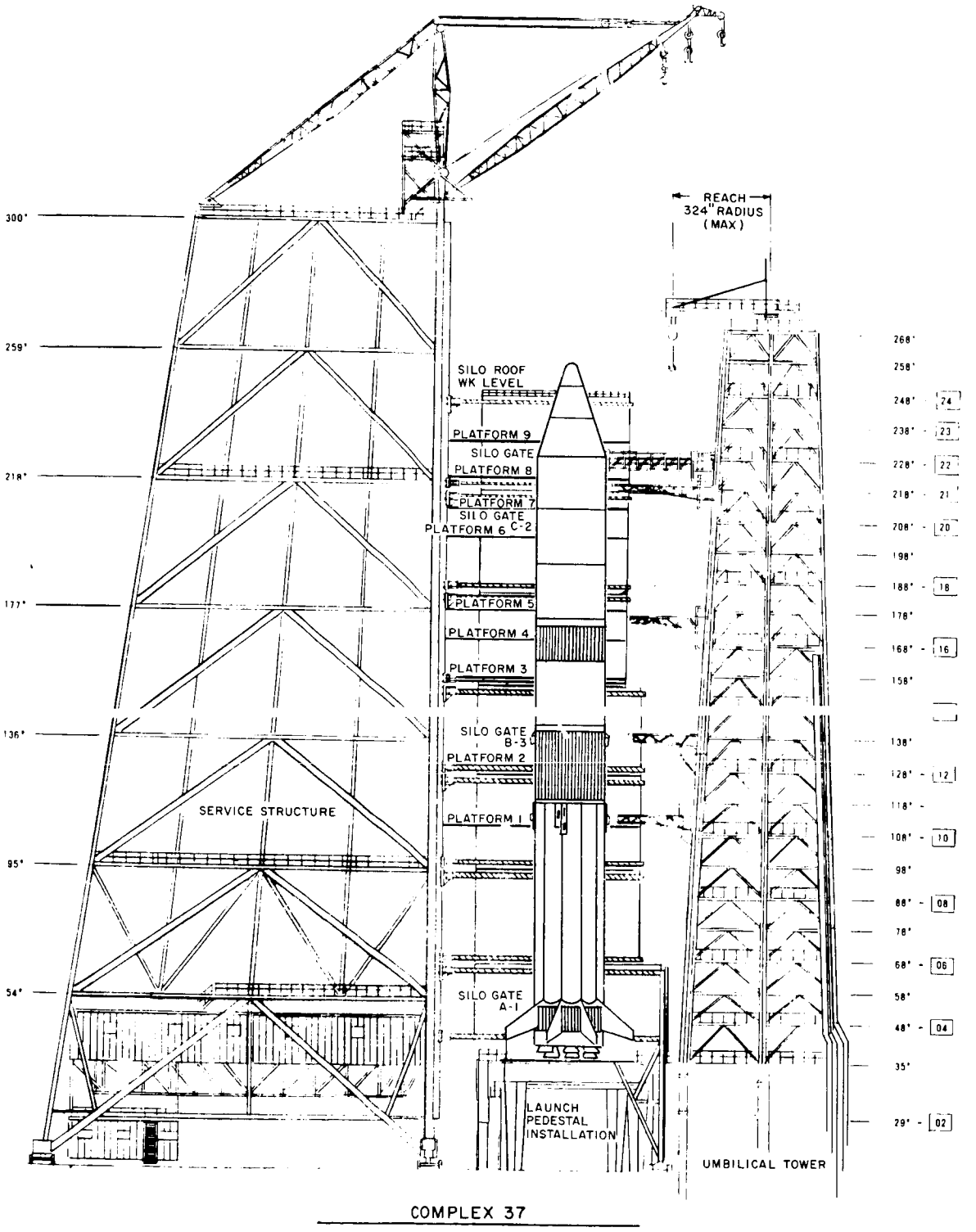

Figure 4-22. Service Structure for Launch Complex 37, KSC

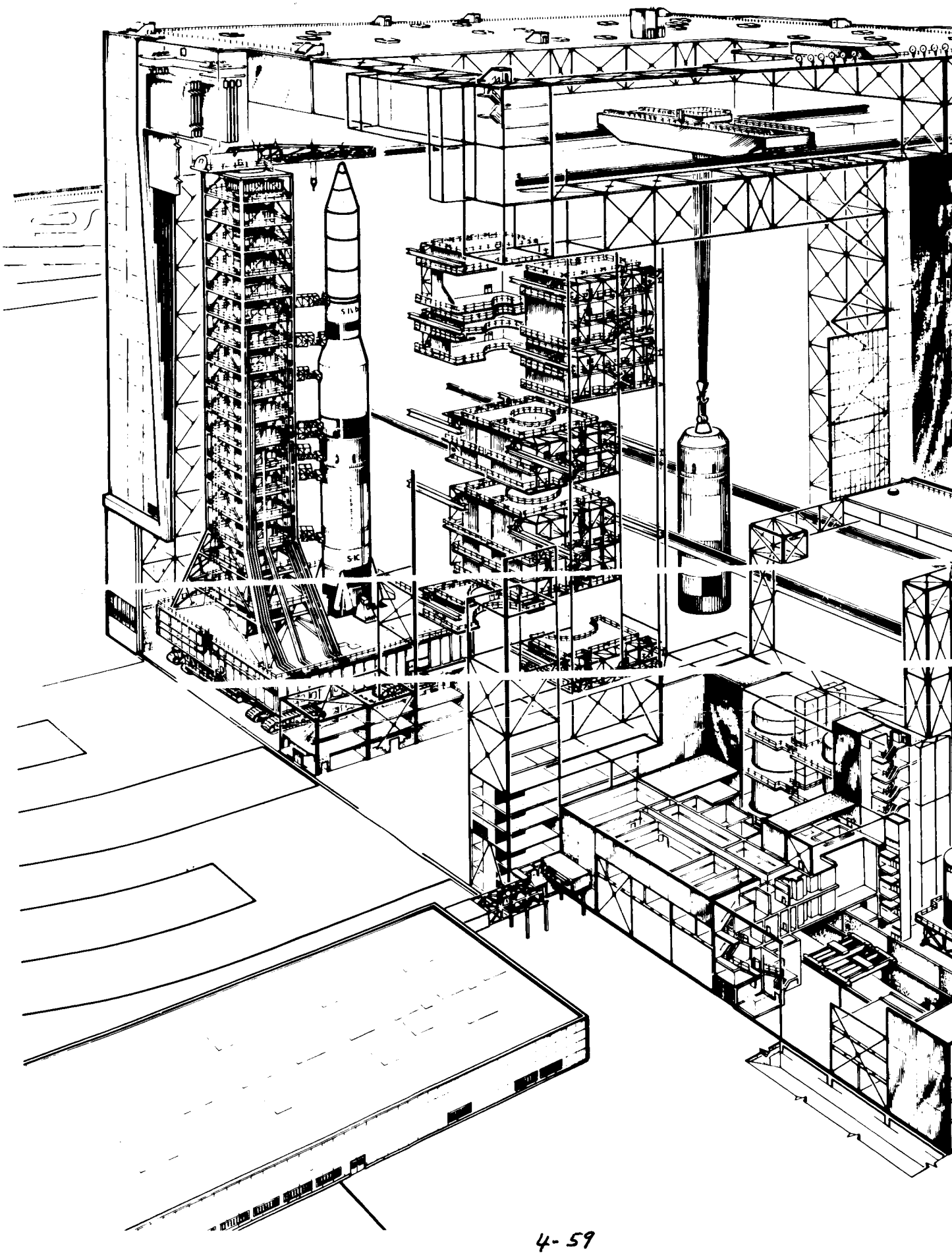

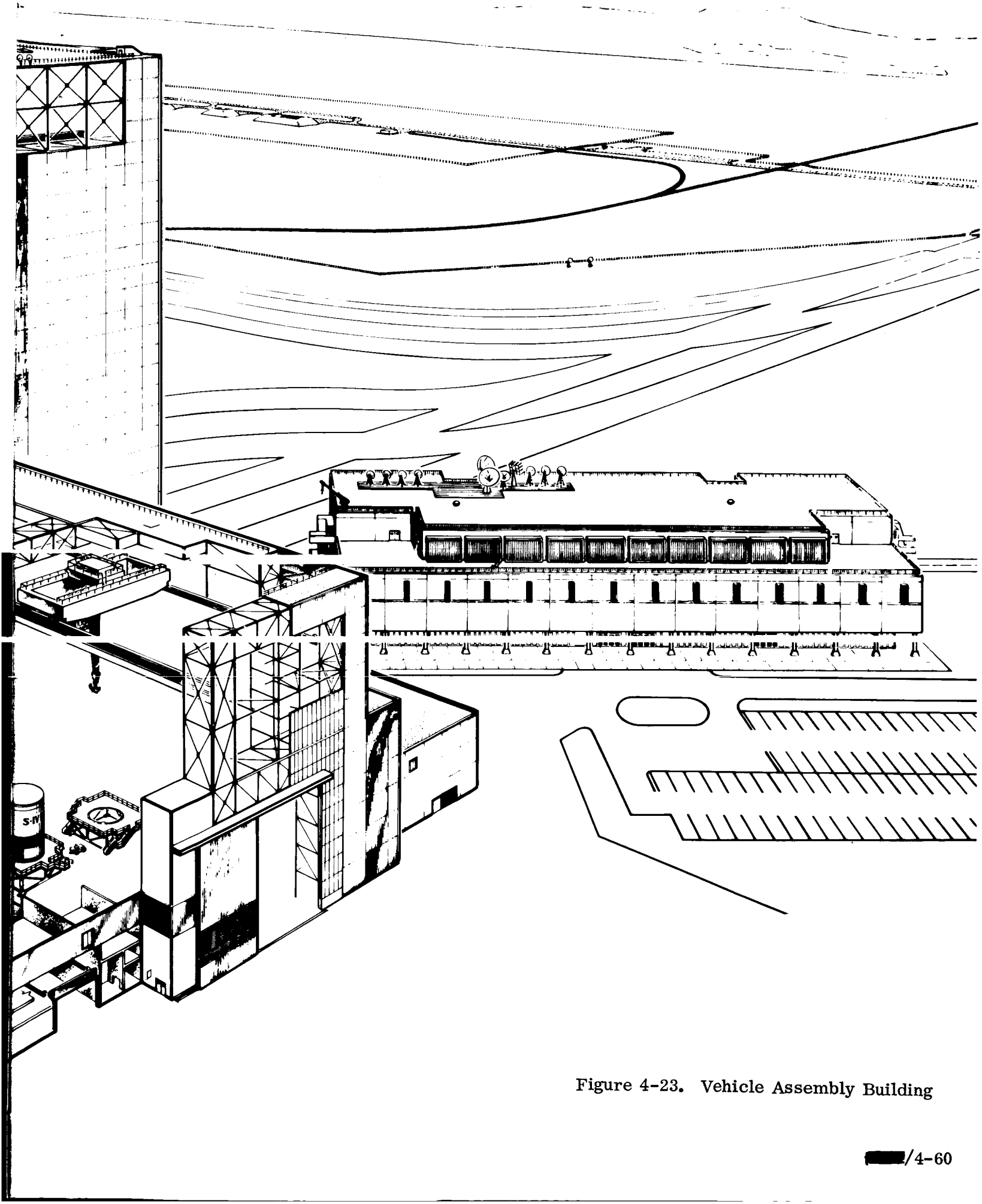

Figure 4-23. Vehicle Assembly Building

For "modified" Saturn V vehicles, the corresponding maximum payload lengths would be less because of the increased lengths of the lower stages. For example, the top of the IU on the three stage MLV-SAT-V-3 is at Vehicle Station 3884.5, permitting a payload length of 75.0 feet. The top of the IU on the two stage MLV-SAT-V-3 is at Vehicle Station 2982, permitting a payload length of 151.8 feet.

4.4 SUMMARY OF RADIATOR AREA CAPABILITIES

It is concluded from the investigation of launch loads in Section 3. that the loads at maximum "$q\alpha$" determine the critical design condition and limit the maximum radiator area that can be obtained above the launch vehicle interface. These areas were listed in Table 3-3. Even for the minimum 10-degree cone angle considered, the powerplant length at which maximum area occurred did not exceed the length limitations imposed by the launch facilities, as discussed in Section 4.3. This was true for the standard launch vehicles defined for the Apollo program. For improved Saturn V vehicles, however, the door height on the Vehicle Assembly Building (VAB) is the critical limitation.

To the radiator area limits established by launch loads can be added the radiator area obtained by utilization of the upper stages. These areas are summarized in Table 4-1. The negative areas shown for the sheath radiators are the areas required for an adapter section. This area must be subtracted from the area that would normally be available above the launch vehicle interface.

The total area available, as a function of the degree of upper stage utilization, is shown in Figures 4-24, 4-25 and 4-26. The curves are drawn for unmanned and manned missions, corresponding to factors of safety of 1.25 and 1.40, as discussed previously. Nominal payload weights were assumed for each launch vehicle. As shown in Figure 4-27, the variation in payload weight has a small effect on the maximum radiator area.

TABLE 4-1. SUMMARY OF AREA AVAILABLE (FT^2)

RADIATOR CONFIGURATION \ LAUNCH VEHICLE / TOTAL PAYLOAD WT. (LB)		SATURN IB 30,000	SATURN V (THREE-STAGE) 100,000	SATURN V (TWO-STAGE) 250,000
1	Above IU (10^{o} cone angle)	3,078	3,235	12,435
2	Sheath over IU and forward skirt	636 (- 98)	636 - 98	---
3	Sheath over forward skirt	654 (- 98)	654 - 98	757 (- 86)
4	Sheath over skirt and tank	1,935 (- 98	1,935 (- 98)	4,576 (- 121)
5	Integral with IU	186	186	302
6	Integral with IU and forward skirt	604	604	776
7	Integral with IU forward skirt and tank	2,208	2,208	5,045
8	Maximum area (payload and integral radiator over IU, skirt and tank)	5,286	5,443	17,490

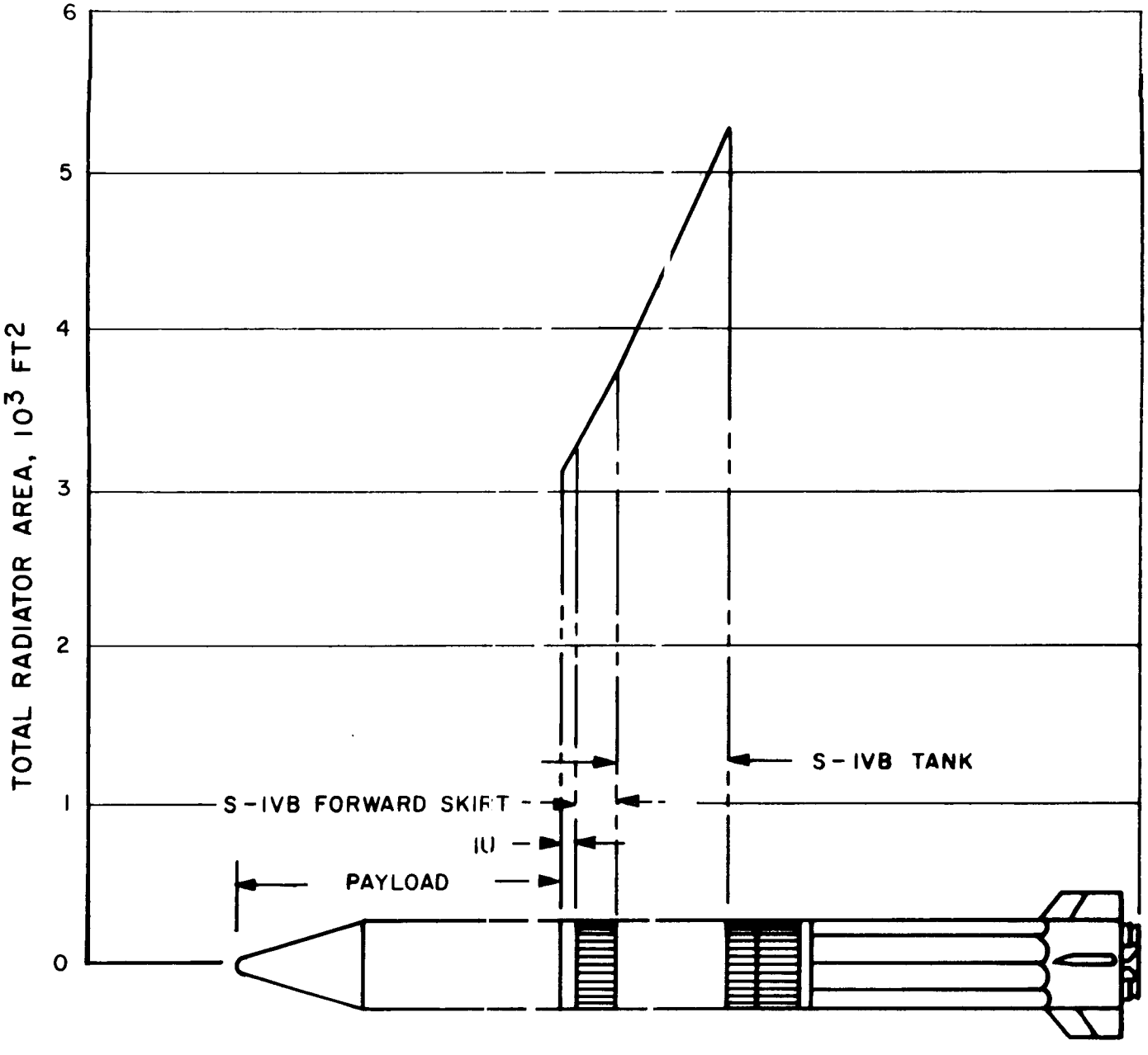

Figure 4-24. Radiator Area Utiliz ng Upper Stage-Saturn 1B Launch Vehicle

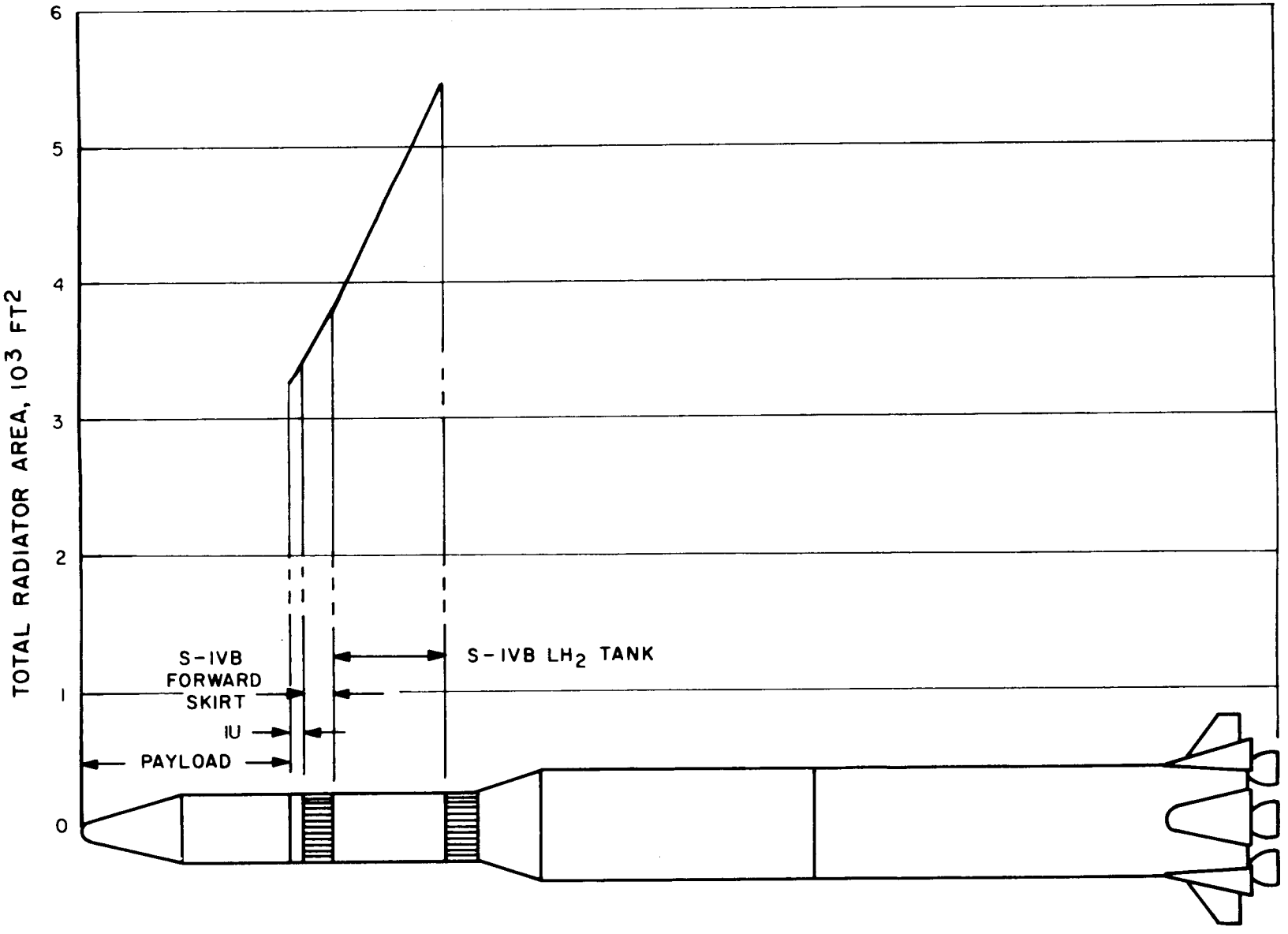

Figure 4-25. Radiator Area Utilizing Upper Stage-Saturn V Launch Vehicle (Three-Stage)

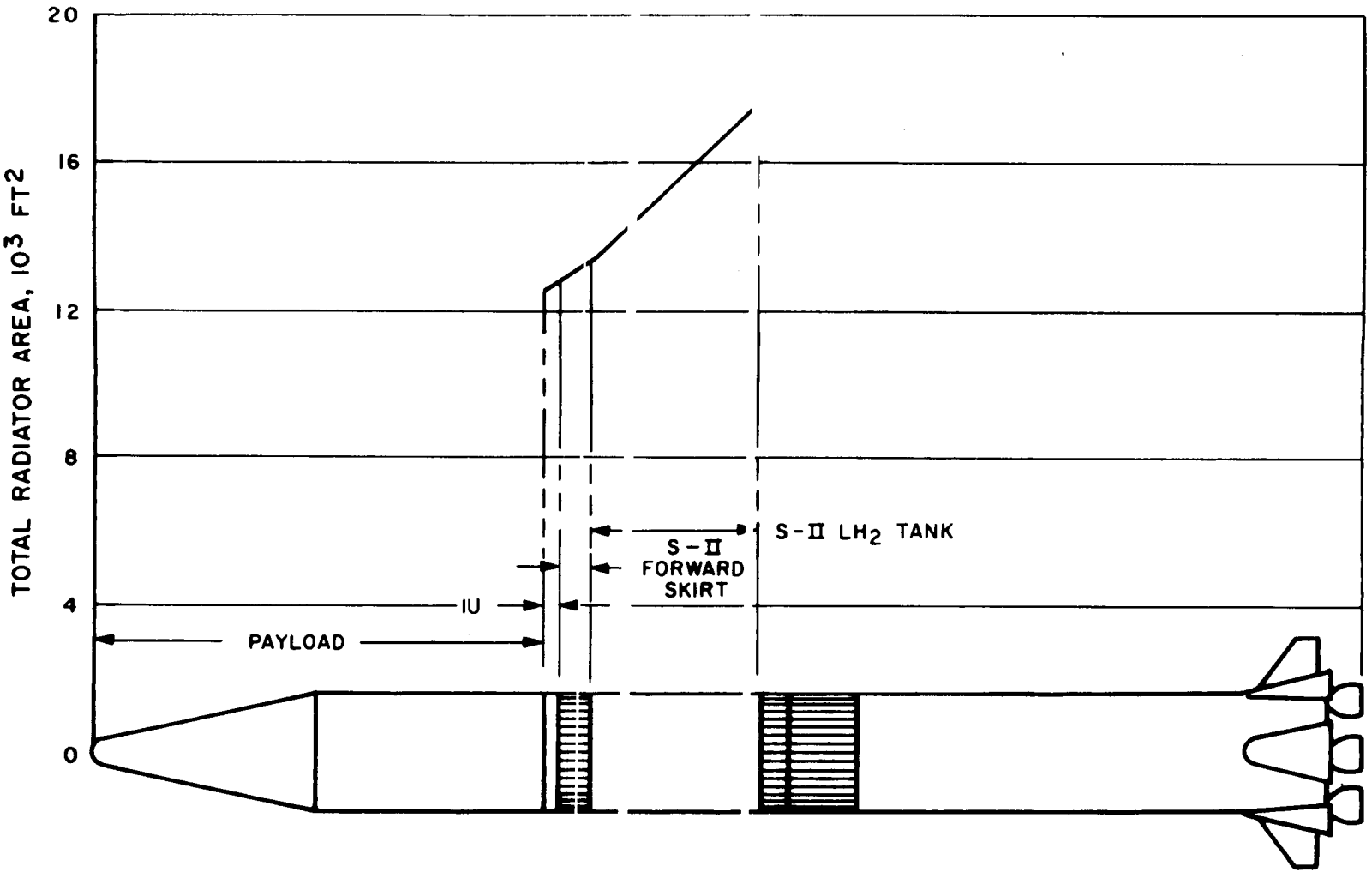

Figure 4-26. Radiator Area Utilizing Upper Stage-Saturn V Launch Vehicle (Two-Stage)

4.5 REFERENCES

4-1. Saturn IB Improvement Study (Solid First Stage) Phase II, Final Detailed Report," Douglas Report SM-51896, 30 March 1966.

4-2. "Saturn V Improvement Study, Final Summary Document," Boeing Report D5-13109-1, April 30, 1965.

4-3. "Saturn Antenna Systems SA-204," 60C09060 Chrysler Corporation (Contract NAS8-4016).

4-4. "Study of Kennedy Space Center Safety Hazards," TRW (Contract NAS10-3082), 22 September 1966.

4-5. Perkins, P. J. and Esgar, J. B. "A Lightweight Insulation System for Liquid Hydrogen Tanks of Boost Vehicles," AIAA Fifth Annual Structures & Materials Conference, April, 1964.

5. EFFECT OF LIMITATIONS ON RADIATOR DESIGN

5.1 AREA-LIMITED OPTIMA

Having determined the radiator area available, as limited by launch loads and the degree of utilization of the upper stages, the effect of these limitations on the design of the radiator will now be examined.

For a radiator of specified heat rejection capability and meteoroid survival probability, there are unique values of fin thickness and tube spacing which result in the minimum weight radiator. If the fin thickness or tube spacing are changed from these optimum values, the radiator weight will increase in the manner shown in Figure 5-1. If the fin thickness is increased (point A), the weight change can be attributed to the increased fin weight. If the fin thickness is decreased, (point B), the loss in bumper effect causes an increase in the tube armor on the back side of the tube, causing the weight to increase. A decrease in the tube spacing (point C) means more tubes, increasing the vulnerable area which causes an increase in armor weight. When the tube spacing is increased (point D), the vulnerable area decreases and armor thickness is less. However, this is offset by an increase in radiator area as a result of a decrease in fin efficiency. The result is that the total radiator weight increases.

Fin efficiency is also decreased when the fin thickness is decreased, as at point B. The larger area required accounts for additional weight increases. As a result, when contours of constant weight are drawn, the slope is steepest in this direction, as shown in Figure 5-2.

The weights shown in this figure are for a radiator rejecting 5,000 kw and having a meteoroid survival probability of 0.90. Figures 5-3 and 5-4 show similar curves for probabilities of 0.95 and 0.99 respectively. The other assumptions used in the analysis from which these curves are derived are listed in Table 5-1.

Superimposed on the weight contours of Figures 5-2, 5-3 and 5-4 are lines of constant fin efficiency. Since the heat rejected is a constant, these lines may be regarded as lines of constant area, the area being inversely proportional to fin efficiency. Where the weight contours are tangent to the fin efficiency, lines are points of minimum weight for a fixed fin efficiency or radiator area. The locus of these tangent points, therefore, is the line of area limited optima. The radiator weights of these optima are plotted in Figure 5-5.

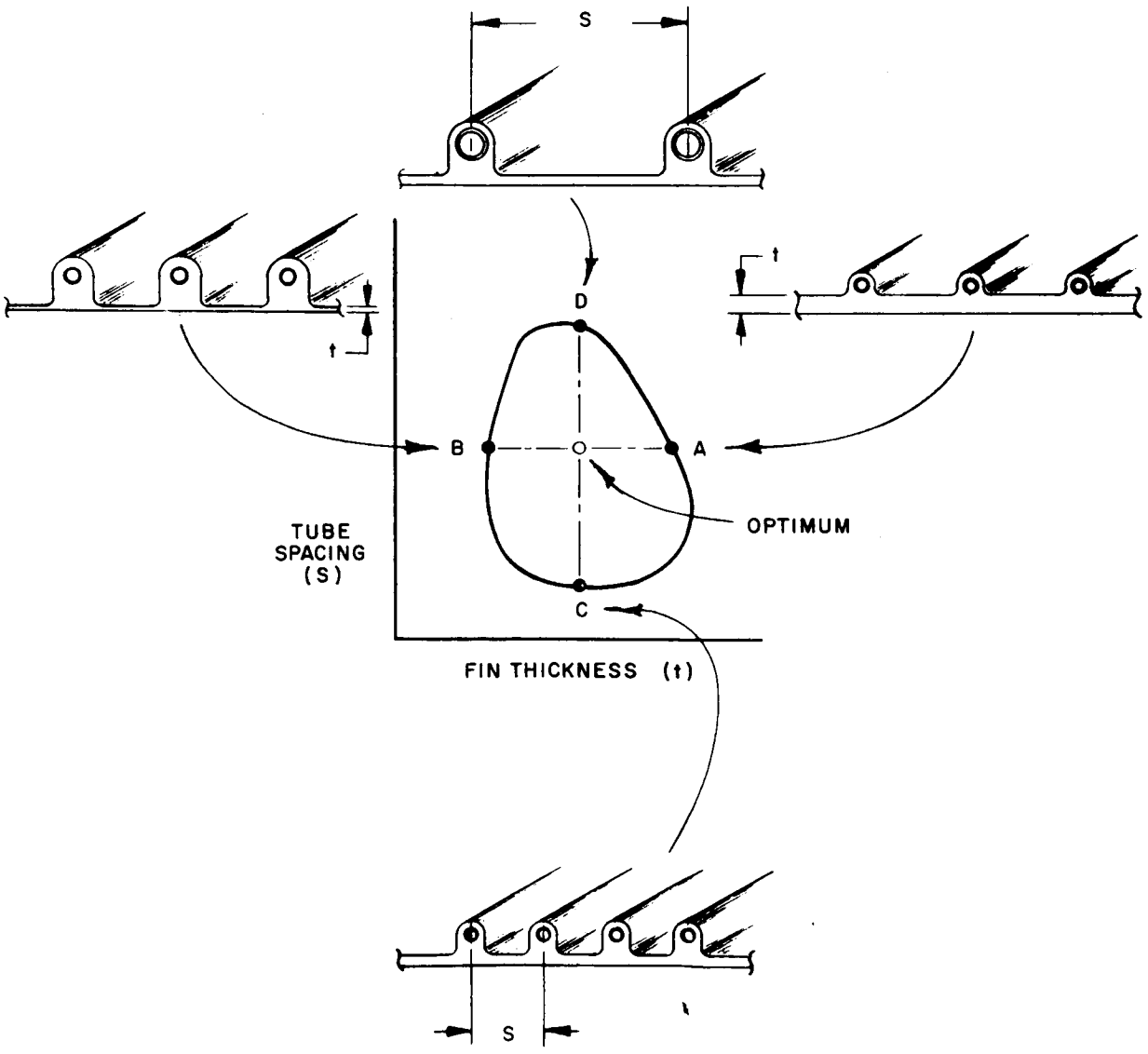

Figure 5-1. Optimum Radiator Geometry

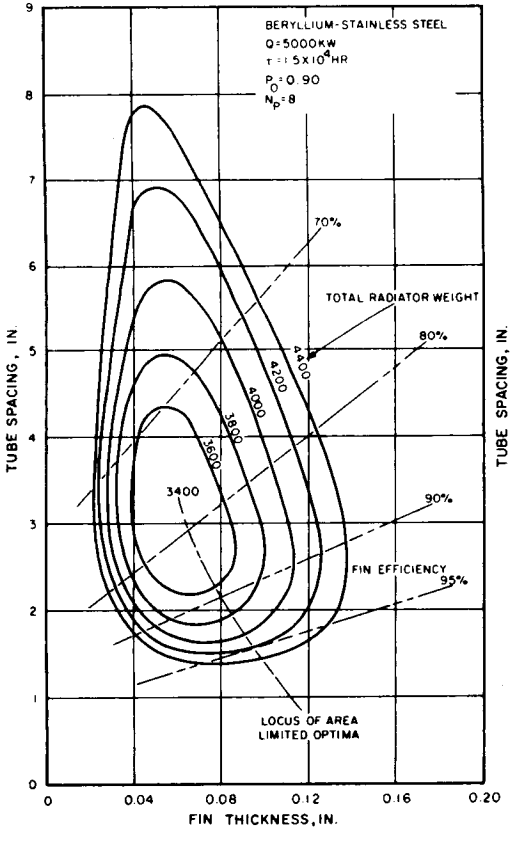

Figure 5-2. Beryllium "Thumbprint", P_O=0.90

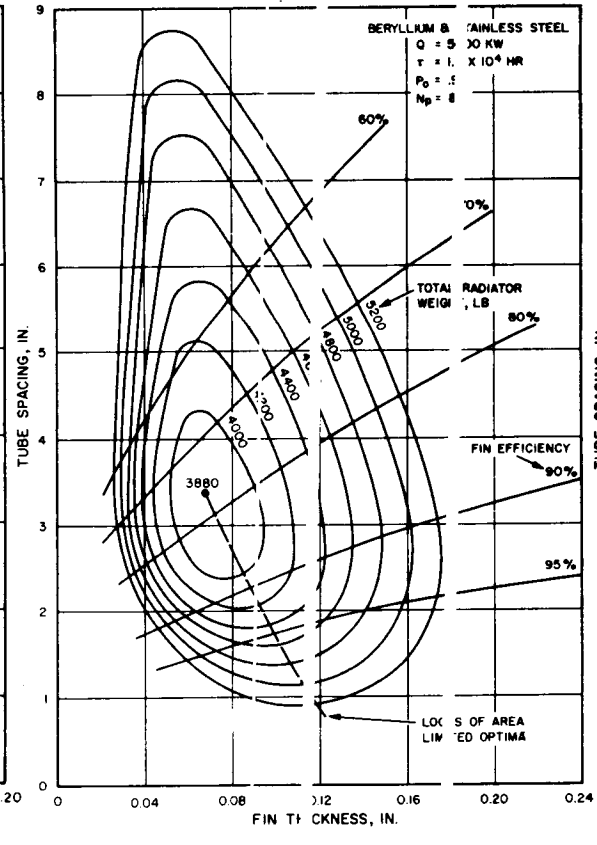

Figure 5-3. Beryllium "Thumbprint", P_O=0.95

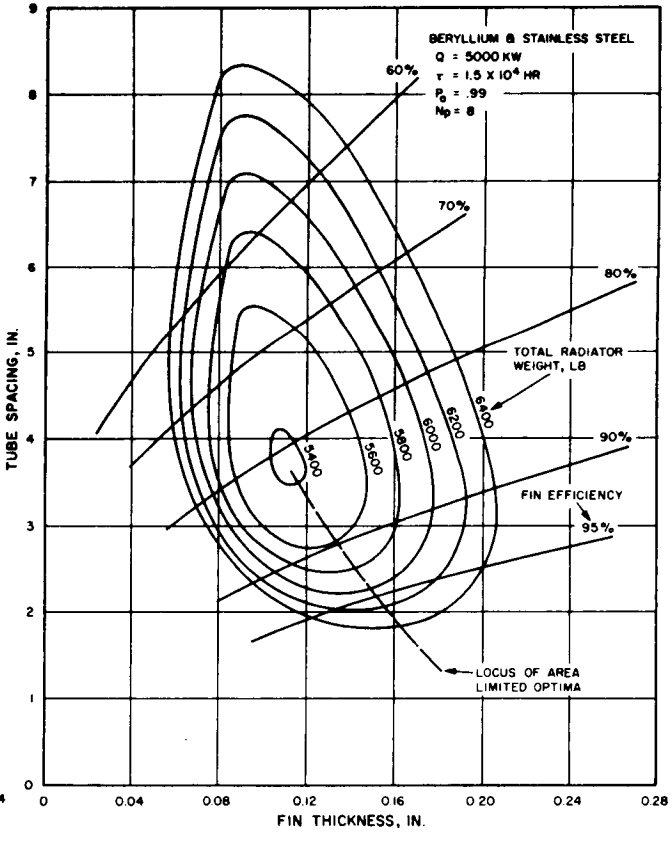

Figure 5-4. Beryllium "Thumbprint", P_O=0.99

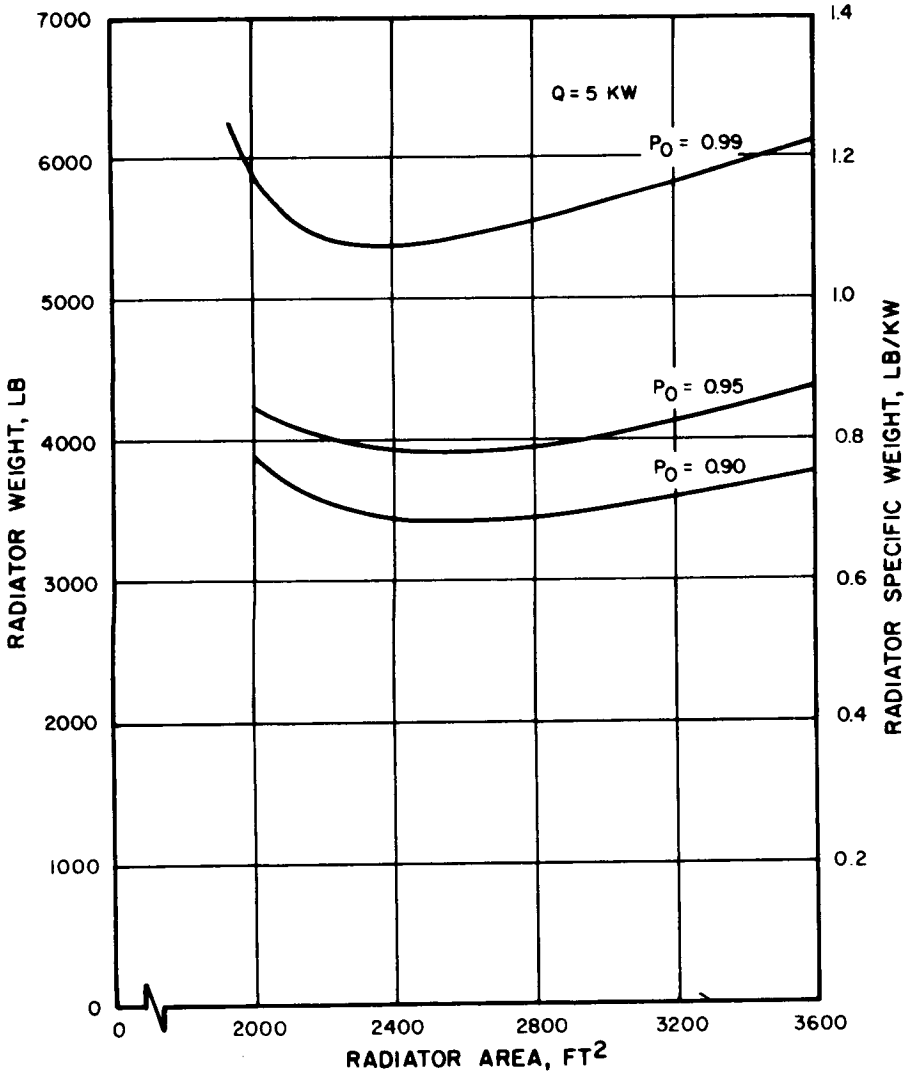

Figure 5-5. Effect of Area Limit on Radiator Weight

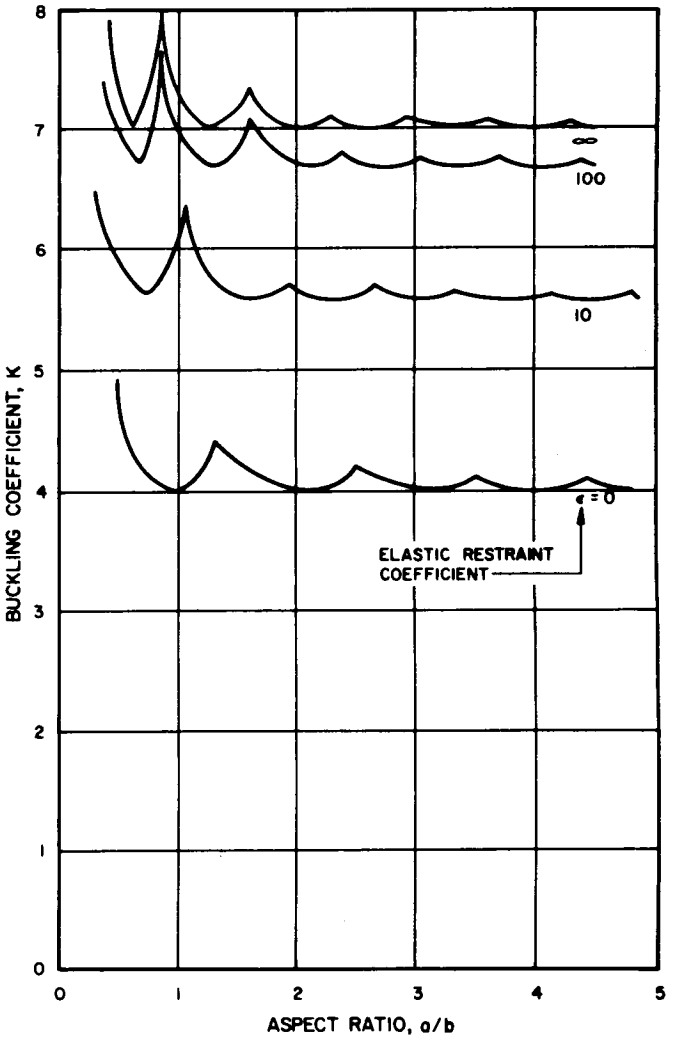

Figure 5-6. Buckling Coefficient for Plates Under Axial Compression

TABLE 5-1. ASSUMPTIONS USED IN RADIATOR ANALYSIS

Inlet temperature	1250°F
Coolant	NaK
Fin and armor material	Beryllium
Liner and feed line material	Stainless steel
Header length	17 feet
Number of panels	Eight
Meteoroid flux model	Whipple - 1963A
Meteoroid penetration criteria	NASA-Lewis
Survival time	15,000 hours

The data shown for a 5,000 kw radiator can be extrapolated to other power levels with little error, if the differences in feed line length can be neglected and the vulnerable area is assumed proportional to the total radiator area. From the meteoroid penetration criteria, the armor thickness is related to vulnerable area and survival probability by

$$t \alpha \left(\frac{A}{-\ln Po}\right)^{0.2485}$$

where t = armor thickness

A = vulnerable area

P_o = no puncture probability

Therefore, radiators for which the term $\left(\frac{A}{-\ln Po}\right)$ is the same, will have the same cross-sectional dimensions or the same specific weight. For example, a radiator rejecting 10,000 kw and having a survival probability of 0.95 has the same specific weight as a radiator rejecting 5,000 kw and having a survival probability of 0.9897. From Figure 5-5, this radiator would have an optimum specific weight of approximately 1.075 lb/kw or the 10,000 kw radiator would weigh 10,750 pounds.

The radiators defined by the line of area limited optima are minimum in area for a given weight, as well as being minimum in weight for a given area. Stated in other terms, these

radiators are minimum in weight for a given "density"; that is, weight divided by area. The "density" is significant, as will be shown, in evaluating the structural capability of the radiator.

5.2 STRUCTURAL FAILURE CRITERIA

Before discussing the structural optimization of radiators, it is first necessary to explain the criteria by which structural capability is determined.

Structurally, the radiator is regarded as a longitudinally stiffened shell in axial compression. The possible failure modes and their definitions are listed in Table 5-2. Of these modes, the two which are of primary concern, and which lend themselves to optimization are local instability and general instability.

The critical buckling stress for local instability is given by

$$\sigma_{\ell} = \frac{k \pi^2 E}{12 (1-\nu^2)} \left(\frac{t}{b}\right)^2$$

where σ_{ℓ} = critical buckling stress

k = buckling coefficient

E = elastic modulus

υ = Poisson's ratio

t = thickness

b = width

For the radiator, the thickness is that of the fin and the width is the tube spacing. The buckling coefficient is determined by the aspect ratio of the panel and the elastic restraint provided by the stiffeners, as shown in Figure 5-6 (Reference 5-1). Usual practice is to consider all edges simply supported, giving a buckling coefficient of 4.0 for "long" panels (a>b). For the radiator diameters of usual interest, the effect of curvature may be neglected.

Figure 5-7 shows lines of constant local instability buckling load for beryllium panels. In plotting these curves, the panel width was assumed to be measured from the fin root, i.e., the panel width is less than the tube spacing by one tube diameter.

TABLE 5-2. DEFINITIONS OF STRUCTURAL FAILURE MODES

Local Instability	Buckling of the skin between the boundaries formed by the longitudinal and circumferential stiffeners	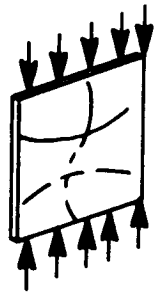
Panel Instability	Buckling of the longitudinal stiffeners by bowing into one or more longitudinal half-waves between circumferential stiffeners	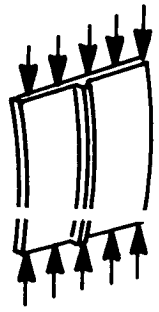
Crippling	The final ultimate compressive failure of a longitudinal stiffener which has sufficient support to prevent panel instability	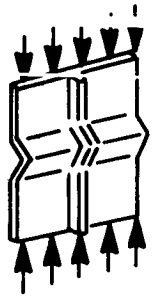
General Instability	The simultaneous buckling of skin, longitudinal and circumferential stiffeners. The mode may be asymmetric (diamond shaped buckles) or axisymmetric (convolutions)	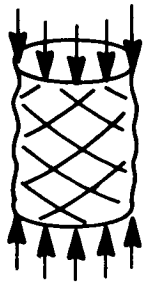

General instability of a shell is best summarized by results shown in Figure 5-10, where density index, $\rho \bar{t}/R$, is plotted versus load index N_x/R

where ρ = material density ($lb/in.^3$)

$\bar{t}$ = equivalent thickness (in.)

R = shell radius (in.)

N_x = axial load intensity (lb/in.)

The upper curve in Figure 5-10 for isotropic cylinders was derived using the modified classical equation from Reference 5-2.

$$\sigma = CE(t/R)$$

In this equation, the coefficient C is a function of t/R and the imperfection factor U, and the other terms are as previously defined. The factor U is chosen to best fit test data from Reference 5-3.

The lower curve in Figure 5-10 was derived from Reference 5-4 and is typical of commonly used stiffening systems. The longitudinal stiffening provided by a radiator is seen to lie midway in efficiency between a grid stiffened shell and an isotropic shell. The middle curve was derived by analyzing a large number of typical radiator configurations, using the theory of Reference 5-5. Since these radiator configurations were not optimized solely for structural efficiency, some scatter was noted. The curve shown was conservatively drawn as the upper boundary of the scattered points.

Using Figure 5-10, it is now possible to determine the radiator "density" (lb/ft^2) necessary to withstand a given load intensity, or equivalent axial load.

A more complete discussion of the methods of analysis for stiffened shells may be found in Reference 5-6.

5.3 STRUCTURAL OPTIMUM

Using the same data from which Figures 5-2, 5-3 and 5-4 were derived, curves of constant radiator "density" are plotted in Figures 5-7, 5-8 and 5-9. To agree with the structural criteria, the weight used is that of the shell only; that is, the tubes, armor and fins. These

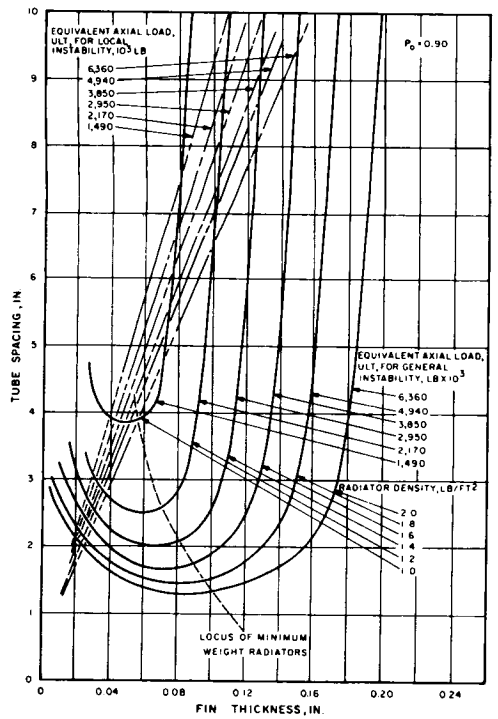

Figure 5-7. Radiator Buckling Stability, P_O=0.90

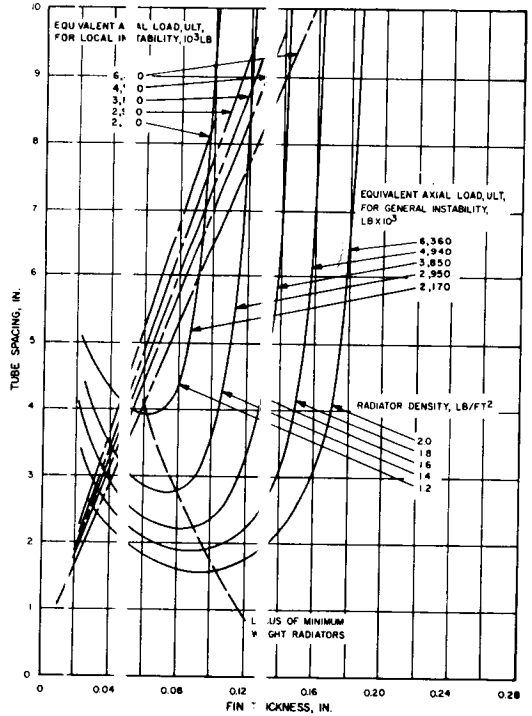

Figure 5-8. Radiator Buckling Stability, P_O=0.95

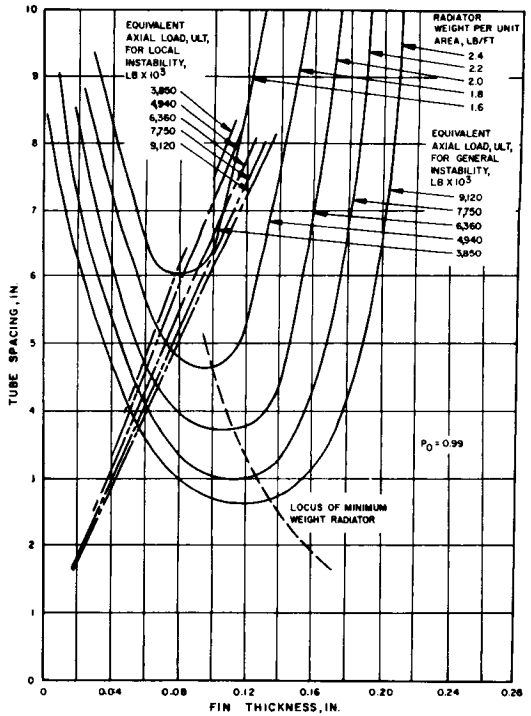

Figure 5-9. Radiator Buckling Stability, P_O=0.99

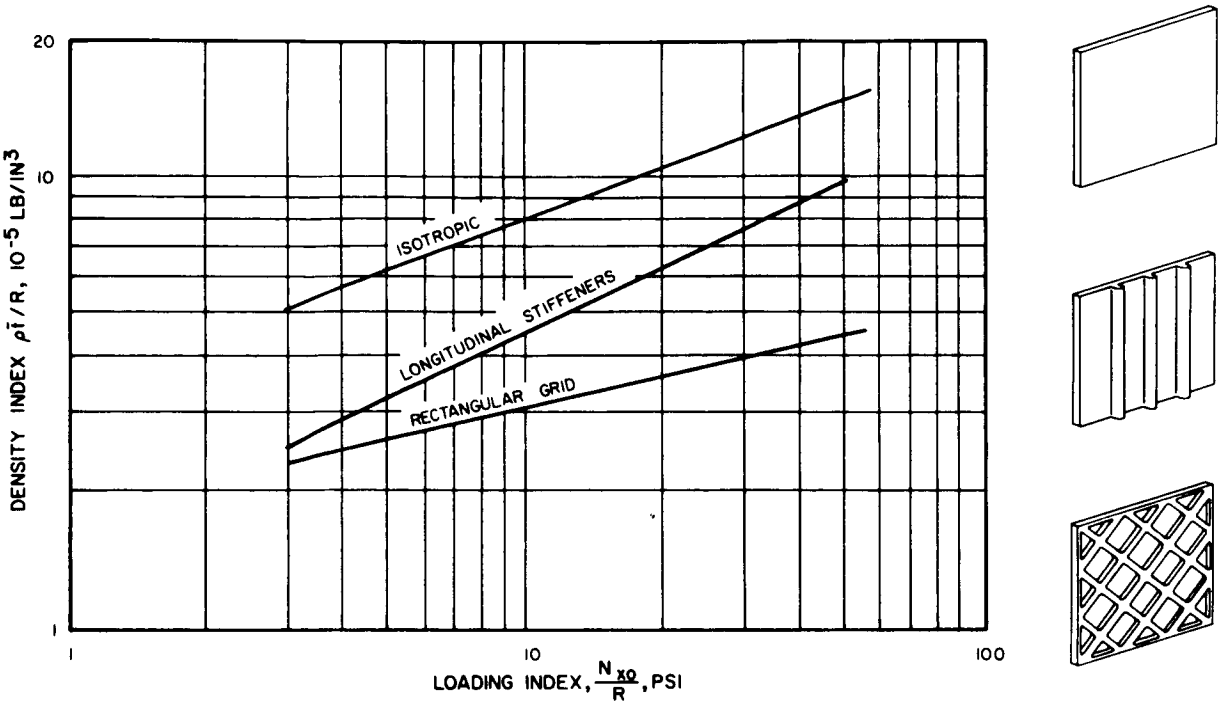

Figure 5-10. Comparitive Efficiencies of Beryllium Cylinders in Axial Compression

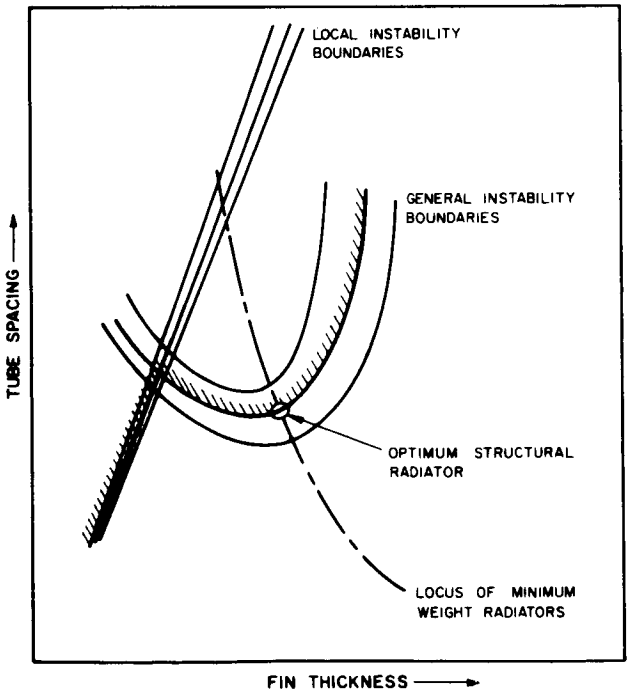

Figure 5-11. Selection of Structurally Optimum Radiator Parameters

curves correspond to lines of constant general instability buckling load. Together with the corresponding curve for local instability, they define a structural stability boundary. For a given load, the radiator design must lie below and to the right of the boundary. The structurally optimum radiator will lie somewhere on this line. In the discussion of Figure 5-2, it was pointed out that the minimum weight radiator for a specified "density" is defined by the locus of area limited optima. Therefore, the structurally optimum radiator, also satisfying the thermal and meteoroid protection requirements, is located at the intersection of the stability boundary and the area limited optima curve. This is shown schematically by Figure 5-11.

By comparing Figures 5-7, 5-8 and 5-9 with the loads derived in Section 3.0, it can be seen that the structural requirements can generally be met by an unlimited optimum radiator. This is characteristic of beryllium radiators and is not generally true for radiators fabricated from aluminum of stainless steel. If redundant panels are used, the survival probability of individual panels would be less than for corresponding non-redundant panels. In this case, the survival probability of individual panels may be low enough, and the radiator "density" low enough that additional stiffening is required, even with beryllium construction.

5.4 REFERENCES

5-1. Steinbacher, F.R. and Gerard, G. "Aircraft Structural Mechanics," Pitman Publishing Corporation, 1952.

5-2. Gerard, G. and Becker, H. "Handbook of Structural Stability, Part III - Buckling of Curved Plates and Shells," NACA TN-3783, August, 1957.

5-3. Batdorf, S.B. et al. "Critical Stress of Thin-Walled Cylinders in Axial Compression," NACA TN 1343, 1947.

5-4. Gerard, G. "Minimum Weight Design of Stiffened Cylinders for Launch Vehicle Applications," Allied Research Associates, Technical Report 235-5, March 13, 1964.

5-5. Gerard, G. and Becker, H. "Elastic Stability of Orthotropic Shells," Journal of the Aerospace Sciences, May, 1962.

5-6. Smith, G.W. and Dittoe, F.A. "Study of Stability of Unpressurized Shell Structures Under Static Loading-Final Report," General Dynamics Report GDC-DDG66-008, April, 1966.

6. CONCLUSIONS

The following conclusions are reached as a result of this study:

a. The launch parameters effecting structural loads have some flexibility and are mission dependent. However, the use of data applicable to Apollo payloads can be used for preliminary design of other payloads on the Saturn launch vehicles.

b. The significant payload parameters in determining launch loads are nose shape and overall length. Mass distribution of the payload has a secondary effect.

c. Optimum shield weight and radiator area favor a cone-cylinder payload shape with a half-cone angle of approximately 10 degrees.

d. There is no advantage in increasing nose bluntness to gain radiator area beyond a bluntness ratio of approximately 0.2.

e. There is little advantage in reduced shield weight for a flat plate radiator when the half-cone angle is 10 degrees or less.

f. The launch facilities are not critical in limiting the payload size on the standard Saturn IB and Saturn V launch vehicles. However, the door height on the Vehicle Assembly Building becomes a limitation for modified Saturn V vehicles having extended propulsion stage lengths.

g. It is feasible to gain substantial radiator area by utilizing the upper stages. However, the adverse effects on the launch vehicle must be weighed against other means of gaining radiator area, such as by deployment.

h. The sensitivity of the Instrument Unit and the large number of external antennas discourages the use of sheath type radiators over the upper stages.

i. Radiators integral with the upper stage structure appear feasible with little or no weight penalty. Use of the skirt area is more easily accomplished than use of the tank area, which would require requalification of the propulsion stage.

j. The use of fixed position charges for propellant dispersion rather than a linear charge in the systems tunnel would facilitate use of the liquid hydrogen tank wall as a radiator.

k. Redesign of the Instrument Unit structure as an integral radiator is an attractive proposal, particularly if a radiator is required for the IU's own power system.

l. Initial design of the IU for the two-stage Saturn V should consider integral radiators.

m. Beryllium radiators designed for operation at 1250°F in a cylindrical configuration are a good structural match for the launch loads on the Saturn IB and Saturn V launch vehicles.

n. Simultaneous optimization to meet the thermal, meteoroid protection and structural requirements can result in appreciable saving in radiator weight.